Charles University
Faculty of Science

Study programme:
Special Chemical and Biological Programmes

Study branch:
Molecular Biology and Biochemistry of Organisms

Michal Ptáček

Excitation Energy Transfer in Photosynthetic Reaction Centres

Přenos excitační energie ve fotosyntetických reakčních centrech

BACHELOR'S THESIS

Supervisor: doc. Mgr. Tomáš Mančal, PhD.

Prague 2020

Prohlašuji, že jsem závěrečnou práci vypracoval samostatně, a že jsem v ní uvedl všechny mnou použité informační zdroje a literaturu. Tato práce nebyla předložena k získání jiného nebo stejného akademického titulu.

Jsem plně srozuměn právům a povinnostem kterým tato práce podléhá dle zákona č. 121/2000 Sb., Autorského zákona, a že Univerzita Karlova má právo na uzavření licenční smlouvy o užití této práce jako školního díla dle § 60 odst. 1 Autorského zákona.

V ..... dne ....

Podpis autora

Acknowledgements:
In the first place, I'd like to thank my supervisor for his unfailing patience as well as for his radiating enthusiasm for the whole topic. I cannot even express what the opportunity of collaboration has meant to me. Besides, I'd like to thank my university and both concerned faculties for enabling me such an interfaculty and interdisciplinary approach to my studies. Last but not least, sincere gratitude belongs also to my parents and the rest of my family for their everlasting support.

Title: Excitation Energy Transfer in Photosynthetic Reaction Centres

Author: Michal Ptáček

Department: Department of Experimental Plant Biology, Faculty of Science, Charles University

Supervisor: doc. Mgr. Tomáš Mančal, PhD.
Institute of Physics, Faculty of Mathematics and Physics, Charles University

Advisor: Mgr. Miloš Duchoslav
Department of Experimental Plant Biology, Faculty of Science, Charles University

Abstract: The photosynthetic reaction centres have uppermost importance in photosynthesis. They represent the actual place where the energy carried by photons is turned into charge-separated states which then enable to establish the electrochemical H^+ transmembrane gradient used by ATP synthases. The photosynthetic light-harvesting complexes gather the energy of light radiation and direct it in the form of electronic excitation energy into the reaction centres. The efficiency of this process is exceptionally high, close to unity, what is capturing the interest of researchers for decades. The development of experimental techniques has led to better understanding of this process down to atomic scale. Nowadays, this insight along with the theoretical basis stemming from quantum mechanics can be used to perform accurate computer simulations which can determine properties of the whole molecular aggregates independently of experiments. This thesis provides an introduction into the field of theoretical photosynthesis research, and it summarises the progress made in past two decades. The detailed theoretical approaches are being put into perspective of the reaction centres of photosynthetic purple bacterium *Rhodobacter sphaeroides* which is a valuable model organism. Both experimental and theoretical results of excitation energy transfer times are compared on this model example.

Keywords: photosynthesis, reaction centre, excitation energy transfer, purple photosynthetic bacteria, *Rhodobacter sphaeroides*, quantum biology, quantum mechanics

Název práce: Přenos excitační energie ve fotosyntetických reakčních centrech

Autor: Michal Ptáček

Katedra: Katedra experimentální biologie rostlin, Přírodovědecká fakulta, Univerzita Karlova

Vedoucí práce: doc. Mgr. Tomáš Mančal, PhD.
Fyzikální ústav, Matematicko-fyzikální fakulta, Univerzita Karlova

Konzultant: Mgr. Miloš Duchoslav
Katedra experimentální biologie rostlin, Přírodovědecká fakulta, Univerzita Karlova

Abstrakt: Fotosyntetická reakční centra mají pro fotosyntetizující organismy kruciální roli. Právě zde totiž dochází k tzv. separaci náboje, kdy je energie excitovaného stavu elektronu využita na ionizaci molekul a uvolněný elektron se pak podílí na ustanovení transmembránového elektrochemického gradientu H^+ iontů využívaného ATP syntázami. Světlosběrné komplexy absorbují energii dopadajících fotonů a s vysokou účinností blížící se jedné ji přenášejí právě do reakčních center. Efektivita tohoto přenosu budí zájem vědců již mnoho dekád a rozvoj experimentálních metod umožnil značné porozumění jeho původu. Získané poznatky, v kombinaci s kvantově mechanickými přístupy, lze navíc využít i na ryze teoretický výzkum zahrnující detailní počítačové simulace. Vlastnosti celých molekulární komplexů tak mohou být určeny s vysokou přesností a nezávisle na experimentech. Text této práce přestavuje úvod do teoretického studia fotosyntézy a shrnuje vývoj odvětví za poslední dvě dekády. Popsané hlavní teoretické přístupy a modely jsou dále prezentovány na příkladu reakčních center purpurové fotosyntetizující bakterie *Rhodobacter sphaeroides*, která představuje důležitý modelový organismus. Na tomto příkladě jsou také srovnány experimentálně i teoreticky získané hodnoty časů přenosu excitační energie.

Klíčová slova: fotosyntéza, reakční centrum, přenos excitační energie, purpurové fotosyntetizující bakterie, *Rhodobacter sphaeroides*, kvantová biologie, kvantová mechanika

Contents

List of Abbreviations

2DES	two-dimensional electronic spectroscopy
AA	amino-acid
ADO	auxiliary density operator
ATP	adenosine-5'-triphospate
BChl$a$	bacteriochlorophyll a
BChl$b$	bacteriochlorophyll b
bCRF	bath correlation function
BPhe	bacteriopheophytine
Chl$a$	chlorophyll a
DOF	degrees of freedom
EET	excitation energy transfer
FGR	Fermi's Golden Rule
FMO	Fenna-Matthews-Olson complex
FRET	Förster Resonance Energy Transfer
HEOM	Hierarchical Equations of Motion
HLA	Heitler-London approximation
IR	infrared light
l.h.s.	left hand side
LH	light-harvesting
LH1	core light-harvesting complex of purple photosynthetic bacteria
LH2	peripheral light-harvesting complex of purple bacteria
LHC	light-harvesting complex
LHO	linear harmonic oscillator
LR	long-range
MRT	modified Redfield theory
NMR	nuclear magnetic resonance spectroscopy
OQS	open quantum system
PAR	photosynthetically active radiation
pbRC	reaction centre of purple (photosynthetic) bacteria
PES	potential energy surface
Phe	pheophytine
PPC	pigment-protein complex
PSI	photosystem I
PSII	photosystem II
PSU	photosynthetic unit
QCh	quantum chemistry
QED	quantum electro-dynamics
QM	quantum mechanics
r.h.s.	right hand side
RC	reaction centre
RDO	reduced density operator
SchrE	Schrödinger equation
SD	spectral density
SDS-PAGE	sodium dodecyl sulphate polyacrylamide gel electrophoresis
SR	short-range
SRT	standard Redfield theory
TD	time-dependent
TDC	transition density cube method
TID	time-independent
TMH	transmembrane α-helix
TrEsp	transition density from electro-static potential method
UV	ultra-violet light
vdW	van der Waals (forces/surface/interactions/...)

List of Physical Constants and Used Notations

Symbol	Notation	Brief description
Å	ångström	unit of distance; 1 Å $= 10^{-10}$ m
c_0	speed of light in vacuum	constant expressing the speed of light in vacuum; $c_0 \approx 299\,792\,458$ m $\cdot$ s^{-1}
$\widehat{\mathbf{p}}$	canonical momentum	vector of canonical momenta in Cartesian coordinates; canonical means it fulfills the canonical commutation relation $[\widehat{q}_n, \widehat{p}_m] = \mathrm{i}\hbar\delta_{nm}$
$\widehat{\mathbf{q}}$	canonical position	vector of position in Cartesian coordinates; canonical means it fulfills the canonical commutation relation $[\widehat{q}_n, \widehat{p}_m] = \mathrm{i}\hbar\delta_{nm}$
$[\,\cdot\,,\,\cdot\,]$	commutator	commutator reflects commutative property of two arbitrary variables or operators, it is defined as $[A, B] = AB - BA$
δ_{nm}	Kronecker delta	Kronecker delta δ_{nm} is used under summation only, it equals to one if index $n = m$, otherwise it's equal to zero, e.g. $\sum_n a_n\delta_{nm} = a_m$
$\delta(x - x_0)$	delta function	delta function $\delta(x - x_0)$ is used under integration only, it equals to infinity in $x = x_0$, elsewhere it's equal to zero, usual definition is: $\int_{-\infty}^{\infty} f(x)\delta(x - x_0)dx = f(x_0)$
$\widehat{\rho}$	density operator	density operator (also called statistical) is an operator fully describing the superposed state of a system (analogously to a wavefunction); it's defined as a outer product of the total system state $\|\psi\rangle$: $\widehat{\rho} = \|\psi\rangle\langle\psi\|$, or alternatively in another basis of states $\|n\rangle$: $\widehat{\rho} = \sum_{n,n'=1}^{N} c_n c_{n'}^* \,\|n\rangle\langle n'\|$. The term *density matrix* is used interchangeably very often yet it stands for one particular representation of the operator.
$\boldsymbol{\mu}$	dipole moment	vector characterising orientation and strength of electric dipole moment; the transition dipole moment is then associated with a transition between two electronic states
e	elementary charge	elementary charge of single electron or e.g. proton; $e = 1.602\,176\,634 \cdot 10^{-19}$ C
ϵ_0	permittivity of vacuum	constant expressing the permittivity of vacuum for electric field; $\epsilon_0 \approx 8.854\,187\,813 \cdot 10^{-12}$ C $\cdot$ V^{-1} $\cdot$ m^{-1}
$\widehat{H}$	Hamiltonian	energy operator, it can be generally expressed as hermitian matrix of dimensions $n \times n$
$\mathcal{H}$	Hilbert space	complex vector space with inner product $\langle f\|g\rangle$, norm is defined as $\|\|f\|\| = \sqrt{\langle f\|f\rangle}$
i	imaginary unit	imaginary unit refers to the domain of complex numbers, it is defined as $\mathrm{i}^2 = -1$
k_B	Boltzmann's constant	constant expressing the proportionality of kinetic energy and thermodynamic temperature of particles; $k_\mathrm{B} = 1.380\,649 \cdot 10^{-23}$ J $\cdot$ K^{-1}

Symbol	Notation	Brief description
$\widehat{T}$	kinetic energy operator	operator of kinetic energy, Hamiltonian can be generally separated into kinetic and potential component: $\widehat{H} = \widehat{T} + \widehat{V}$
λ	light wavelength /læmdə/	wavelength of light is obtainable as fraction of speed of light in vacuum c_0 and light frequency ν: $\lambda = \frac{c_0}{\nu}$
λ_r	reorganisation energy /læmdə/	energy accompanying reorganisation of molecular nuclei in response to excitation
$\widehat{\mathfrak{L}}$	Liouville's superoperator	generalised operator acting on vector space of operators, Liouville's superoperator $\widehat{\mathfrak{L}}$ is defined as commutator with Hamiltonian $\widehat{H}$: $\widehat{\mathfrak{L}} = -\frac{\mathrm{i}}{\hbar}[\,\widehat{H}\,,\,\cdot\,]$
m_e	(non-relativistic) electron mass	mass of a single stationary electron; $m_e = 9.109\,383\,56 \cdot 10^{-31}$ kg
N_A	Avogadro's number	constant expressing the number of particles in one mole; $N_\mathrm{A} \approx 6.02214 \cdot 10^{23}$ mol^{-1}
ν	light frequency /njuː/	frequency of light/photon, corresponds linearly to its energy: $E = h\nu$
$\tilde{\nu}$	wavenumber /njuː tɪldə/	wavenumber is directly proportional to energy by a factor of hc_0 and can be thus regarded as a variable of energy; it equals the reciprocal value of wavelength: $\tilde{\nu} = \frac{1}{\lambda}$; it is frequently used in spectroscopy, usual units are reciprocal centimeters [cm^{-1}]
h	Planck's constant	fundamental constant in QM that represents ratio of energy to wave-frequency of a photon; $h \approx 6.626\,070\,015 \cdot 10^{-34}$ m$^2 \cdot$ kg $\cdot$ s^{-1}
$\hbar$	reduced Planck's constant /eɪtʃ bɑːr/	Planck's constant divided by 2π; $\hbar \approx 1.054\,571\,817 \cdot 10^{-34}$ m$^2 \cdot$ kg $\cdot$ s^{-1}
$\widehat{V}$	potential energy operator	operator of potential energy, Hamiltonian can be generally separated into kinetic and potential component: $\widehat{H} = \widehat{T} + \widehat{V}$
$\prod_{k=1}^{K} c_k$	product	product of all c_k from $k = 1$ to $k = K$; $\prod_{k=1}^{K} c_k = c_1 \cdot c_2 \cdot \ldots \cdot c_K$
$\sum_{k=1}^{K} c_k$	sum	summation of all c_k from $k = 1$ to $k = K$; $\sum_{k=1}^{K} c_k = c_1 + c_2 + \ldots + c_K$
$\mathrm{Tr}(\,\cdot\,)$	trace	trace of an matrix is defined as a sum of all diagonal terms: $\mathrm{Tr}(A) = \sum_{n=1}^{dim(A)} A_{nn}$
$\mathrm{Tr}_{(\,\cdot\,)}(\,\cdot\,)$	partial trace	trace generalised to act on operators on Hilbert space, assume $\widehat{\rho} = \widehat{A} \otimes \widehat{B}$, then $\mathrm{Tr}_A(\widehat{\rho}) = \widehat{B}$
$\mathbb{1}$	unity/identity operator	unity or also identity operator can be defined as $\mathbb{1}A = A$, in matrix representation it has only ones on the main diagonal and zeros elsewhere

List of Notable Equations

Name	Equation & Brief description
Fermi's Golden Rule (FGR)	$$k_{21} = \frac{2\pi}{\hbar}\left\|H_{21}\right\|^2 \rho_2$$ Fermi's Golden Rule describes the rate of electronic transitions from state ψ_1 to ψ_2 in atoms or molecules; H_{21} is the matrix element of electronic interaction Hamiltonian $\widehat{H}$ such that $H_{21} = \langle\psi_2\|\widehat{H}\|\psi_1\rangle$; term ρ_2 is the final density of states.
Hamiltonian of Linear Harmonic Oscillator	$$\widehat{H} = \frac{\widehat{p}^{\,2}}{2m} + \frac{m\omega^2}{2}\,\widehat{q}^{\,2}$$ Hamiltonian of linear harmonic oscillator known from classical physics where classical variables of momentum p and position q are replaced by operators of canonical momentum $\widehat{p}$ and of canonical position $\widehat{q}$. It can be also expressed in terms of creation and annihilation operators what introduces its quantised form. Quantum LHO is known for its infinite number of equidistant energy levels. The energy of nth level is $E_n = \hbar\omega(n + \frac{1}{2})$. Eigenfunctions of the Hamiltonian are called *Hermite polynomials* H_n of nth degree. For further description please see Valkunas et al. (2013, pp 66–69, 91–96).
Liouville-von Neumann equation	$$\frac{\partial}{\partial t}\widehat{\rho}(t) = -\frac{\mathrm{i}}{\hbar}\Big[\widehat{H}, \widehat{\rho}(t)\Big]$$ Liouville-von Neumann equation is a direct analogue of the time-dependent Schrödinger equation. It describes time evolution of a density operator $\widehat{\rho}(t)$ (for derivation please see Valkunas et al. (2013, p 65); alternatively it can be derived from purely classical Liouville equation by its quantisation).
Nakajima-Zwanzig equation	$$\frac{\partial}{\partial t}\widehat{\rho}^{(\mathrm{I})}(t) = \mathrm{Tr}_\mathrm{B}\left\{\widehat{\mathfrak{L}}^{(\mathrm{I})}_{\text{S-B}}(t)\widehat{w}_{EQ}\right\}\widehat{\rho}^{(\mathrm{I})}(t) - \int_0^t \mathrm{d}\tau\, \widehat{\mathcal{M}}(t,\tau)\,\widehat{\rho}^{(\mathrm{I})}(\tau)$$ Nakajima-Zwanzig integro-differential equation describes time evolution in the interaction picture (denoted by a letter 'I' in superscript) of a system part ($\widehat{\rho}^{(\mathrm{I})}(t)$) of a total density operator $\widehat{W}^{(\mathrm{I})}(t)$; $\widehat{P}$ and $\widehat{Q}$ are projector operators such that $\widehat{Q} = \mathbb{1} - \widehat{P}$, $\widehat{P}^2 = \widehat{P}$, $\widehat{P}\widehat{W}^{(\mathrm{I})}(t) = \mathrm{Tr}_\mathrm{B}(\widehat{W}^{(\mathrm{I})}(t))\widehat{w}_{EQ} = \widehat{\rho}^{(\mathrm{I})}(t)\widehat{w}_{EQ}$, and $\mathrm{Tr}_\mathrm{B}(\widehat{w}_{EQ}) = \mathbb{1}$; $\widehat{\mathfrak{L}}^{(\mathrm{I})}_{\text{S-B}}(t)$ is the Liouville's superoperator with system-bath interaction Hamiltonian; $\widehat{w}_{EQ}$ is the bath state in equilibrium. $\widehat{\mathcal{M}}^{(\mathrm{I})}(t,\tau)$ is called the *memory kernel* or the *convolution* in interaction picture and it can be expressed as $\widehat{\mathcal{M}}^{(\mathrm{I})}(t,\tau) = \mathrm{Tr}_\mathrm{B}\left\{\widehat{\mathfrak{L}}^{(\mathrm{I})}_{\text{S-B}}(t)\,\overrightarrow{\exp}\left\{\int_\tau^t \mathrm{d}\tau'\,\widehat{Q}\widehat{\mathfrak{L}}^{(\mathrm{I})}_{\text{S-B}}(t)\right\}\widehat{Q}\widehat{\mathfrak{L}}^{(\mathrm{I})}_{\text{S-B}}(\tau)\widehat{w}_{EQ}\right\}$. The term $\overrightarrow{\exp}\{\}$ stands for the *time-ordered exponential*. The equation can be derived from Liouville-von Neumann equation in a couple of steps, see May and Kühn (2011, pp 183–184).
Planck-Einstein formula	$$E = h\nu = \hbar\omega$$ Planck-Einstein formula puts in relation energy and frequency of electromagnetic radiation. It can be expressed either in terms of transverse frequency ν, or using the circular frequency $\omega = 2\pi\nu$.

Name	Equation & Brief description
Redfield equation	$$\frac{\partial}{\partial t}\widehat{\rho}(t) = -\frac{\mathrm{i}}{\hbar}\Big[\widehat{H}, \widehat{\rho}(t)\Big] - \widehat{\mathcal{K}}\widehat{\rho}(t)$$ Redfield equation describes time evolution of a density operator which characterises a system weakly coupled to its bath. $\widehat{\mathcal{K}}$ is called the Redfield tensor (or alternatively Redfield relaxation (super)operator). For more detailed description please see Valkunas et al. (2013, pp 246–256).
time-independent Schrödinger equation (TID SchrE)	$$\widehat{H}\,|\psi\rangle = \mathcal{E}\,|\psi\rangle$$ Time-independent (also called stationary) Schrödinger equation states that the eigenvalue associated with an eigenfunction (eigenstate) $|\psi\rangle$ of an arbitrary Hamiltonian $\widehat{H}$ stands for the energy of the state.
time-dependent Schrödinger equation (TD SchrE)	$$\frac{\partial}{\partial t}\,|\psi(t)\rangle = -\frac{\mathrm{i}}{\hbar}\widehat{H}\,|\psi(t)\rangle$$ Time-dependent Schrödinger equation describes time evolution of an arbitrary wave function $|\psi(t)\rangle$. Usually, such wave function can be split into two parts, time-dependent and time independent, $|\psi(t)\rangle = \exp\left\{\frac{-i\hat{H}t}{\hbar}\right\}|\psi\rangle$ where $|\psi\rangle$ is the stationary solution of TID SchrE.

Introduction

Photosynthesis is undoubtedly the most essential biochemical reaction on planet Earth. It has triggered the rise of aerobic life forms what changed the planet climate once and for all. Although photosynthesis is considered as purely biological process, it is a subject of interest of much more research fields than just the biology; including even computational chemistry and quantum physics. Several authors proposed a new name for such a broad research area—quantum biology (for review see Lambert et al., 2013).

In 2014, Al-Khalili and McFadden published a science popularisation book subtitled 'Dawn of Quantum Biology'. Besides other topics mentioned in the book, the photosynthesis was described there as a quantum process fully exploited and fine-tuned by organic life. The text was apparently riding on the then wave of thrill about a couple of spectroscopic experiments, started by Engel et al. (2007), which threw into question the role of quantum coherence in living organisms. The book tried to follow some of the ideas of quantum mechanics (QM) co-founder Erwin Schrödinger whose book 'What is life?' (1944) actually inspired molecular biologists and biochemists and led to important discoveries (Dronamraju, 1999). However, Al-Khalili's book cannot be considered that revolutionary at all. At least in terms of photosynthesis, many statements remained controversial up to now and they frequently lead to overestimated assumptions and misinterpretations (see Cao et al., 2020).

For example, one particular phenomenon in photosynthesis is captivating scientists for decades—efficiency and high quantum yield of excitation energy transfer (EET). Despite the presumably hostile and thermodynamically noisy environment of wiggling proteins and membranous phospholipids, nearly every captured photon have potential to reach the reaction center and to be actually further utilised by the cell. The quantum yield is above 80 %, usually even close to unity (Wraight and Clayton, 1974). Such counter-intuitive behavior is obviously triggering the imagination of scientists who are after the explanation. Electronic quantum coherence was one of the candidates.

The aim of this thesis is to provide insight into the topics of such an interdisciplinary field as photosynthesis research. For the sake of clarity, only the 'traditional photosynthesis' of prokaryotes and eukaryotes is taken into consideration. Archeal bacteriorhodopsin-based photosynthesis will not be matter of discussion here. Moreover, only the light-harvesting part of photosynthesis is scrutinised—from photon capture to charge separation event. The biochemical steps that follow can be found in majority of biochemistry textbooks, e.g. Buchanan et al. (2015); Nelson and Cox (2013).

The text of this thesis is divided into three main parts. The first chapter introduces the general principles of light capture and energy transfer, and also describes the structure of pigments as light-absorbing and energy-transferring molecules. The second part is dedicated to the physical point of view and presents overview of basic concepts as well as the most important theories in use. Additionally, some light is also shed on the controversial topic of quantum coherence in photosynthesis. In the last part, everything is put into perspective of experimental work and biological research topics. The reaction centres—core complexes of the photosynthesis—are scrutinised in terms of their structure, function, optical properties, and EET dynamics. As a simple model organism worth more detailed description, purple photosynthetic bacterium *Rhodobacter sphaeroides* is introduced. The side by side comparison of experimentally obtained data and theoretical calculations is presented too.

Regarding the references, there are two particular books worth highlighting. Croce et al. (2018) and Golbeck and van der Est (2014) covered not only all the topics being discussed here but they developed many more interesting points that were unfortunately outside the scope of this thesis.

1 | Light Harvesting in Photosynthesis

1.1 The Pathway to RC

Photosynthetic light-harvesting (LH) machinery consists mostly of transmembrane protein complexes located either in cytoplasmic membrane (Eubacteria), or in thylakoid membrane of chloroplasts (Eukaryota). Two basic functional structures can be identified — the *light-harvesting antennas* and the *reaction centre* (RC). The purpose of the antennas is apparent, they both increase the spatial area where light capture takes place, and they broaden the utilised part of light spectrum. The absorbed energy of light, which is converted into the excitation energy of electronic states of the antenna, has to be somehow delivered to the other compartment, the reaction centre, where it can be utilised. This has to happen before the excitation decays or before it cause collateral photodamage. The major driving force for this transport is the dissipation of excitation energy due to interaction between electronic excited states and the protein surrounding the pigment molecules, which forces the excitation to follow the negative gradient of excited state energy formed by the antennas. That is, the pigments with the lowest energy within the whole EET pathway is always the final acceptor state of the RC, where the energy is converted into a charge travelling across the membrane and establishing the transmembrane electrochemical gradient. This principle is usually referred to as the energy funnelling (Blankenship, 2014).

The number of antennas and RCs in a given photosynthentic system can be experimentally measured. At the beginning of photosynthesis research a concept of *photosynthetic unit* (PSU) was introduced. PSU declares the number of LH antennas belonging to a single RC, i.e. their proportional ratio (Mirkovic and Scholes, 2015; Mirkovic et al., 2017). The bigger the PSU is, the more antennas it contains and the higher would be the total number of absorbed photons with potential to reach RC. On the other hand, the longer travel they would need to undergo to actually reach the RC, and the more likely it is to loose the excitation in a recombination processes, since the excited states have always a finite lifetime. To sum up, there are three factors that can affect the efficiency of light-harvesting so far—the size of PSU (ratio of antennas to RCs), the EET transfer rates (how fast the excitation can 'hop' between antenna-antenna or antenna-RC), and then the energy gradient towards the RC which also declares the strength of energy trapping[1]. All these parameters offer plenty of space for environment specific modifications for the sake of efficient exploitation of sunlight.

The structure of light-harvesting complexes (LHCs) reflects their common evolutionary origin. The functional design of core complexes is pretty much conserved and immune to modifications of significant importance throughout the evolutionary 'tree of life' (see Hohmann-Marriott and Blankenship, 2011). That is the reason for only two basic types of reaction centres, see chapter 3. The LH antennas, especially the peripheral ones, are not so tightly restricted, though, since they do not influence the functionality but only contribute to the efficiency of the processes. They stand for the main hot spot of evolutionary adaptations in photosynthetic organisms (see Green, 2003).

As an example of the evolutionary variety of photosynthetic antennas, we can mention two notable exceptions of LH antennas located completely in cytoplasm. An enormous light absorbing complex called *chlorosome* can be found adjacent to the inner side of cytoplasmic membrane of the sulfur and non-sulfur green bacteria as well as of Chloroacidobacteria (Blankenship, 2014). Chlorosomes contain

[1] Trapping of the excitation occurs in the RC. It minimises the probability of leaving the RC before the charge separation occurs.

crystal-like structure of self-assembled bacteriochlorophylls *c,d*, and *e* embedded in a phospholipid monolayer (see reviews by Orf and Blankenship, 2013; Pšenčík et al., 2014). Proteins contribute to the overall structure only partially, since they form only about 30 % of dry weight. The much smaller in size bacteriochlorophylls represent ca 50 % of the dry weight(Blankenship and Matsuura, 2003). Proteins are located only on the cytoplasm-exposed surface. In some species of bacteria, chlorosomes are linked to RCs by the so-called Fenna-Matthews-Olson (FMO) proteins.

The other exception of a cytoplasmic antenna are the *phycobilisomes*; PPC with covalently bound pigments called *bilins*. They can be either adjacent directly to RCs, similarly to chlorosomes and FMO, or be freely dissolved in cytoplasm/stroma. Bilins along with the phycobiliproteins will be mentioned in section 1.2. As we will discuss further on in this essay, there are many different ways how to tune the optical properties of LHCs and the efficiency of photosynthesis besides adding macromolecular entities. It has been even speculated that the evolution has exploited quantum phenomena to achieve higher efficiency of light-harvesting. For instance, the energy doesn't have to travel by hopping between individual pigments, it can rather spread as a wave delocalised across several molecules in the complex. Elucidation and description of such ideas is one of many key points of the following chapters.

1.2 Photosynthetic Pigments

Photosynthesis is a process of converting energy of electromagnetic radiation into electrochemical potential in form of transmembrane H^+ gradient. This potential, along with the also obtained reducing agents, is then converted further into energy of chemical bonds (Blankenship, 2014). Besides the necessary enzymes, scaffold proteins, lipids, and regulatory pathways, the most crucial part, which conditions the whole energy flux, is the starting point—photon capture by the pigments.

Throughout this essay, the terms *pigment* and *chromophore* are being used interchangeably. Both refer to a molecule capable of electronic transition from a ground state into its higher excited states by absorbing energy quantum of the visible or near-infrared part of radiation spectra. Unfortunately, no unifying term is commonly used for this spectral range. The term *photosynthetically active radiation* (PAR) is frequently used in literature, but it is defined in context of chlorophyll *a* (Chl*a*) only, with the PAR range being between 400–700 nm (Blankenship, 2014).

The energy carried by a photon can be expressed in terms of either the wavelength λ or the frequency ν using the Planck-Einstein formula $E = h\nu$. The part of spectrum which can be exploited by known photosynthetic organisms is defined by the following limits. Speaking of wavelength, the shorter limit is marked out by the strong absorption of proteins, DNA, and also water in the far-UV region ($\lambda < 300$ nm). The longer limit is then set by the fact that from some particular wavelength the IR light doesn't have enough energy to cause the so-called *charge separation*. This process takes place at the heart of RCs on molecular dimer called the *special pair* (see chapter 3), and is closely coupled with oxidation of primary electron donor, e.g. water or inorganic substrates (Blankenship, 2014).

The necessary and common feature to all pigments absorbing visible and IR light is the presence of conjugated double bonds resulting in delocalised molecular orbitals. It is this 'disperse cloud' of π-electrons that enables the excitation in visible region of light (Björn and Ghiradella, 2015). As a rule of thumb, the more the π-electron system is delocalised, the lower in energy the excited state should be. And the other way around. In terms of light-matter interaction, the principle suggests the wavelength which corresponds to molecule's peak absorption should increase with the extent of delocalisation since less energy would be needed for excitation.

Three distinct groups of pigments are present in LHCs—*chlorophylls*, *bilins*, and *carotenoids*. Each group has its own structural characteristics as can be seen in Figure 1.1a–d. However, the molecular optical properties can vary greatly within each group. The absorption spectra of selected chromophores are depicted at Figure 1.1e,f.

Chlorophylls are by far the most common pigments, since they are able to exploit nearly the whole part of the above outlined spectrum, except the so-called 'green gap'. They can be found throughout all LH compartments, and chlorophyll *a* (Chl*a*) is even the most abundant LH pigment on Earth (Björn et al., 2009). About eleven basic types of chlorophylls, distinguished by letters from latin alphabet, can be described and divided into three groups by their structure. Chlorophylls *c* (Chl*c*) are derived from the well-known porphin ring. Chl*a*,*b*,*d*,*f* together with bacteriochlorophylls BChl*c*,*d*,*e* [2] origin from dihydroporphin (also called chlorin[3], see Figure 1.1a). Finally, BChl*a*,*b*,*g* contain tetrahydroporphin (also called bacteriochlorin, see Figure 1.1b) (Scheer, 2003, 2008). The here omitted Chl*f* was only synthesised in laboratory and haven't been discovered in nature yet, and for its unsuitable properties it probably never will (Vogl et al., 2012; Orf et al., 2013). For a detailed description of each chlorophyll, see Blankenship (2014).

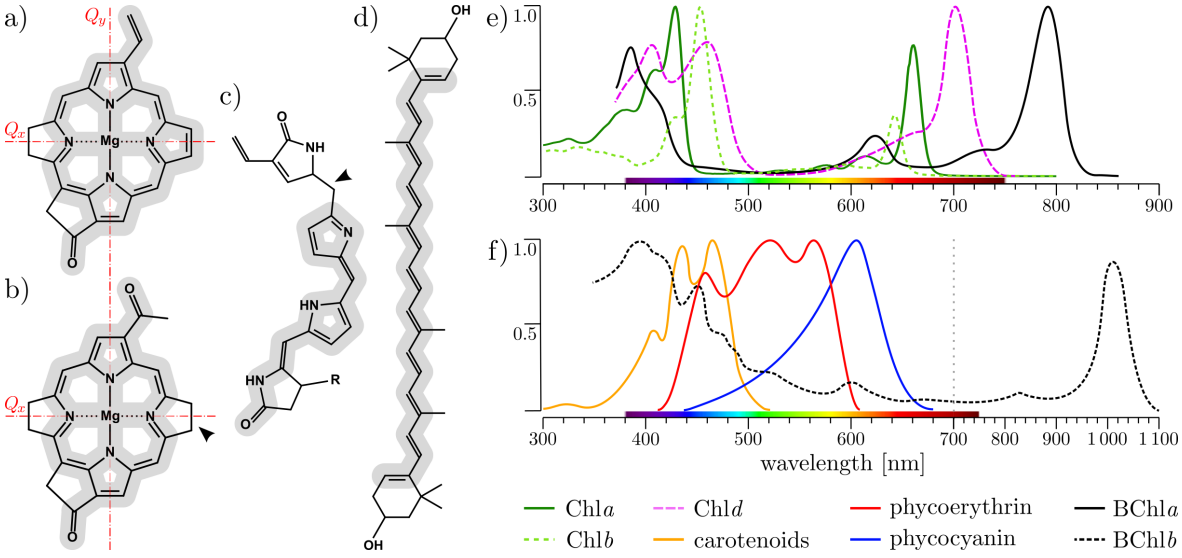

Figure 1.1: Overview of general structure and optical properties of LHC pigments. For clarity, most of the peripheral substituents are omitted here and only the main backbone is shown. The grey shading highlights the extent of conjugated double bonds system.
Left: Representatives of three main types of LH pigments are shown, chlorophylls (a,b), bilin (c), and carotenoid (d). Three separate subgroups of chlorophylls can be additionally distinguished according to the structure of their porphyrin ring. Two of them—chlorin and bacteriochlorin—are depicted here. Small arrow in picture (b) emphasize the major difference between these two rings. Axes Q_x and Q_y corresponds to the orientation of electronic transitions as defined by Gouterman (1961). Bilins are represented by phycoerythrobilin (c). The letter R at the bottom right corner denotes the site where all bilins are covalently linked to a cystein AA of phycobiliprotein. The small arrow shows a bond which desaturation leads to significant expansion of the conjugated double bonds system[4]. As a result, the absorption peak of free dissolved molecules would be red-shifted from ca 600 nm to 700 nm (Scheer, 2003). The carotenoids are represented by zeaxanthin (d).
Right: Graphs of relative absorption spectra of selected pigments and PPCs. Data are normalised to one. On picture (e) are depicted chlorophylls *a*,*b*,*d*, and bacteriochlorophyll *a* as dissolved in methanol. On picture (f) are schematically shown carotenoids in general, then bilins-containing biliproteins (phycoerythrin with phycoerythrobilin and phycocyanin with phyocyanobilin), and on partially scaled axis also BChl*b* measured in the form of PPC.
Figure is based on Scheer (2003, pp 3), Björn and Ghiradella (2015, pp 100) (a–d), and on Chen and Blankenship (2011, pp 429), Mirkovic and Scholes (2015, pp 232), Oelze (1985, pp 280) and on PhotoChemCAD3™ database (Taniguchi et al., 2018; Taniguchi and Lindsey, 2018) (e,f).

[2] Bacteriochlorophylls *c*,*d*,*e* form the chlorosome of green bacteria. Despite being bacterial, they are not derived from bacteriochlorin but rather from chlorin.
[3] not to be mistaken for *chlorine*, the chemical element Cl

Photosynthetic bilins (phycobilins) have mainly just a supportive role in LH, since they occur in peripheral antennas only. In contrast to other pigments, bilins are covalently bound[5] to the protein scaffold—forming *phycobiliproteins*. Phycobiliproteins then aggregate into *phycobilisomes*, supramolecular LH protein complexes present in majority of Cyanobacteria, Glaucophytes, Rhodophytes, and also in Cryptophytes and few heterokonts[6]. For a detailed review of phycobiliproteins please see Marx et al. (2014). Bilins in general consist of four pyrroles linked in a linear molecule what corresponds to a linearised open-chain porphin ring, see Figure 1.1c. Their peak absorbance lays in the otherwise unexploited green region of the spectrum (main peaks between 495–671 nm) so they can efficiently increase the effective absorption cross-section of chlorophylls, which lay lower in energy, see Figure 1.1e,f (Björn and Ghiradella, 2015).

Finally, carotenoids are the most diverse group of photosynthetic pigments. They absorb light mainly in the blue spectral region of 420–570 nm (Chen and Blankenship, 2011). Presence of carotenoids in LHCs has uppermost importance. Firstly, they work as accessory pigments funnelling the captured energy to chlorophylls. And secondly, they stabilise the PPC environment and protect it from photodamage. Carotenoids posses a variety of mechanisms how to deal with excess of excited states energy for the sake of preventing the *reactive oxygen species* (ROS) formation (for overview see Pinnola et al., 2018). The most studied mechanism of excess excitation disposal is the so-called *nonphotochemical quenching*, probably better known as dissipation of energy into heat. Carotenoids usually consist of about 40 carbons forming a system of ca 10–13 conjugated double bonds (Chen and Blankenship, 2011). Structure of a representative species, zeaxanthin, is depicted on Figure 1.1d.

In this thesis, we will focus on the most pertinent pigments commonly present in the photosynthetic RCs. Chlorophylls Chl*a*, BChl*a,b*, and bacteriopheophytins are the most crucial pigments directly participating in EET. Rarely, Chl*a* can be replaced by Chl*d* in case of a few Cyanobacteria (Björn et al., 2009). Atomic structure of chlorophylls is rather variable what gives them a wide range of optical properties. By and large, the default structure consist of somehow modified porphin ring (i.e. porphyrins in general), a single metal ion, and a long saturated hydrocarbon chain. In each of these parts, significant alterations can be observed.

The planar porphyrin ring is the most important unit where all the double bonds are located. Plethora of different substituents can be bound to the peripheral carbons what may not only bolster the specificity of placement within the protein scaffold, but also enlarge the delocalisation of molecular orbital and thus again tune their absorbance. A single metal ion is usually placed inside the porphyrin ring. The most abundant is magnesium ion Mg^{2+} present in all chlorophylls *sensu stricto* and a majority of bacteriochlorophylls. The second most frequent situation is the complete lack of cation. Such metal-free molecules can be found in bacterial RCs or in PSII and they are called *(bacterio)pheophytins*. A much less frequent is the presence of zinc cation Zn^{2+}. This modification of natural origin was described in two distinct taxons of bacteria only—*Candidatus* Chloracidobacterium thermophilum (Bryant et al., 2007; Tsukatani et al., 2012) and *Acidiphilium rubrum* (Wakao et al., 1996). In both cases it is their conserved phenotype. However, rare observations in other species, stemming from either random mutations or high concentration exposures, were also made (see Jaschke et al., 2011; Küpper et al., 1998).

More transmetallated chlorophylls containing Hg, Cd, Ni, Cu, La, or Pb were observed in natural LHCs, including RCs, as a result of higher concentration of the element in the environment (Küpper

[5]Usually they are bound by a single thioether bond, but two can occur as well (Scheer, 2003; Björn and Ghiradella, 2015).

[6]The phycobilisomes were obviously just inherited by multiple processes of endosymbiosys. Secondary endosymbiosys with a Rhodophyte alga gave rise to Cryptophytes, and tertiary endosymbiosys with a Cryptophyte resulted in few groups within heterokonts (e.g. taxon *Dinophysis* sp.). Even the Rhodophytes and Glaucophytes are obviously cases of primary endosymbiosys, pointing towards Cyanobacteria.

et al., 1998). However, the above-mentioned zinc seems to be the only one which can be purposefully utilised and does not disrupt the photosynthesis. The other transmetallated chlorophylls are sometimes described as 'energy black holes' since their vacant *d*-orbitals enable instant dissipation of any kind of excitation energy (see Scheer, 2003, 2008).

Last but not least, the long non-polar saturated hydrocarbon chain, usually *phytyl* (it is thus generally called 'phytyl-tail'; Blankenship, 2014), ensures the solubility of the whole molecule in the transmembrane scaffold protein. Despite its structural importance, the chain is not directly involved in EET, and thus it is not usually even shown in illustrations.

Albeit structurally diverse, general shape of the chlorophylls is the same as well as their spectroscopic and quantum-chemical (QCh) description. Traditionally, the four-molecular-orbital model formalised by Gouterman (1961) is used for all porphyrin-like molecules. The model takes into account two highest occupied molecular orbitals (HOMO, HOMO−1) and two lowest unoccupied molecular orbitals (LUMO, LUMO−1). Four different one-electron HOMO to LUMO transitions can be then described. As a result of mutual interactions between the MO, the transitions are spatially polarised into two directions, described by two perpendicular axis laying in the plane of porphyrin ring. The orientation of axes is a matter of consensus and it's depicted on Figure 1.1a,b (named Q_x and Q_y therein). Once the orientation is assigned to the electronic transitions, they can be called transition dipoles. The four transition dipoles are also split in terms of their energy (for great illustration see Frank and Cogdell (2012), pp 96). The two lower in energy are called Q_x and Q_y, with the latin letters referring to their orientation. Then there are two higher energy transition dipoles called B_x and B_y which are frequently called by an unifying term *Soret bands* (Curutchet and Mennucci, 2018). According to the model, all these transition dipoles directly correspond to peaks observable in spectroscopic signal (see Scheer, 2003, pp 47, Fig. 3).

Precise QCh tools are used nowadays preferably to determine the molecular orbitals where also the peripheral substituents and even the surrounding protein environment with different AA chains are taken into account. Besides, there are various combined QM/QCh approaches. The interested readers are referred to the exhaustive reviews and comparisons made by Linnanto and Korppi-Tommola (2006), König and Neugebauer (2012), and by Curutchet and Mennucci (2017).

To exemplify the close relation between protein environment and optical properties of embedded pigments (i.e. the above-mentioned spectral tuning), let us have a look at the bacteriochlorophyll *b*, the furthest absorbing natural LH pigment known so far. It is utilised for anoxygenic photosynthesis by a purple non-sulphur bacterium *Blastochloris viridis*[7]. Bacteriochlorophyll *b* (BChl*b*) is situated at the RCs, and it reaches the maximum absorbance at ca 1 020 nm when measured *in vivo* (Trissl, 1993; Scheer, 2003; Björn and Ghiradella, 2015). It differs from the common BChl*a* in one single double bond on one of the peripheral substituents. However, such modification results in a shift of only ca 25 nm when solution of chlorophylls in diethylether is measured (Oelze, 1985). That means that the distinct far-IR red-shift of more than 160 nm[8], which is visible on Figure 1.1f, has to be caused by the protein environment. The scaffold protein both ensures the right organisation and orientation of molecules as it also directly interacts with the pigments by various AA chains and can the affect the charge distributions (van Amerongen et al., 2000; Tsukatani et al., 2013). The mentioned measurements are very temperature dependent, though. Kiang et al. (2007) thus proposed that the actual maximal wavelength value could go even higher, beyond 1 073 nm where the peak of water transmittance is located. The transmittance then plummets and at 1 173 nm approaches to zero. That is the final thinkable boundary. The close relation between LH pigments absorption spectra and water transmittance was elucidated by Stomp et al. (2007).

[7] in the literature, it can be also found under an older name *Rhodopseudomonas viridis*
[8] when compared to BChl*a* measured *in vivo*

2 | Physical Description of Excitation Energy Transfer

2.1 Physical Model of Light-Harvesting Complexes

The complexity of photosynthetic light-harvesting complexes (LHCs) does not go hand in hand with exact quantum calculations. It is well-known that analytical solution of Schrödinger equation is obtainable only for very small model systems, such as isolated hydrogen atom. Every more complicated system has to be somehow approximated to be even solvable. There is no doubt that solutions obtained from such approximate methods must still correspond to experimental measurements to be scientifically relevant. However, natural phenomena on sub-atomic level are far more sophisticated then one would ever think, and many processes can evolve in different directions depending on the subtle interactions with the environment (see e.g. Harrop et al., 2014). To be able to properly describe all EET phenomena, tremendous amount of work had to be done to lay down the unifying theoretical foundations.

At the beginning of developing the general physical model of LHC, a few crucial concepts of uppermost importance in EET will be introduced. Firstly, for the sake of clarity, we will focus on the description of individual chromophore molecules and the interactions between them, omitting the environment for a while. Consequently, we will describe the concept of exciton—electronic states delocalised over several molecules—and we will clarify the meaning of coherence in energy transfer processes.

2.1.1 Physical Description of Chromophore Molecule

The chromophore molecules present in LHC can be generally regarded as neutrally charged, with zero magnetic moment, and negligible mass. They are firmly embedded in the protein scaffold so their average relative position and orientation can be generally assumed as rigid. However, things get changed as we start evaluating separate electrons and atomic nuclei. The general Hamiltonian of a single chromophore molecule reads:

$$\widehat{H}_{\text{mol}} = \widehat{T}_{\text{nuc}} + \widehat{T}_{\text{el}} + \widehat{V}_{\text{nuc-nuc}} + \widehat{V}_{\text{nuc-el}} + \widehat{V}_{\text{el-el}} \,, \tag{2.1}$$

where $\widehat{T}$ and $\widehat{V}$ stand for the kinetic and the potential energies, respectively, *nuc* and *el* in subscript stand for nuclei and electrons. Potential energies arise from Coulombic interactions between charged particles. Electronic states of atoms and molecules can be described either in terms of wave function or in our case preferably using the so-called *charge density* $\rho(\mathbf{r})$. On the other hand, the nuclei can be regarded as charged mass points. Because of the mass discrepancy between electrons and nuclei (i.e. carbon nuclei is more than $1\,000\times$ heavier than a single electron), the Born-Oppenheimer approximation[1] is usually used (Valkunas et al., 2018). Let us assume that the nuclei are fixed in space and $\mathbf{R}$ represents all their Cartesian coordinates. The nuclear kinetic energy $\widehat{T}_{\text{nuc}}$ from (2.1) can be thus omitted for a while. As a result, the electrons are not influenced by any movement of positive charges, and they behave independently in respect to the fixed parameter $\mathbf{R}$. They also respond adiabatically[2]. This simplifies the $\widehat{H}_{\text{mol}}$ (based on Valkunas et al., 2013):

[1] also called *adiabatic approximation*

[2] the electrons react instantaneously on change of nuclei position—parameter $\mathbf{R}$ (May and Kühn, 2011)

$$\begin{aligned} \widehat{T}_{\text{el}} &= \sum_{n}^{N_{\text{el}}} \frac{\mathbf{p}_n^2}{2m_e} & \qquad \widehat{V}_{\text{nuc-el}} &= \sum_{k}^{N_{\text{nuc}}} \sum_{n}^{N_{el}} \xi \frac{-z_k e^2}{|\mathbf{r}_n - \mathbf{R}_k|} \\ \widehat{V}_{\text{el-el}} &= \sum_{n<m}^{N_{\text{el}}} \xi \frac{e^2}{|\mathbf{r}_n - \mathbf{r}_m|} & \qquad \widehat{V}_{\text{nuc-nuc}} &= \sum_{k<l}^{N_{\text{nuc}}} \xi \frac{z_k z_l e^2}{|\mathbf{R}_k - \mathbf{R}_l|} \end{aligned} \tag{2.2}$$

where N_{nuc} and N_{el} are the total numbers of nuclei (atoms) and electrons of described molecule, respectively; $\mathbf{R}$, $\mathbf{r}$, $\mathbf{p}$, and $\mathbf{z}$ are the whole sets of nuclear and electronic coordinates, conjugated momenta of electrons, and atomic (proton) numbers, respectively[3]; m_e is the electron mass; e is the elementary charge; ξ equals to $(4\pi\epsilon)^{-1}$, where ϵ is the environment specific dielectric constant.

The separation of the Hamiltonian with respect to the parameter $\mathbf{R}$ is visible in equations of (2.2). The parameter occurs explicitly only in the right column of (2.2) in operators of potential energy. The right-hand-side seems to be $\mathbf{R}$-independent. However, even the left column is implicitly $\mathbf{R}$-dependent as the fixed position of nuclei is setting an initial condition for the electrons. To define the initial equilibrium state of the molecule, the value of parameter $\mathbf{R}$ minimising the electronic part is sought (Valkunas et al., 2013). The Hamiltonian of a fixed molecule then reads:

$$\widehat{H}_{\text{mol}} = \widehat{H}_{\text{el}}(\mathbf{r}, \mathbf{R}) + \widehat{V}(\mathbf{r}, \mathbf{R})\,. \tag{2.3}$$

The TID SchrE with this Hamiltonian would have to be evaluated for every $\mathbf{R}$ separately (Müh and Renger, 2014). For our purposes, only the aforementioned equilibrium state is relevant. One then obtains the molecular adiabatic electronic eigenstates and adjoint eigenenergies:

$$\psi^{(i)}(\mathbf{r}, \mathbf{R})\,, \quad \mathcal{E}^{(i)}(\mathbf{R})\,. \tag{2.4}$$

The superscript stands for the ith electronic (eigen)state of the molecule (Valkunas et al., 2018). This 'electronic' solution can be then used as a part of *ansatz*[4] for determining the total molecular wave function $\Psi(\mathbf{r}, \mathbf{R})$, along with the corresponding eigenergies, by re-establishing the nuclear kinetic energy $\widehat{T}_{\text{nuc}}$ into the Hamiltonian and by solving the TID SchrE.

Complete derivation was skipped as May and Kühn (2011), Valkunas et al. (2013), and Jang (2020) offer fairly detailed insight and step-by-step solution. More general descriptions is then provided by Valkunas et al. (2018).

The last term worth of mentioning here is the *potential energy surface* (PES). The PES arise from previous calculations of molecular Hamiltonian, and it has exceptional importance in description of EET (May and Kühn, 2011). PES expresses the total potential energy of the molecule as a function of all its nuclear coordinates $\mathbf{R}$. That is to say, it puts into relation the excited molecular electronic states with the molecular structure. The PES is obviously convoluted many-dimensional hypersurface, which is difficult to depict. Hence, it is often expressed in terms of the so-called *normal modes*—non-interacting degrees of freedom (DOF) (Valkunas et al., 2013) obtained as linear transformation of Cartesian displacements (May and Kühn, 2011). The advantage of such a normal mode is that it describes a collective displacement of multiple particles rather than a precise position of a single one.

As a decent simplification, one generalised normal mode can be identified with the x-axis what enables us to plot the molecular PES. Additionally, the function behaviour around its global minimum can be assumed harmonic what leads to the well-known type of problem—quantum linear harmonic oscillator (LHO). Hence, under these approximations, the PES can be drawn as a parabola (see Figure 2.1) enclosing equidistant energy levels—*normal vibrational energy levels*.

[3] i.e. $\mathbf{R} = (\mathbf{R}_1, \mathbf{R}_2, \ldots \mathbf{R}_{N_{\text{nuc}}})$, $\mathbf{r} = (\mathbf{r}_1, \mathbf{r}_2, \ldots \mathbf{r}_{N_{\text{el}}})$, $\mathbf{z} = (z_1, z_2, \ldots z_{N_{\text{nuc}}})$

[4] The term *ansatz* is used frequently in all QM-related fields of science. It comes from German and it stands for an arbitrary function we use to try to solve our mathematical problem. A trial function, so to speak.

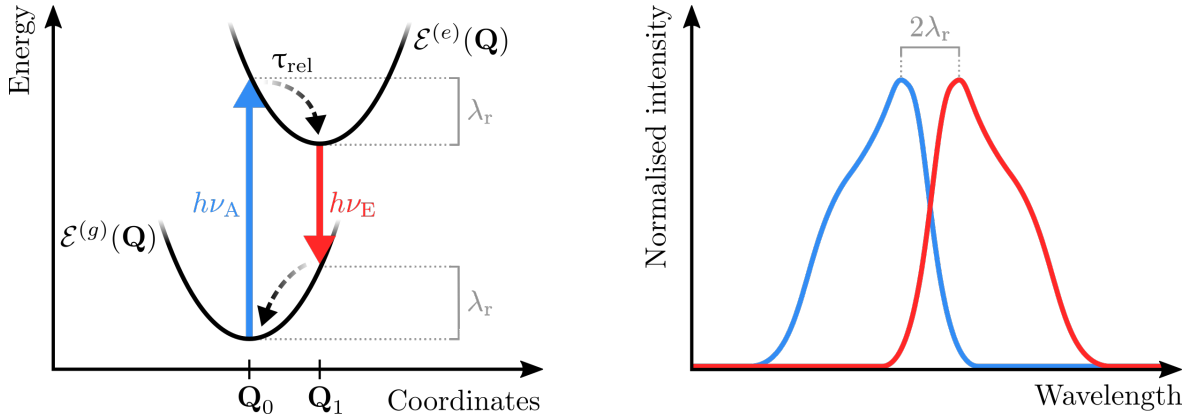

Figure 2.1: Simplified schematic depiction of reorganisation energy λ_{r} (approximated by harmonic oscillators around global minima).
Left: Scheme of a generalised potential energy surfaces (PES) of ground ($\mathcal{E}^{(g)}(\mathbf{Q})$) and excited ($\mathcal{E}^{(e)}(\mathbf{Q})$) state of a molecule. Both depends on general displacement $\mathbf{Q}$ quadratically. The excitation from ground state to excited state occurs by absorbing energy quantum $h\nu_{\mathrm{A}}$ (solid blue arrow). Consequently, the molecule is not in stable equilibrium any longer, with respect to potential energy of nuclei. The equilibrium of the excited molecule is re-established by releasing the so-called *reorganisation energy* λ_{r} (dashed black arrows) accompanied by a change of nuclear position Q_0 to Q_1. The duration of this process is called *relaxation time* τ_{rel}. The molecule can then relax back to its ground state while emitting energy quantum $h\nu_{\mathrm{E}}$. However, yet in ground state, the nuclei have to undergo reorganisation again. Hence, the emitted energy differs from the absorbed by twice the reorganisation energy λ_{r}. Both excitation and relaxation are considered adiabatic, following the *Franck-Condon principle* (Braslavsky, 2007).
Right: The plot shows absorption and emission spectra of an arbitrary molecule as they could be experimentally measured. The observable energy shift between two peaks is called *Stokes shift* and it's equal twice the reorganisation energy (May and Kühn, 2011; Valkunas et al., 2018).
Adapted from Ishizaki and Fleming (2012, pp 335) (*left*), and from Collini et al. (2009, pp 21) (*right*).

2.1.2 Intermolecular Interactions

Every single particle and molecule interacts with its neighbouring counterparts and with the surrounding environment. Such interactions can be covalent or non-covalent. Generally, the latter can be result of electric, magnetic, gravitational, or van der Waals[5] forces. Action radius of all non-covalent interactions is theoretically infinite. However, the strength of such interactions always weakens significantly with the distance.

Pigments present in LHC are predominantly bound to the protein scaffold non-covalently (Renger and Müh, 2013). However, is's worth noting that cases of covalent binding are also well-known, e.g. aforementioned bilins. Two limiting cases of non-covalent interactions can be further distinguished—long-range (LR) and short-range (SR). The latter correspond to direct overlap of electronic orbitals, what may result even in occasional electron exchange between the molecules (Madjet et al., 2009)[6]. The SR effects become negligible beyond ca 4 Å (Collini et al., 2009; Müh and Renger, 2014). To put it into perspective, the diameter of porphyrine ring[7] is ca 9 Å and distances between neighbouring chromophores (center to center) in LHC vary in range of 5–20 Å (Mirkovic et al., 2017). Hence, LR electrostatic (Coulombic) interactions between chromophores are far the most predominant (van Amerongen et al., 2000; Renger and Müh, 2013). Apparently, many exceptions where the SR interactions cannot be disregarded are also known.

The interplanar distance between two parallel (bacterio)chlorophylls forming the so-called *special pair* (see chapter 3) is only ca 3–3.8 Å (Deisenhofer and Norris, 1993). The SR orbital-overlapping interaction thus should be considered and treated in model Hamiltonian. The importance of SR

[5]The term van der Waals (vdW) force is usually used as a general name for a group of dispersion forces; in contrast with previously mentioned 'classical' forces, vdW forces act between every particles or molecules, regardless of their net charge, structure, or polarisation. They have very complex character, and include also electrodynamic interactions or entropy.
[6]Occasionally, the term short-range interaction is used in context of the validity of dipole-dipole approximation, as will be mentioned further on. However, in this text it is defined as an interaction which involves direct orbital overlap.
[7]Main structural component of many light-capturing molecules, e.g. chlorophylls; see section 1.2

interaction and possible EET mediated by excited electron exchange was first proposed by Dexter (1953), and thus it is usually called *Dexter exchange mechanism* of excitation energy transfer. The theory was then fundamentally revised by Harcourt et al. (1994) and Scholes et al. (1995). Unlike the SR interactions, in general, the Dexter transfer of excited electron can occur at greater distance; at up to 10 Å (van der Meer et al., 1994; van der Meer, 2013). Madjet et al. (2009) then discovered that 70–80 % of all interactions in photosynthetic RCs have SR character. Speaking of RCs, Madjet et al. (2009) described a convenient approach how to treat such closely separated dimer. They combined the approach of (Madjet et al., 2006) (TrEsp method for calculation of Coulombic interaction) and the QCh description of separated SR interactions proposed by Scholes et al. (1999).

Both SR and LR interactions between molecules stand for the so-called *coupling*. If the relative strength of the intermolecular coupling is sufficiently large compared to the fluctuations of environmental fluctuations, it can result in the so-called *delocalised molecular exciton* (see subsection 2.1.3). As was already mentioned, the LR couplings of pigments are caused mainly by Coulombic interaction. It can be usually observed between two charged monopoles, or two dipoles. However, neither is applicable on net neutral molecules—what majority of photosynthetic pigments is. In this case, we describe the so-called *charge density Coulomb coupling* (Madjet et al., 2009). That is to say, two reciprocally interacting molecular charge distributions.

One possible approach is to assume the intermolecular distance is much larger than the diameters of individual molecules. Under this LR assumption the interaction can be approximated into two separate point-charge-density parts. Hence, it is called the *point-dipole approximation*. The charge densities arise from the previous treatment of molecular Hamiltonian where the molecular wave function $\Psi_\alpha(\mathbf{r},\mathbf{R})$ was introduced (see subsection 2.1.1). The letter α represents the index of individual chromophores. Corresponding charge density $\rho_\alpha(\mathbf{x})$ in an arbitrary spatial point of observation $\mathbf{x}$ is then defined as (based on May and Kühn, 2011):

$$\rho_\alpha(\mathbf{x}) = \sum_k^{N_{nuc}} \iint ez_k |\Psi_\alpha(\mathbf{r},\mathbf{R})|^2 \delta(\mathbf{R}_k - \mathbf{x})\ \mathrm{d}\mathbf{r}\,\mathrm{d}\mathbf{R} - \sum_n^{N_{el}} \iint e|\Psi_\alpha(\mathbf{r},\mathbf{R})|^2 \delta(\mathbf{r}_n - \mathbf{x})\ \mathrm{d}\mathbf{r}\,\mathrm{d}\mathbf{R}\ , \quad (2.5)$$

where the notation corresponds to the one used in equations (2.2). Integration of net neutrally charged molecule α over the whole space would necessarily give zero. Dipole moment of such molecule can be written as:

$$\boldsymbol{\mu}_\alpha = \int \rho_\alpha(\mathbf{x}_\alpha)\,\mathbf{x}_\alpha\ \mathrm{d}^3\mathbf{x}_\alpha\ . \quad (2.6)$$

The spatial coordinates $\mathbf{x}_\alpha$ are expressed there relatively to the middle point $\boldsymbol{\chi}_\alpha$ of molecule α. That is to say, the point of origin of Cartesian coordinates is placed in $\boldsymbol{\chi}_\alpha$. Since we want to investigate interaction between two molecules (α and α'), the coordinate system have to be unified and the terms $(\boldsymbol{\chi}_\alpha + \mathbf{x}_\alpha)$ (and analogous one for molecule α') needs to be used instead:

$$V_{\alpha\alpha'} = \xi \iint \frac{\rho_\alpha(\boldsymbol{\chi}_\alpha + \mathbf{x}_\alpha)\,\rho_{\alpha'}(\boldsymbol{\chi}_{\alpha'} + \mathbf{x}_{\alpha'})}{|(\boldsymbol{\chi}_\alpha + \mathbf{x}_\alpha) - (\boldsymbol{\chi}_{\alpha'} + \mathbf{x}_{\alpha'})|}\ \mathrm{d}^3\mathbf{x}_\alpha\,\mathrm{d}^3\mathbf{x}_{\alpha'}\ . \quad (2.7)$$

Usually, the so-called *binomial multipole expansion* proceeded by *dipole approximation* (see Hassani, 2009) is used for a pair of well separated chromophores [8]. The Coulombic dipole-dipole interaction between neutral molecule α and α' then reads (Abramavicius et al., 2011; Sener et al., 2011):

$$V_{\alpha\alpha'} = \xi \left[\frac{(\boldsymbol{\mu}_\alpha \cdot \boldsymbol{\mu}_{\alpha'})}{|\boldsymbol{\chi}_{\alpha\alpha'}|^3} - 3\frac{(\boldsymbol{\chi}_{\alpha\alpha'} \cdot \boldsymbol{\mu}_\alpha)\,(\boldsymbol{\chi}_{\alpha\alpha'} \cdot \boldsymbol{\mu}_{\alpha'})}{|\boldsymbol{\chi}_{\alpha\alpha'}|^5} \right]\ , \quad (2.8)$$

[8] The size of interacting molecules must be much smaller than their intermolecular distance (i.e. the LR limiting case). Then, the SR orbital interaction as well as the variables $\mathbf{x}_\alpha$ and $\mathbf{x}_{\alpha'}$ can be conveniently neglected. The series expansion of $V_{\alpha\alpha'}$ in $(\boldsymbol{\chi}_\alpha - \boldsymbol{\chi}_{\alpha'})^{-1} = \boldsymbol{\chi}_{\alpha\alpha'}^{-1}$ then converges (van Amerongen et al., 2000). The first two expansion terms equals zero, hence, only the leading term (called first order dipole term) is taken (Sener et al., 2011, Appendix A).

where $\boldsymbol{\chi}_{\alpha\alpha'} = \boldsymbol{\chi}_\alpha - \boldsymbol{\chi}_{\alpha'}$, and the molecular dipole moment $\boldsymbol{\mu}$ is defined in (2.6). In fact, the equations (2.5-2.8) would describe only static interaction between the molecules. For the sake of describing EET dynamics, one has to adopt the transition charge densities and the transition dipole moments that express, as the name suggests, the transition from one electronic state of the molecule to another[9].

To sum up, the Coulombic interaction depends so far mainly on the structure and the charge distribution of the interacting molecules, and on their intermolecular distance. However, we have had to assume the molecules are well separated due to disregarding SR orbital overlaps, and due to using the multi-pole expansion and dipole approximation.

This approach is not convenient for many real cases but it is still used for its low computational cost. The main issue of the dipole approximation is that it completely disregards the shape of interacting molecules (Scholes et al., 2001). Much more sophisticated QCh methods need to be utilised for proper treatment. They are predominantly based on the transition densities calculated *ab initio* for each molecule separately (see Krueger et al., 1998). Commonly used methods for the calculation of Coulombic coupling are e.g. the *transition density cube* (TDC) method (Krueger et al., 1998) or the aforementioned *transition charge from electrostatic potential* (TrEsp) method (Madjet et al., 2006).

2.1.3 Concept of Molecular Exciton

The idea of delocalised electronic states—excitons—was first proposed in context of molecular crystals by Frenkel (1931). Hence, this type of excitons is traditionally called the *Frenkel exciton*[10]. The model was further developed by Davydov (1971)[11] and finally adopted for application in biological molecular aggregates by Kasha (1963); Kasha et al. (1965). In QM, the term delocalisation is closely related to the principle of superposition. Roughly speaking, quantum systems are not in any way restricted to a representation by a single state of a selected basis. The system can be in multiple such states at once. Schrödinger's dead/alive cat is probably the best known example. Additionally, another notable example of superposition (in this case from classical physics) is linearly polarised light, what is just superposition of two circular polarisations of the same amplitude, but contrary orientation. The principle of superposition is one of the most fundamental concepts in QM. It says that every normalised state is an eigenstate of a linear operator if it can be expressed as a linear combination of its orthonormal basis.

The formulation of exciton theory as a description of an aggregate of strongly interacting spatially separated molecules was triggered by experiments in spectroscopy. The strong molecular coupling has significant effect on the optical properties of such aggregate as it leads to splitting of the exciton energy levels compared to the ones observed on monomers, see Figure 2.2. This phenomenon was lately named *Davydov splitting* (Davydov, 1948, 2008, 1971; Braslavsky, 2007). The distribution of exciton excited energy levels always directly depends on the strength of intermolecular coupling $V_{\alpha\alpha'}$ and on the number of molecules engaged. Usually, the so-called red-shift of absorption spectrum is primarily observed. That is, strongly coupled chromophores absorb at longer wavelengths (Chenu and Scholes, 2015; Mirkovic et al., 2017). This feature is very meaningful in EET as it can ensure effective excitation energy funneling from higher-energy absorbing antennas to lower-energy absorbing RCs.

Let us assume that our system consists of N molecules considered as individual two-level systems. That is, each molecule can possess two electronic states only. Molecule α can be either in its electronic ground state $\psi_\alpha^{(g)}$, or in its excited state $\psi_\alpha^{(e)}$ (or their superposition). To put into perspective, the

[9] An elucidation of transition dipoles and their graphical visualisation offers Parson (2015), pp 132–137.

[10] Also called zero-radius exciton. Another type of exciton is the Wannier-Mott exciton, also called large-radius exciton. Here, the word *radius* refers to the co-localisation and molecular distance between an excited electron and a hole left after it.

[11] To clarify the time gap, the first edition was published in Russian in 1951, English translation then in 1962. The second extended edition, which is referred to here, was published directly in English in 1971.

excitation to the first excited state assumed here could correspond, for example, to the Q_y transition band of chlorophylls (van Grondelle and Novoderezhkin, 2009), see section 1.2. Now, we can write the so-called *collective states* in terms of the *Heitler-London approximation* (HLA) (Abramavicius et al., 2011). The collective ground state $|G\rangle$ is a product of all molecular ground states, and an excited state $|\beta\rangle$ is a product of $N-1$ molecular ground states and a single singly-excited state localised at the molecule β. As an example only, the double-excited collective state $|\beta\gamma\rangle$ is mentioned in (2.11) as well. Here, the *Dirac bra-ket notation*[12] is introduced.

$$|G\rangle = \prod_{\alpha}^{N} \psi_{\alpha}^{(g)}(\mathbf{r}, \mathbf{R}) \tag{2.9}$$

$$|\beta\rangle = \psi_{\beta}^{(e)}(\mathbf{r}, \mathbf{R}) \prod_{\alpha \neq \beta}^{N} \psi_{\alpha}^{(g)}(\mathbf{r}, \mathbf{R}) \tag{2.10}$$

$$|\beta\gamma\rangle = \psi_{\beta}^{(e)}(\mathbf{r}, \mathbf{R})\, \psi_{\gamma}^{(e)}(\mathbf{r}, \mathbf{R}) \prod_{\alpha \neq \beta,\gamma}^{N} \psi_{\alpha}^{(g)}(\mathbf{r}, \mathbf{R}) \tag{2.11}$$

It's worth mentioning that by adopting this *ansatz* for exciton states, we have to immediately presume the molecules are conveniently separated and direct electron exchange cannot occur. Otherwise, the ansatz would have to be much more complex to satisfy Pauli antisymmetry (exclusion) principle (König and Neugebauer, 2012). Although the HLA is mostly sufficient, it is not an universal tool. In some cases, corrections to the ansatz might be necessarily adopted (Agranovich and Basko, 2000).

The ground state $|G\rangle$ in (2.9) is unique, non-degenerate. On the other hand, the single excited state $|\beta\rangle$ can be described for each of N molecules. The aggregate single excited state $|\Phi\rangle$ can thus be a superposition of all possible site states $|\beta\rangle$ from (2.10) with weighing coefficients c_β such that $\sum_{\beta}^{N} |c_\beta|^2 = 1$.

$$|\Phi\rangle = \sum_{\beta}^{N} c_\beta\, |\beta\rangle \tag{2.12}$$

The square of coefficient c_β can be interpreted as a probability of finding the exciton in the particular state $|\beta\rangle$, as long as the state $|\Phi\rangle$ is normalised. However, there is not only one state $|\Phi\rangle$. Different coefficients c_β and their combinations can solve the TID SchrE. In fact, there is exactly N of such states that form a new complete orthonormal basis set of the system Hamiltonian, the so-called *energy basis*:

$$|\Phi_b\rangle = \sum_{b,\beta}^{N} c_{b\beta}\, |\beta\rangle \ , \tag{2.13}$$

$$\widehat{H}_{\mathrm{S}}\, |\Phi_b\rangle = \mathcal{E}_b\, |\Phi_b\rangle \ , \tag{2.14}$$

where coefficients $c_{b\beta}$ are now matrix elements of a unitary transformation matrix (Valkunas et al., 2018). The system Hamiltonian $\widehat{H}_{\mathrm{S}}$ from (2.14) must contain a contribution of every molecular Hamiltonian[13] $\widehat{H}_\alpha$, as well as every thinkable intermolecular interaction $\widehat{V}_{\alpha,\alpha'}$ as proposed in the previous subsection 2.1.2.

$$\widehat{H}_{\mathrm{S}} = \sum_{\alpha}^{N} \widehat{H}_\alpha + \sum_{\alpha \neq \alpha'}^{N} \widehat{V}_{\alpha\alpha'} \tag{2.15}$$

Solutions of Eq. (2.14), i.e. values of energies $\mathcal{E}_b$, always differ from the site-energies obtained by the so-called monomeric Hamiltonian $\widehat{H}_\alpha$ if the interaction terms are non-zero. The possible expectation values of the monomeric Hamiltonian are:

[12] Dirac notation consists of two basic elements. *Ket* $|\phi\rangle$ stands for an arbitrary wave function ϕ while *bra* $\langle\phi|$ is its complex conjugate ϕ^*. From mathematical point of view, both *bra*s and *ket*s are vectors. Hence, $\langle\phi|\phi\rangle$ denotes inner product (scalar) while $|\phi\rangle\langle\phi|$ is the outer product (matrix). See summarising description by Valkunas et al. (2013), pp. 56

[13] also called *site Hamiltonians* since each molecule of the aggregate sits on a rather stable site

$$\langle\beta|\widehat{H}_\alpha|\beta\rangle = \mathcal{E}_\alpha = \begin{cases} \mathcal{E}_\alpha^{(g)} \\ \mathcal{E}_\alpha^{(e)} \end{cases} \qquad (2.16)$$
$$\langle G|\widehat{H}_\alpha|G\rangle = \mathcal{E}_\alpha^{(g)}$$

The energy of a single molecule is meant when index α is used. The energy can be either $\mathcal{E}_\alpha^{(g)}$ for ground state or $\mathcal{E}_\alpha^{(e)}$ for excited state. Index β refers to the collective state (2.10), where only the βth molecule is excited. The energy of such a collective state $|\beta\rangle$ (in the site basis) is then $\mathcal{E}_\beta = \mathcal{E}_{\alpha=\beta}^{(e)} + \sum_{\alpha\neq\beta}^{N} \mathcal{E}_\alpha^{(g)}$. And finally, the true observable energies and corresponding optical transitions also include the intermolecular interactions $V_{\alpha\alpha'}$, they belong to the superposition states $|\Phi_b\rangle$, and are noted $\mathcal{E}_b$ as in (2.14).

The extent of exciton energy level shift depends on the strength of intermolecular coupling $V_{\alpha\alpha'}$, on the number of interacting molecules N, and on the dispersion of site-energies of the interacting molecules $\mathcal{E}_\alpha^{(e)}$. The latter predominantly applies in the case of different chemical identity and structure of the molecules. However, site-energy tuning by the environment also definitely takes place here.

The mentioned discrepancy also reflects the delocalisation of such aggregate states. A very simple approach is frequently used for quantifying the delocalisation based on the coefficients $c_{b\beta}$. Since the superposed states are normalised, the sum of coefficients fourth power $\sum_\beta^N |c_{b\beta}|^4$ denotes the *inverse participation ratio* (IPR) straightforwardly. IPR value varies from $1/N$ in case of completely delocalised state, up to one for purely localised state (Bell and Dean, 1970; Thouless, 1974; Fassioli et al., 2014). Also, its inverse power describes the length of delocalisation in units of molecules (Scholes, 2020). However, its applicability in the field of open quantum system (OQS) is disputable (Jang, 2020) as it cannot reflect the effects of the environment, e.g. decoherence (see subsection 2.1.5). Better methods, which overcome this issues, were already developed (Fassioli et al., 2014).

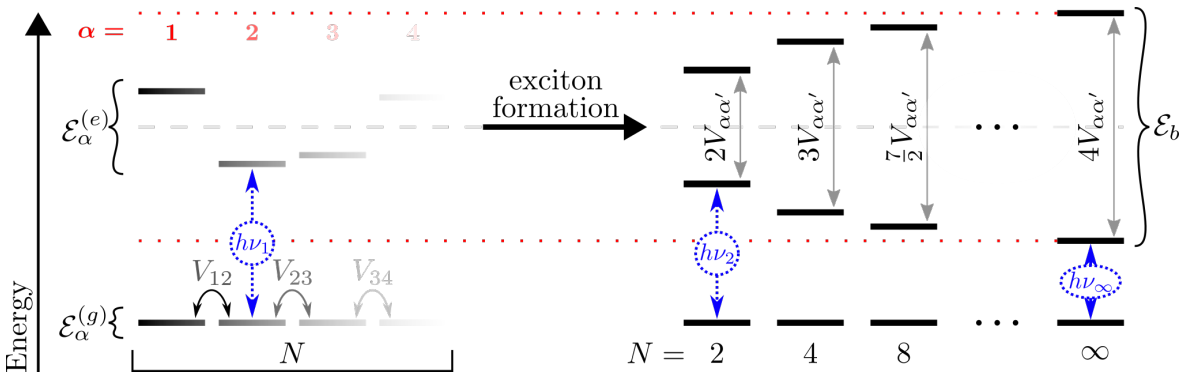

Figure 2.2: Thorough illustration of molecular energy levels giving origin to an exciton.
Left side: individual monomeric energy levels in the basis of localised states (i.e. solution of SchrE (2.16)). α runs from 1 to N labeling the participating molecules. Terms $V_{\alpha\alpha'}$ stands for intermolecular interaction (coupling). Unlike the simplified situation on the picture, every molecule is interacting with each of the others. Here, every molecule is depicted with different site-energies. That corresponds to reality in PPC. By the way, diluted solution of identical molecules would have these energies always identical.
Right side: simplified depiction of excitonic energy levels in the basis of delocalised superposed exciton basis where only the lowest and the highest non-degenerate energy levels are pictured. In reality, many more intermediate and usually degenerated levels are present in-between these two limiting single-excitonic states. Every column here accounts for different number of molecules participating in the exciton ($N = 2, 4, 8, ...$). An progressive increase of energy gap between the split lines can be observed as the size of exciton enlarges. The limit approaches equivalent of $4V_{\alpha\alpha'}$ as $N \to \infty$ (Scholes, 2020). The marked boundary is highlighted by two red dotted lines. The splitting is always symmetric, centered around the average value of monomeric excited energy levels (grey dashed line). Examples of a few possible electronic transitions resulted from external excitation are depicted in blue. The phenomenon of red-shift, caused by the formation of delocalised excitonic states, can be observed as well ($h\nu_1 > h\nu_2 > h\nu_\infty$).
Image is based on Renger and Holzwarth (2008, pp 428), Valkunas et al. (2013, pp 110), Valkunas et al. (2018, pp 257), and on data of Scholes (2020).

A notable example from photosynthesis where the effects of multimolecular exciton aggregate takes exceptional place is the light-harvesting antenna complex LH2 of purple photosynthetic bacteria (see section 3.2).

2.1.4 Description of Molecular Aggregate Hamiltonian

LHC is regarded as an OQS. That means our quantum system of main interest—chromophores—is surrounded by the so-called 'bath'—the environment consisting of the protein scaffold, molecules of solvent, membrane lipids, etc. The bath is a very dynamic system rich in molecular movements, vibrations, and includes many excitable electrons. The immense number of DOF typical for the bath makes it truly impossible to treat its interaction with the electronic states of our system analytically. However, such system can be often satisfactory approximated as an aggregate of infinite number of one-dimensional linear harmonic oscillators (LHOs). LHO is a very well described physical model with infinite number of equidistant energy levels. Unfortunately, even such model cannot be solved exactly. More physically motivated approximations and assumptions have to be made for the sake of formulating a solvable problem.

Here, one of many possible approaches to total Hamiltonian description is presented (e.g. Yang and Fleming, 2002; Cheng and Fleming, 2009; Hwang-Fu et al., 2015). It was chosen in the context of subsequently discussed methods. The general approach is essentially always the same although some significant theory-specific characteristics can be present (see section 2.2).

Let's assume that the studied molecular aggregate consists of two distinct parts. The chromophores, which directly participate in excitation energy transfer (EET), and the environment[14], which represents the protein scaffold and nearby molecules of the solvent. Energy of these two parts is described by two different Hamiltonians; $\widehat{H}_{\mathrm{S}}$ and $\widehat{H}_{\mathrm{B}}$ respectively[15]. However, the interaction Hamiltonian $\widehat{H}_{\mathrm{S\text{-}B}}$ of these two independent spaces must be present as well. The word 'space' is meant literally in this case. For the sake of correct mathematical description, operators $\widehat{H}_{\mathrm{S}}$ and $\widehat{H}_{\mathrm{B}}$ each exists on two distinct Hilbert spaces $\mathcal{H}_{\mathrm{S}}$ and $\mathcal{H}_{\mathrm{B}}$. The interaction Hamiltonian $\widehat{H}_{\mathrm{S\text{-}B}}$ must then exist on a *tensor product*[16] of both, i.e. $\widehat{H}_{\mathrm{S\text{-}B}} \in \mathcal{H}_{\mathrm{S}} \otimes \mathcal{H}_{\mathrm{B}}$. The total Hamiltonian of the problem reads as:

$$\widehat{H} = \widehat{H}_{\mathrm{S}} + \widehat{H}_{\mathrm{B}} + \widehat{H}_{\mathrm{S\text{-}B}} \,. \tag{2.17}$$

The $\widehat{H}_{\mathrm{B}}$ and $\widehat{H}_{\mathrm{S}}$ can be also expressed in matrix representation[17]. Energies $\mathcal{E}$ then form the diagonal elements of the system Hamiltonian $\widehat{H}$ while the interaction terms V are off-diagonal.

$$\widehat{H}_{\mathrm{S}} = \mathcal{E}_G \left|G\right\rangle\!\left\langle G\right| + \sum_{\beta=1}^{N} \mathcal{E}_\beta \left|\beta\right\rangle\!\left\langle\beta\right| + \sum_{\beta\neq\beta'}^{N} V_{\beta\beta'} \left|\beta\right\rangle\!\left\langle\beta'\right| \,. \tag{2.18}$$

The system Hamiltonian of this form is referred to as a *Frenkel exciton Hamiltonian* (Fassioli et al., 2014). Collective states $|G\rangle$ and $|\beta\rangle$ are defined in Eqs. (2.9) and (2.10). $V_{\beta\beta'}$ is an interaction term between two collective states. We can shift the energy in such a way that the energy $\mathcal{E}_G$ of the total ground state $|G\rangle$ will be zero. The new energies $\mathcal{E}'_\beta = \mathcal{E}_\beta - \mathcal{E}_G$ are then referred to as *site-energies* or *Franck-Condon transition energies* (Ishizaki and Fleming, 2012) since they directly correspond to the energy necessary to excite the βth molecule of the exciton. Consequentially, the first term on the r.h.s. of (2.18) vanishes.

The bath is usually considered as an infinite set of LHOs interacting with each chromophore of the system linearly and independently of each other. The bath is presented in many different ways in

[14] The environment (bath) is considered as *open* (in thermodynamic manner) since its size is so vast that any absorbed energy diminish quickly and the overall bath state don't change on a reasonable timescale.

[15] standard notation is used, 'S' in $\widehat{H}_{\mathrm{S}}$ stands for 'system', 'B' in $\widehat{H}_{\mathrm{B}}$ stands for 'bath'

[16] also called *direct product*

[17] A detailed explanation of the operator matrix representation, and many more topics, can be found in Appendix of Cogdell et al. (2006).

literature, using different field-specific nomenclature. From physics of condensed matter and crystal lattices, for example, the term *phonon* is frequently used. Phonon is in fact an auxiliary artificial analogue of photon. In the same way as photon is a quantum of electromagnetic wave, phonon is a quantum of vibration, either atomic or molecular. The bath Hamiltonian $\widehat{H}_{\mathrm{B}}$ can be expressed as:

$$\widehat{H}_{\mathrm{B}} = \sum_{\alpha=1}^{N} \left(\sum_{k=1}^{\infty} \frac{\widehat{p}_k^2}{2m_k} + \frac{m_k \omega_k^2}{2} \widehat{q}_k^2 \right)_{\alpha} = \sum_{\alpha=1}^{N} \sum_{k=1}^{\infty} \hbar \omega_{\alpha k} \left(n_{\alpha k} + \frac{1}{2} \right) , \tag{2.19}$$

where $\widehat{p}_k$, $\widehat{q}_k$, m_k, and ω_k are the canonical momenta, canonical position, mass, and oscillation frequency of kth vibrational mode, in corresponding order. The vibrational levels (phonons) of each mode are labeled by $n_{\alpha k}$ which run from zero to infinity. Everything is then summed over all N molecules of the system. Despite the vibrational modes are quantised, and they can be expressed also in terms of the *creation* and *annihilation* operators, it is also feasible to write them as a real continuous function (due to the great assumed number of them), the *spectral density* (*function*) (here abbreviated as SD) $J(\omega)$ (Jang, 2020). The SD is time-independent and it should be thus perceived as a persisting pool of bath thermal noise. Various standard SDs are defined and used for different models of the bath, e.g. the Brownian SD, or the Drude SD (see Mukamel, 1995). Since the SD directly influence e.g. the decoherence rate (to be mentioned in subsection 2.1.5), the choose of SD should be done with care and better based on experimental data (Kreisbeck and Kramer, 2012). The interaction Hamiltonian $\widehat{H}_{\text{S-B}}$ combines both the system ($\widehat{d}_k$) and the bath ($\widehat{q}_k$) variables:

$$\widehat{H}_{\text{S-B}} = \sum_{\beta=1}^{N} \left(\sum_{k=1}^{\infty} \gamma_k \widehat{q}_k \widehat{d}_k \right)_{\beta} |\beta\rangle\langle\beta| , \tag{2.20}$$

where $\widehat{d}_k$ is an operator of chromophore position displacement from its equilibrium, and γ_k is a coefficient of the interaction strength. Other notation corresponds to the (2.19). As can be seen, $\widehat{H}_{\text{S-B}}$ is a diagonal matrix similar to the second term of (2.18). The S-B interaction thus only causes fluctuations to the site-energies of our system. In a couple of manipulations the $\widehat{H}_{\text{S-B}}$ can be redistributed to the other terms of the total Hamiltonian. Namely, the interaction causes a shift in coordinates $\widehat{q}_k$ of the harmonic bath, and additionally a new term appears—the reorganisation energy λ_{r} (see Figure 2.1 on page 9). It has a constant value for each molecule of the system can be thus implemented to the molecular potential Hamiltonians. If the bath is described by the SD $J(\omega)$, the overall reorganisation energy is related to its integral $\lambda_{\mathrm{r}} = \pi^{-1} \int_0^{\infty} \frac{J(\omega)}{\omega} \mathrm{d}\omega$ (Mukamel, 1995; Jang, 2020).

There is one more important entity which governs all the mentioned—the *bath correlation function* (bCRF) $C(\tau)$. It is time-dependent and describes how the environment is influencing the system between two time points (see May and Kühn, 2011). The bCRF can be calculated for a particular SD accordingly (Mukamel, 1995):

$$C(\tau) = \int_{-\infty}^{\infty} \left(\coth \left(\frac{\hbar\omega}{2k_{\mathrm{B}}T} \right) \cos(\omega\tau) - \mathrm{i} \sin(\omega\tau) \right) \mathrm{d}\omega . \tag{2.21}$$

The bCRF originates in statistical physics and for our purposes can be generally expressed as:

$$C_{uv}(\tau) = \frac{1}{\hbar^2} \mathrm{Tr}_{\mathrm{B}} \left\{ \widehat{U}_u(\tau)\, \widehat{U}_v(0)\, w_{EQ} \right\} , \tag{2.22}$$

where $\widehat{U}_u(0)$ and $\widehat{U}_v(\tau)$ are general operators expressing the fluctuations of bath included in $\widehat{H}_{\text{S-B}}$ in two time points, and w_{EQ} is the equilibrium bath state. The bCRF is also related to the so-called *line-shape function* $g(\tau'') = \int_0^{\tau''} \mathrm{d}\tau' \int_0^{\tau'} \mathrm{d}\tau\, C(\tau)$, which describes the absorption spectrum shape.

2.1.5 Meaning of Coherence

Hereinafter, the term *coherence* will be occurring quite frequently. Before this starts happening, an attempt to decipher its meaning—on which there is unfortunately only a limited consensus (Cao

et al., 2020)—will be made here. The word *coherence* is slowly meeting a similar destiny in the field of physics as the word *quantum* in pop-culture. Both are tremendously overused and often adopted out of their original context causing a great deal of confusion. The forthcoming overview is mainly based on Kassal et al. (2013), Chenu and Scholes (2015), and Rathbone et al. (2018a,b).

The main source of necessary experimental data about EET and also about the coherent processes during photosynthesis is the ultra-fast laser 2D electronic spectroscopy (2DES). Comprehensive theoretical introduction into multidimensional spectroscopy offers Hamm (2005), Gelzinis et al. (2019), Li and Cundiff (2017), and Schlau-Cohen et al. (2011). Advanced insight can provided by the all-embracing book of Mukamel (1995), and also articles of Cho (2009) and Abramavicius et al. (2009).

The term *coherence* generally expresses the property of a collective or in-phase behaviour. Detailed definition is highly field-specific, though. What is important, the term is used in both classical and quantum physics.

In classical physics, it is used in the context of fluctuating fields (e.g. electric or magnetic field) and it describes either spatial, temporal, or spectral correlation. For example, in the famous Young's double-slit experiment (see Björn, 2015), the maxima of interference pattern appear at points (spatial coherence), where the electromagnetic waves, which originated in one source (spectral coherence) but propagate from two different sites, are constructively correlated, i.e. coherent.

In quantum physics the term has even more meanings. Before describing them, let us introduce one more important entity, the *density matrix* $\widehat{\rho}$, alternatively called *density operator*. The density matrix is a tool for describing the studied system in an exhaustive, albeit simple way. The formalism of density operator is especially useful in the cases which involve superposition of states since it is defined as a sum of all outer products of all states weighed by probability of their realisation. For example, in case of our previously introduced exciton (Equation 2.9–2.12), we have actually two levels of superposition. Firstly, the exciton state $|\Phi_b\rangle$ is a superposition of different collective states $|\beta\rangle$. Secondly, there are N possible states $|\Phi_b\rangle$ which are linked with various probabilities of realisation p_b what can also result in a regular state $|\Xi\rangle$. The density operator would look like accordingly with a sum of N terms occupying each element of $N\times N$ dimensional matrix:

$$\widehat{\rho} = |\Xi\rangle\langle\Xi| = \sum_{bb'}^{N} p_b p_{b'}^{*} \, |\Phi_b\rangle\langle\Phi_{b'}| = \sum_{b\beta}^{N}\sum_{b'\beta'}^{N} p_b p_{b'}^{*} c_{b\beta} c_{b'\beta'}^{*} \, |\beta\rangle\langle\beta'| \ . \tag{2.23}$$

The total system state is represented by $|\Xi\rangle$; star in superscript denotes complex conjugate. The diagonal terms ($\beta{=}\beta'$) of such matrix representation are called *site populations* since they straightforwardly represent the probability of finding the corresponding molecule excited. The off-diagonal matrix elements ($\beta{\neq}\beta'$) may then be called *coherences*, or to be more precise, *state coherences*, as will be clarified soon after. In addition, only these off-diagonal terms can evolve in time and stand behind the oscillating spectroscopic signals. More details about density operators can be found in (Valkunas et al., 2013, pp 61–64).

Three meanings of coherence are differentiated by QM. (i) *Coherent states* are firmly defined in quantum optics; (ii) *state coherence* arises from superposition of states and their interference; (iii) the term *process coherence* is then used in context of EET mechanisms.

i *Coherent state* in context of quantum optics is, roughly speaking, an eigenstate of photonic annihilation operator (besides vacuum state). This interpretation is not found in EET-related literature very often and would not be matter of the discussion in this essay.

ii *State coherence* or *steady state coherence* (Mančal, 2013) was already introduced in equation (2.23) and in the paragraph below. The issue of such definition stems from the nature of matrices; they can be expressed equivalently in different bases. Such manipulation does not

influence the carried information but it doubtless changes the values of matrix elements. Only the off-diagonal matrix elements in the site basis representation—in our case that corresponds to the states $|\beta\rangle$—should be called coherences.

iii *Process coherence* is directly related to the EET and it describes the regime in which it proceeds. There are two pertinent contrary phenomena—dissipative relaxation and unitary evolution. The former is caused by strong coupling with the bath and results in fast decay of any oscillations, i.e. the off-diagonal elements evolving in time. On the other hand, the unitary evolution stems from the strong intermolecular coupling so in case of total system isolation from the environment the energy and the oscillations would be preserved till the relaxation by fluorescence. So the excitation energy would not be effectively transferred anywhere. The first case (limit of $\lambda_{\mathrm{r}}^{\alpha} \gg V_{\alpha\alpha'}$) leads to Förster incoherent transfer (see section 2.2). However, the coherent transfer, which involves both the oscillations and the bath-induced damping, corresponds to the situation in-between the two phenomena ($\lambda_{\mathrm{r}}^{\alpha} \approx V_{\alpha\alpha'}$) (see Mirkovic et al., 2017, pp 75). This intermediate regime reaches the effectively highest transfer rates (Plenio and Huelga, 2008; Caruso et al., 2009; Rebentrost et al., 2009; Mohseni et al., 2008, 2014).

These definitions are not, however, preserved by the authors very often, and occasional confusion is thus imminent. Two more terms worth mentioning are related to the quantum coherence as a whole. Quantum coherence is generally considered as fragile since the noisy environment and vibrational movement of surrounding particles easily causes its decay—the so-called *decoherence*[18]. Sometimes the term *dephasing* is used interchangeably but, in fact, they have two different meanings (May and Kühn, 2011; Scholes et al., 2017). The time of coherence survival is then called the *coherence life-time*. The apparent temperature dependence of coherence life-time was inspected by Panitchayangkoon et al. (2010).

Probably the most provocative but nonetheless influential article about quantum coherence in photosynthesis was published in 2007. Engel et al. detected surprisingly long-lasting[19] oscillations—identified with the state coherences evolving in time—in 2DES spectrum of FMO complex of green sulphur bacteria. This observation of quantum effects actually manifesting in living cells[20] for a considerable amount of time brought very much attention to the topic. Regardless of the fact that a similar article was already published ten years before (Savikhin et al., 1997). Since then, similar results were obtained from measurements of, for example, pbRC of *Rhodobacter sphaeroides* (Lee et al., 2007) or LHCII of *Arabidopsis thaliana* (Calhoun et al., 2009). Complexes of phycocyanin and phycoerythrin of various marine cryptophytes were scrutinised too, even at ambient temperature (Collini et al., 2010; Turner et al., 2012; Wong et al., 2012). The presence of oscillations have instantly become suspected of the high efficiency of the energy transfer in photosynthesis. Moreover, the function of coherence as a trait in terms of the natural selection and evolution have also been discussed.

The critics of these conclusions mostly point out the relevance of these measurements since the values depend on the basis set we use for the matrix representation. Besides, even though the coherence life-times would actually reach the timescale on which the EET between molecules is occurring, as the authors suggest, the timescale of the EET limiting steps still surpass these values by a factor of more than 50, and the subsequent electron transfer even by a factor of about 1 000 (see subsection 3.2.2).

Unfortunately, the space limitation here doesn't allow us to develop this incredibly captivating topic any further. Just to sum up, any consensus or unified point of view have not been reached yet. New supporting as well as dismissing articles are still frequently published in prestigious peer-reviewed

[18]The strength of influence is characterised by *rate of decoherence* γ $[time^{-1}]$. Two contributing terms can be distinguished—*relaxation rate* γ_{r} and *pure dephasing rate* γ_{d}: $\gamma = \gamma_{\mathrm{r}}/2 + \gamma_{\mathrm{d}}$ (May and Kühn, 2011)

[19]Their life-time was comparable with the energy transfer rates.

[20]However, this first experiment was performed at not-that-physiological temperature of 77 K.

journals. On the one hand, there are experimental results presenting the long-lasting quantum beats. On the other hand, number of theorists are providing a reasonable explanation for these observations, without employing quantum effects into such a questionable extent (e.g. see Paleček et al., 2017; Duan et al., 2016). The critical points of the theory were recently summarised by Cao et al. (2020).

2.2 Theoretical Descriptions of Excitation Energy Transfer

The energy transfer can be classified in terms of several viewpoints. Fairly important is the chemical identity of interacting chromophores. The molecules can be either the same (homotransfer) or different (heterotransfer). This aspect has an influence on the energy funneling, the rate of transfer, and the coupling strength. Another important feature is the mechanism of transfer itself. In general, the energy can be either transmitted indirectly via 'real photons' (radiative transfer), or directly without any occurrence of emission or absorption (nonradiative transfer)[21]. In LHCs, only the nonradiative way is known and it contributes to the exceptional transfer efficiency. The quantum efficiency of nonradiative EET can reach even unity what is far from the radiative as the wavevector of emitted light can point any direction (Olaya-Castro and Scholes, 2011). The differentiation between radiative/nonradiative transfer is widely accepted and used although Andrews (1989) and Andrews and Bradshaw (2004) have shown that both are just manifestation of a single QED phenomenon.

Strength of intermolecular coupling is another crucial factor aforementioned in subsection 2.1.2. Specifically, it is necessary to compare the coupling strength between chromophores ($V_{\alpha\alpha'}$) with the coupling to the bath (reorganisation energy $\lambda_{\mathrm{r}}^{\alpha}$).

Three separate categories of couplings, EET regimes, and pertinent standard theoretical approaches can be distinguished. The Förster-type theory (see next subsection 2.2.1) describes limiting case of *weak intermolecular coupling* (the interaction between chromophores is much weaker than the interaction with bath, $\lambda_{\mathrm{r}}^{\alpha} \gg V_{\alpha\alpha'}$) resulting in localised states. The energy transfer is then described as incoherent 'hopping' between individual molecules. On the contrary, the Redfield-type theory (see subsection 2.2.2) is used for the limit of *strong intermolecular coupling* (the interaction between chromophores is much stronger than the one with bath, $\lambda_{\mathrm{r}}^{\alpha} \ll V_{\alpha\alpha'}$) causing delocalised excitonic states. The energy transfer in space thus resembles a spreading of a wave[22] over the coupled molecules, superposing various electronic states. Both approaches usually lead to approximate (second-order) perturbation theory in either of the small coupling parameters.

However, the natural processes do not tend to our idealised limiting cases very often. In fact, the both kinds of coupling can be comparable in strength (i.e. $\lambda_{\mathrm{r}}^{\alpha} \approx V_{\alpha\alpha'}$). The term *intermediate coupling* is used in that case. Necessarily much more involved theoretical methods need to be adopted then. They can either arise as a variation on the limiting-case treatments (e.g. modified Redfield theory) or as a brand-new non-perturbative one. Recently, the most popular methodologies are the so-called hierarchical equations of motion (see subsection 2.2.3), the density matrix renormalisation method (Chin et al., 2010; Prior et al., 2010), and many techniques based on Feynman's integration over path (Feynman, 1948), e.g. QUAPI—*quasi-adiabatic propagator path integral* (Makarov and Makri, 1994; Makri and Makarov, 1995a,b).

Another alternative comparative parameters are sometimes used. The excitation *transfer time* $\tau_{\mathrm{trans}}^{\alpha\alpha'}$ can be conveniently introduced instead of the $V_{\alpha\alpha'}$. Its counterpart is the *intramolecular vibrational relaxation time* $\tau_{\mathrm{rel}}^{\alpha}$ which expresses the time necessary to reestablish equilibrium after the excitation (see Figure 2.1). Although this notation currently dominates in the literature, the former formalism will be preferred here since it's more related to the discussed topics.

[21] term 'virtual photons' is sometimes used in this context
[22] The correct term is quantum mechanical wave-packet.

2.2.1 Förster Resonance Energy Transfer (FRET)

Förster resonance energy transfer (FRET)[23] is probably the best known theory of nonradiative energy transfer, which found an irreplaceable utilisation in a variety of fields of chemistry and biology. It was firstly derived by Förster (1946, 1948)[24] who studied molecular absorption and emission spectra alongside with phenomenon of concentration depolarisation and quenching. The complete history and evolution of Förster theory was mapped by Clegg (2006).

The original theory describes the interaction of two weakly-coupled molecules which are regarded as transition dipole moments. The condition of weak-coupling enables us to describe the interaction as only a small perturbation of the stationary-state Hamiltonian. Besides, the weak-coupling results in strictly localised excitation which propagates by 'hopping' within individual pairs of chromophores[25]. The two molecules are usually referred to as a *donor* (D) and an *acceptor* (A). Let D^* and A^* denote excited states of the molecules. The notation of FRET with transfer rate $k_{D\to A}$ can be then boiled down to:

$$|D^*A\rangle \xrightarrow{k_{D\to A}} |DA^*\rangle \tag{2.24}$$

The theory itself poses many restrictions for its validity as a result of making several approximations. Firstly, only Coulombic intermolecular interactions are considered so the molecules have to be spatially well separated (see subsection 2.1.2), at least 10 Å apart (van der Meer et al., 1994; van der Meer, 2013). Secondly, the theory might operate within the *point-dipole* and *dipole-dipole* approximation what poses even stricter demands on relative dimensions[26]. The diameter of the molecules has to be much smaller (according to Parson (2015) at least four or five times) compared to the intermolecular distance. Thirdly, the leading term of Förster rate (2.26) decreases with sixth power of intermolecular distance and thus effectively vanishes beyond ca 100 Å (van der Meer et al., 1994; van der Meer, 2013).

Another restrictive condition of the theory is referenced literally in its name—resonance. That is to say, the energy of electronic transition of the donor from its excited state to the ground state (ΔE_{DD^*}) has to be the same (i.e. in resonance) as the energy gap between ground and excited state of the acceptor (ΔE_{AA^*}). This condition can be expressed mathematically in terms of Dirac delta function $\delta(\Delta E_{AA^*} - \Delta E_{DD^*})$. The relaxation of donor and the excitation of acceptor occurs simultaneously without mediation by a photon. The energy exchange is also essentially conditioned by the *spectral overlap*. That is to say, the donor emission spectrum has to overlap the acceptor absorption spectrum.

The TD perturbative treatment of donor-acceptor pair (for comprehensive derivation and description see van der Meer, 2013; Parson, 2015; Govorov et al., 2016) leads to the *Fermi's Golden Rule* (see List of Notable Equations) which was already proposed before Förster by Dirac (1927). Fermi's Golden Rule (FGR) describes electronic transition rates caused by the perturbative Hamiltonian in atoms and molecules. In case of the original FRET, the Coulombic interaction in dipole-dipole approximation accounts for the perturbation:

$$V_{DA} = \frac{f^2}{n^2}\left(\frac{\boldsymbol{\mu}_D \cdot \boldsymbol{\mu}_A}{|\mathbf{R}_{DA}|^3} - \frac{3(\boldsymbol{\mu}_D \cdot \mathbf{R}_{DA})(\boldsymbol{\mu}_A \cdot \mathbf{R}_{DA})}{|\mathbf{R}_{DA}|^5}\right), \tag{2.25}$$

[23] The term 'FRET' is still sometimes referred to as an acronym of *fluorescence (resonance) energy transfer*. However, this interpretation is incorrect (Braslavsky, 2007; Braslavsky et al., 2008; van der Meer et al., 1994; Masters, 2014) since fluorescence is clearly a radiative process. In contrast, the resonance energy transfer is strictly nonradiative. Doubtlessly, the fluorescence-involving experiments had uppermost importance in derivation of FRET as they offered the necessary data. And after the theory was published, it has found even larger application in this experimental field. Nonetheless, the resonance energy transfer itself is completely independent of the process of fluorescence, and the occasional misnomer should be avoided.

[24] For english translations see Förster (2012, 1993), respectively.

[25] FRET thus belongs to the so-called *incoherent rate equation approaches* (May and Kühn, 2011)

[26] This is the case of the original formulation only. However, FRET can be also used with the exact QCh calculations of intermolecular couplings and thus some of the restrictions can be avoided.

where $\boldsymbol{\mu}_D$ and $\boldsymbol{\mu}_A$ are transition dipole moments belonging to the molecules of donor and acceptor, respectively. Here, $\mathbf{R}_{DA}$ denotes the vector from the centre of donor to the centre of acceptor. The prefactor $\frac{f^2}{n^2}$ stands approximately for the local screening effects caused by the environment with refraction index n. Screening effects, and influence of surrounding proteins on EET in general, were scrutinised by Scholes et al. (2007). After proper treatment of units (see van der Meer, 2013; Parson, 2015) we obtain in few steps the Förster formula for transfer rate per unit of time[27]:

$$k_{D\to A} = \frac{1}{\tau_D} \cdot \left(\frac{R_0}{|\mathbf{R}_{DA}|} \right)^6 ; \qquad R_0^6 = \frac{9,000\,(\ln 10)\,\kappa^2\,\phi_D\,I}{128\,\pi^5\,N_A\,n^4} ; \tag{2.26}$$

$$I = \int_0^\infty f_D(\lambda)\epsilon_A(\lambda)\lambda^4\,\mathrm{d}\lambda\,; \qquad \kappa = \cos\theta - 3\cos\alpha\cos\beta \tag{2.27}$$

τ_D and ϕ_D are the lifetime and the fluorescence quantum yield of the donor excited state in absence of other molecules, respectively. N_A is the number of molecules in one mole (i.e. Avogadro's number), n is the averaged refractive index of the surrounding environment for the spectral overlap interval. I is the overlap integral of donor emission spectrum $f_D(\lambda)$ and acceptor absorption spectrum $\epsilon_A(\lambda)$. κ is the so-called orientation factor. It expresses the mutual orientation of donor and acceptor transition dipole moments by angles θ, α, and β (see equation (2.27) and Figure 2.3). Its value can vary from -2 to 2 only; the square than between 0 and 4. R_0 is called *Förster radius* and corresponds to a distance from the donor where the probability of excited state relaxation (e.g. by radiative fluorescence) is the same as the probability of resonance energy transfer to the molecule of acceptor in that distance (van der Meer, 2013). That is to say, $k_{D\to A} = 0.5$ (Masters, 2014; Parson, 2015). If the spectral overlap is expressed in units of $\mathrm{mol}^{-1}\cdot\mathrm{dm}^3\cdot\mathrm{cm}^3$, the Förster radius would be in centimeters.

One might conclude that the application of FRET is very limited in terms of LHCs since the chromophores are often closer than 10 Å and the coupling is not strictly weak. This is true only partially. Obviously, FRET cannot be conveniently applied on tightly packed molecules. However, the Förster theory can be generalised from a pair of interacting molecules to a pair of interacting molecular aggregates. Both aggregates can consist of many strongly coupled molecules, but as far as the interaction between them is weak, the *Generalised Förster theory*[28] holds (Renger and Holzwarth,

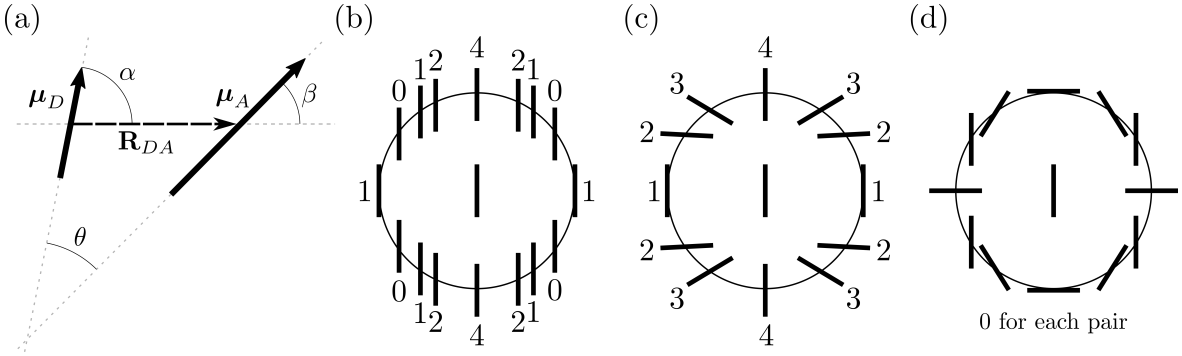

Figure 2.3: Schematic depiction of the orientation factor κ^2. (a) Scheme of the donor-acceptor pair with the notation used in equation (2.27). $\boldsymbol{\mu}_D$ and $\boldsymbol{\mu}_A$ stands for the transition dipole moments, $\mathbf{R}_{DA}$ is vector connecting centres of both molecules. Adapted from Parson (2015, pp 331). (b, c, d) Images showing different values of κ^2 as they depends on the relative position and orientation of transition dipoles moments of the donor (in the middle of circles) and the acceptor (around the circle). Since κ^2 doesn't depend on the relative direction (plus/minus orientation) of transition moments, the depicted vectors lack arrowheads. Adapted from van der Meer et al. (2013, pp 68).

[27] Braslavsky et al. (2008) pointed out several difficulties which accompany the Förster formula. The first Förster publications weren't free of typos and misprints, e.g. π^6 instead of correct π^5. Besides, Förster preference of using millimoles for expressing Avogadro constant, which traditionally references moles, also caused much confusion. Unfortunately, these original articles have obviously become the most frequently cited so the misunderstandings are spreading throughout literature ever since. Förster himself have corrected his formulas in his later papers (e.g. Förster, 1967) but it did not save the situation at all. However, the factor of 1 000, whose presence also varies within the literature, is only maintaining correct units introduced to the formula by the spectral overlap I.

[28] also referred to as *Multichromophoric Förster Resonance Transfer* (MC-FRET) (Jang et al., 2004; Bondarenko et al., 2020), what is, in fact, just a special case of the generalisation (see Mohseni et al., 2014)

2008). This is exactly the case of many pigment-protein complexes (PPCs) where the protein scaffold maintains the proper separation (Sumi, 1999; Mukai et al., 1999; Scholes and Fleming, 2000; Jang et al., 2004). Thorough review and derivation of various generalisations of Förster theory was made by Mohseni et al. (2014); their application are also being discussed.

To sum up, FRET was a breakthrough in chemical physics. It successfully shed light on several optical processes, and enabled further development of both the theory and the experimental approaches (van der Meer, 2013). However, it has many limitations, especially regarding the spatial dimensions of the system. On the one hand, the intermolecular distance between donor and acceptor cannot be shorter than ca 10 Å as orbital overlap and Dexter mechanism of EET could occur. And on the other hand, the transfer rate decreases rapidly with the sixth power of the distance and thus effectively vanishes beyond several dozens of ångströms. Beyond this range, other effects predominate and the Förster theory does not hold. And for last but not least, the intermolecular interaction has to be much weaker than with the bath. Nonetheless, FRET theory is still very popular, and it is often applied even to systems which meet the above mentioned conditions rather questionably (Valkunas et al., 2013)[29].

2.2.2 Redfield Theory

The so-called *standard Redfield theory* (SRT) was derived for the sake of describing dynamics in the limit of weak chromophore-bath coupling (Redfield, 1957, 1965). Originally, it found implementation in nuclear magnetic resonance spectroscopy (NMR), but it was readily adopted by condensed matter physicist, chemical physicist, and finally by biophysicist. Generally speaking, the theory can be applied on all OQS systems that display delocalisation of electronic states as a result of strong intermolecular coupling, i.e. excitons (see subsection 2.1.3). As long as the system-environment coupling strength is weak ($\lambda_{\mathrm{r}}^{\alpha} \ll V_{\alpha\alpha'}$), it can be treated with the perturbation theory. Redfield theory thus belongs to approximate methods alongside with FRET.

The Redfield's approach is based on the (reduced) density operator formalism which was already briefly introduced in subsection 2.1.5. Since the environment is considered as a large system, and its interaction with chromophores as weak, we can assume that the initial bath thermal equilibrium will not change during the examined period of time. Only the states of the chromophores will evolve in response to the excitation. The form of total density operator is written below. Pursuing this notation, the system density operator $\widehat{\rho}_{\mathrm{S}}(t)$ can be obtained from the total density operator $\widehat{W}(t)$ by averaging out the irrelevant[30] bath DOF represented by $\widehat{\rho}_{\mathrm{B}}$ (i.e. tracing them out):

$$\widehat{W}(t) = \widehat{\rho}_{\mathrm{S}}(t) \otimes \widehat{\rho}_{\mathrm{B}} \,; \qquad \widehat{\rho}_{\mathrm{S}}(t) = \mathrm{Tr}_{\mathrm{B}}(\widehat{W}(t)) \,; \tag{2.28}$$

where Tr_{B} is the *partial trace* over the bath (see List of Physical Constants and Used Notations). Hence, the system density operator $\widehat{\rho}_{\mathrm{S}}(t)$ is called the *reduced density operator* (RDO). Just to clarify, although the partial trace effectively eliminates the description of bath from our equation, the obtained system part remains affected by the bath.

Time evolution of the total density operator is generally described by Liouville-von Neumann equation, which is equivalent to the TD SchrE. For the RDO, the so-called *quantum master equation* can be systematically derived. First, by adopting the Liouville's superoperator $\widehat{\mathfrak{L}}$ notation (see List of Physical Constants and Used Notations), and by using the projection operator technique (see Renger et al., 2001; Yang and Fleming, 2002; May and Kühn, 2011; Jang, 2020), one can obtain master equation in form of the so-called Nakajima-Zwanzig equation (Nakajima, 1958; Zwanzig, 1960, 1964).

[29] The FRET don't have to necessarily operate under the dipole-approximation—as it was mentioned in footnote 26—what may avoid some of the restrictions.

[30] Although they are irrelevant, we cannot simply discard them since they still are an important source of the perturbation. Otherwise the excited system might evolve unitarily until the universe ends.

At this point, the derived equation is still formally exact and analogous to the Liouville-von Neumann equation. However, it cannot be solved any better than the original so several approximations must be applied to derive a practical master equation.

The full derivation is again beyond the scope of this essay. It was done comprehensively by Abramavicius et al. (2011), May and Kühn (2011), and Valkunas et al. (2013). Only the key points of the theory will be presented and discussed here.

Consider exciton states derived in subsection 2.1.3, equations (2.13) and (2.14). Such exciton basis diagonalises the system Hamiltonian $\widehat{H}_{\mathrm{S}}$ so that the energies $\mathcal{E}_b$ are found straight on its main diagonal. The perturbation Hamiltonanian $\widehat{H}_{\text{S-B}}$ can be expressed in the form of (2.20). However, it has to be transformed into the same basis—the exciton (energy) basis:

$$\begin{aligned}\widehat{H}_{\text{S-B}} &= \sum_{\beta=1}^{N} \tilde{h}_\beta \,|\beta\rangle\langle\beta| = \sum_{\beta=1}^{N} \tilde{h}_\beta \underbrace{\left(\sum_{b=1}^{N} |\Phi_b\rangle\langle\Phi_b|\right)}_{\mathbb{1}} |\beta\rangle\,\langle\beta| \underbrace{\left(\sum_{b'=1}^{N} |\Phi_{b'}\rangle\langle\Phi_{b'}|\right)}_{\mathbb{1}} \\ &= \sum_{b,b',\beta=1}^{N} \tilde{h}_\beta \underbrace{\langle\Phi_b|\beta\rangle}_{c^*_{b\beta}} \underbrace{\langle\beta|\Phi_{b'}\rangle}_{c_{b'\beta}} |\Phi_b\rangle\langle\Phi_{b'}| = \sum_{b,b'=1}^{N} \tilde{h}_{bb'} \,|\Phi_b\rangle\langle\Phi_{b'}| \ ,\end{aligned} \tag{2.29}$$

where indices bb' stands for 'coordinates' within the matrix representation of $\widehat{H}_{\text{S-B}}$ in the exciton basis, i.e. $\tilde{h}_{bb'}$ is a single matrix element. Coefficients $c_{b\beta}$ are the expansion coefficients from equation (2.13), the asterisk in superscript stands for the complex conjugate:

$$\tilde{h}_{bb'} = \sum_{\beta} \tilde{h}_\beta \, c^*_{b\beta} \, c_{b'\beta} \ . \tag{2.30}$$

The perturbation by system-bath Hamiltonian enables two important processes—diagonal terms ($\tilde{h}_{bb}$) participate in *coherence dephasing* (i.e. decay of the RDO off-diagonal terms oscillations, $\widehat{\rho}_{S(b\neq b')}(t)$) while the off-diagonal terms ($\tilde{h}_{b\neq b'}$) ensure the energy transfer between the *populations* of RDO (i.e. diagonal terms $\widehat{\rho}_{S,(bb)}(t)$) (Yang and Fleming, 2002). Finally, the *population transfer rate* $K_{bb\to b'b'}$ from state $|\Phi_b\rangle$ to $|\Phi_{b'}\rangle$ can be formulated.

$$\mathcal{K}_{bb\to b'b'} = \frac{2}{\hbar^2}\,\mathrm{Re}\int_0^\infty \mathrm{d}\tau\, e^{(\mathrm{i}\omega_{b'b}\tau)} \underbrace{\mathrm{Tr}_{\mathrm{B}}\left\{ e^{\left(\frac{\mathrm{i}}{\hbar}\widehat{H}_{\mathrm{B}}\tau\right)} \tilde{h}_{b'b}\, e^{\left(-\frac{\mathrm{i}}{\hbar}\widehat{H}_{\mathrm{B}}\tau\right)} \tilde{h}_{bb'}\, w_{EQ} \right\}}_{C_{bb',b'b}(\tau)} = \frac{1}{\hbar^2}\sum_{\beta=1}^{N} |c_{b\beta}c_{b'\beta}|^2 F_{\beta\beta}(\omega_{b'b}) \tag{2.31}$$

The symbol Re stands for the real part of following complex term, w_{EQ} is the equilibrium bath state. The transition frequency $\omega_{b'b}$ would correspond to circular frequency of light released by the transition between corresponding exciton states; it can be expressed as $\omega_{b'b} = \hbar^{-1}(\mathcal{E}_{b'} - \mathcal{E}_b)$. $C_{bb',b'b}(\tau)$ is the bCRF from subsection 2.1.4, and $F_{\beta\beta}(\omega)$ is its Fourier transform.

Only the *population transfer rate* was presented here. However, the so-called *coherence transfer rates* can be derived analogically. In fact, there are many more terms in the final master equation, since every elements of RDO may be in principle influenced by all the others. The entity which collects all these rates is called the *Redfield tensor*[31] $\mathcal{K}$ with matrix elements $\mathcal{K}_{bb',b''b'''}$. Retaining only the diagonal population dynamics leads to the so-called *secular approximation*[32] of Redfield theory (May and Kühn, 2011; Trushechkin, 2019). Redfield equations in the secular approximation represent a convenient theory for the long-time dynamics where quickly vanishing coherent oscillations do not manifest. The Redfield tensor occurs in the standard form of the *Redfield equation*:

[31] Alternatively, terms like *Redfield relaxation matrix*, *relaxation (super)operator*, or *relaxation tensor* can be found in the literature. All refers to the same.

[32] This approximation is sometimes identified with the *rotating wave approximation* (Breuer and Petruccione, 2007; May and Kühn, 2011), although the theoretical background behind them is somewhat different (Mäkelä and Möttönen, 2013)

$$\frac{\partial}{\partial t}\widehat{\rho}_{\mathrm{S}}(t) = -\frac{\mathrm{i}}{\hbar}\Big[\widehat{H}, \widehat{\rho}_{\mathrm{S}}(t)\Big] - \widehat{\mathcal{K}}\widehat{\rho}_{\mathrm{S}}(t)\,. \tag{2.32}$$

Several other theories were derived from the SRT. The best known example is the *modified Redfield theory* (MRT) formulated by Zhang et al. (1998); (also see Yang and Fleming, 2002). This method simply extracts the diagonal part of the 'perturbation' Hamiltonian $\widehat{H}_{\text{S-B}}$ and treats it non-perturbatively.

2.2.3 Hierarchical Equations of Motion (HEOM)

Hierarchical equations of motion (HEOM) are currently considered as the golden standard for open quantum system dynamics computing (see Bondarenko et al., 2020). This non-perturbative[33] method offers formally exact numerical solution and thus, again, revolutionised the field of theoretical photosynthesis research. Although the theory was published already a couple of decades ago by Tanimura and Kubo (1989), it was reintroduced into this field by Ishizaki and Fleming (2009), and its importance is growing ever since. The theory belongs to the *quantum master equation* approaches which expresses the system dynamics in one all-embracing equation. That is to say, HEOM can be reduced into either Förster or Redfield theory under relevant limiting assumptions (Ishizaki and Fleming, 2009).

The reason for this trend is simple—computational power of computers. The ultimate exactness has come at the expense of computational cost. Hence, its application was fairly limited at the time it was originally published—on systems of few molecules only. Obviously, computational cost increases tremendously with the system size. The optimisation of the computational process on computer clusters is thus one of the main areas of current development (see Kreisbeck et al., 2011; Strümpfer and Schulten, 2012b).

The theory of HEOM was exhaustively reviewed and summarised by Tanimura (2006, 2020) and by Wilkins (2015). Only a brief summary will be made here. Similarly to the SRT, HEOM stands on the density operator formalism. The assumptions made about the Hamiltonian are the same, and also the bath is described as an infinite set of LHOs (usually by the Lorentz-Drude SD). However, unlike other conventional descriptions of the RDO dynamics, the HEOM does not disregard the dynamics of the bath by tracing all the DOF out of the density matrix (Tanimura, 2020). All environmental processes are preserved in the so-called *auxiliary density matrices* (ADOs). ADOs arise from the hierarchical expansion of the time-dependent *correlation functions* (see subsection 2.1.4).

The number of ADOs needed for the correct description of the system dynamics depends on the size of our system (consisting of N molecules), on the number of hierarchy levels[34] taken into account (L), and on the so-called cut-off number K. K expresses how many terms of otherwise infinite hierarchical expansion series are considered. The series converges very quickly so the induced error is negligible for sufficiently large K (Tanimura, 2020). All the ADOs are indexed by matrices of dimensions $N \times K$.

On top of that, the equations of motion, what are complex differential equations describing our system dynamics, establish couplings between 'neighbouring' ADOs. The complexity of the computation thus jumps up again. Having desire for exhaustive numerical results, all these equation of motion containing all the hierarchy of ADOs, and also their interactions, have to be determined. Strümpfer and Schulten (2012b) noted the computation time can take several days using many gigabytes of computer RAM memory if the computation isn't effectively distributed.

[33] That is to say, the introduction of approximative limiting assumptions (e.g. weak interchromophoric coupling), which usually enables us adopting the perturbation theory, can be completely avoided.

[34] Level of hierarchy is an integer, $l = 0, 1, 2, \ldots$. Every ADO $\widehat{\sigma}_{\mathbf{n}}(t)$ can be assigned to one such hierarchy level, if sum of all its indexing matrix elements ($\mathbf{n}$) is equal to the level's number, $l = \sum_j^N \sum_k^K n_{jk}$

3 | Overview of Photosynthetic Reaction Centres

Reaction centres (RCs) are evolutionary the most conserved light-harvesting molecular complexes. It is highly likely that the photosynthetic RCs of all known organisms share one common ancestor (Green, 2003; Orf et al., 2018). All complexes possess the same numbers of transmembrane α-helices[1] and they also have in common the number and the arrangement of chlorophylls, as well as the placement of metal ions and quinones (Heathcote and Jones, 2012). The only major variables left, which are allowing some adaptations, are thus the chemical identity of the pigments (see section 1.2)—which is still rather uniform, though—and then the peripheral parts of scaffolding proteins. The latter becomes significant especially when it enables aggregation of more complexes together, either in terms of dimerisation (e.g. see Figure 3.2c) or by attaching various types of peripheral antennas, both membranous and cytosolic.

The presence of functional RCs conditions the whole photosynthesis since the *primary charge separation* takes place here. That is to say, the complex is capable of photooxidation of a particular substrate molecule using the energy from sunlight, and of guidance of the obtained electrons towards the redox cofactors located in the membrane. Such reduced cofactors are then utilised further by the rest of photosynthetic machinery. To enhance the efficiency and overall turnover of the whole process, RCs are surrounded by great number of LH antennas, as was discussed in section 1.1.

3.1 Types of Photosynthetic Reaction Centres

All known RCs share a twofold symmetry[2] where the pigments—(bacterio)chlorophylls non-covalently bound at their binding pockets—are surrounded by two transmembrane proteins from both sides (structure similar to a sandwich). The protein scaffold is always a dimer where both subunits contain homologous structural motifs of five transmembrane α-helices (TMH). However, many structural alterations occur and species-specific protein names are usually used. The protein names presented below are based on a comprehensive articles of Schubert et al. (1998) and Orf et al. (2018); for the original works elucidating the structure and introducing the nomenclature presented here, see the literature therein. Heathcote and Jones (2012) distinguish four types of reaction centres based on the protein structure, the chlorophylls, and the adjacent LH antennas.

i The simplest type of RC can be found in anoxygenic phototrophic purple bacteria (see Madigan and Jung, 2009) and in anoxygenic filamentous non-sulfur green bacteria. These groups are facultative phototrophs what makes them ideal models for photosynthesis research and mutagenesis-involving experiments. However, their photosynthesis doesn't involve reduction of redox cofactors (ferredoxin, NAD^+, $NADP^+$) directly[3] since it can only create the H^+ transmembrane gradient by the so-called *cyclic electron transfer*. The gradient is then used by F_OF_1 ATP synthases as usual. The structure and function of this type of RC will be scrutinised on example of the purple bacteria *Rhodobacter* (*Rh.*) *sphaeroides* in section 3.2.

   Additionally, the non-sulfur green bacteria—similarly to their sulfur namesakes (to be mentioned shortly)—assemble the chlorosome, a specialised cytosolic LH antenna. However, the FMO

[1] Albeit structurally nearly identical, only about 30 % of the AA sequence is actually conserved (Orf et al., 2018).

[2] In fact, it cannot be called true symmetry because of the heterodimeric rather than homodimeric nature of the scaffolding proteins. Sometimes the term pseudosymmetry is used instead (Jones, 2009).

[3] The cofactor reduction is then performed by subsequent *reversed electron transfer* driven either directly by the established H^+ gradient or by energy from ATP (see Dutton, 1986; Brune, 1989).

protein is not present here. The main subunits of RC core protein are called L and M (also PufL and PufM) and they form a heterodimer.

ii A bit more convoluted structure have the RCs of green sulfur bacteria, Heliobacteria, and Chloroacidobacteria (Heathcote and Jones, 2012; Blankenship, 2014). The two former are obligate anaerobic phototrophs, but Chloroacidobacteria are surprisingly obligately aerobic (Bryant et al., 2007). Unlike the previous type, NAD^+ is involved in the electron flow directly. The two later groups of bacteria presented here also possess the specialised LH structure called chlorosome, connected with RC by the FMO protein, as was already mentioned in section 1.1. The RC core is a homodimer of two polypeptides PscA.

iii+iv The last two types of RCs take part in the well-known oxygenic photosynthesis performed by Cyanobacteria and all so far known eucaryotic photoautotrophs. Both types of RC are usually present and engaged in photosynthesis. That means both RCs are linked into one electron pathway what enables the organisms to use the energy even more efficiently. They are referred to in general as (iii) *photosystem I* (PSI) and (iv) *photosystem II* (PSII). Core proteins of both complexes are heterodimers. In the case of PSI they are called PsaA and PsaB, while in PSII it is D1 and D2 (also called PsbA and PsbD accordingly).

In fact, all these four types can be rearranged into just two categories. Such classification is older (Blankenship, 1992; Allen and Williams, 1998), and can be found in literature more frequently. The sort key is in this case based on the terminal electron acceptor which is leaving the RC.

The first type is usually called the *Fe-S type* (alternatively also *PSI type* or simply *Type I*) and it unites groups (ii) and (iii) from above. As the first presented name suggests, it is recognisable by the presence of iron-sulfur [4Fe—4S] cluster on the cytoplasmic/thylakoidal stromal side (see Vassiliev et al., 2001). In addition to the group-specific structural characteristics already mentioned, there is in fact a six-TMH-containing antenna protein linked to the N-terminus of both core subunits of all Fe-S type RCs. That is to say, the RC core dimer actually consists of 2× 11 TMH proteins called PsaA and PsaB (Schubert et al., 1998).

The second type of RC is mostly referenced as the *Q type* (Q standing for quinone; or again alternative names like *PSII type*, *pheophytin-quinone (Phe-Q) type*, or just *Type II* are frequently used) and it represents groups (i) and (iv) from above. Here, the final acceptor is a mobile molecule of quinone which enters and leaves the RC directly from the membranous space (Orf et al., 2018). RCs of type (iv) (i.e. Cyanobacterial and chloroplastidal PSII) have also their core antennas with 6 TMH—CP43 and CP47 (alternatively called PsbC and PsbB respectively). Unlike the FeS type, neither of the proteins is covalently linked to the core (Schubert et al., 1998). Hence, the whole RC complex is in fact a tetramer of 2× 5 TMH and 2× 6 TMH proteins.

The Figure 3.1 maps the occurrence and the general structure of above mentioned RC types in various taxonomic groups. In upcoming paragraphs, I'd like to just briefly characterise the molecular structure of both RC types with main emphasis on the pigments. As suggested above, the Q type RC of purple bacteria *Rh. sphaeroides* will be then presented in greater detail in section 3.2.

RCs contain numbers of different pigments and cofactors. Most frequently, there can be found (bacterio)chlorophylls, (bacterio)pheophytines, carotenoids, quinones, non-heme ions, and FeS clusters. Their distribution and orientation are tightly bound. Nonetheless, it is also highly species-specific as pointed out by Heathcote and Jones (2012). Since the description of the whole taxonomic clades is usually based on a few model organisms only, some established generalisations might be brought into question as more species will be scrutinised by the time.

Due to the dimeric nature of RCs, the main backbone of pigments is arranged into two separate branches (usually called simply 'A' and 'B') shaped—if one takes it with a grain of salt—as a letter 'V' (oriented perpendicular to the membrane surface). Consequently, four 'vertical' levels, each parallel to the membrane surface, can be described as well. The imaginary tip of the 'V' always points into the thylakoid lumen/periplasm, i.e. in the direction of light-driven H^+ transfer. At the tip is located the *special pair* consisting of two closely separated (bacterio)chlorophylls. They are usually denoted by letter 'P' (Blankenship, 2014).

One tier higher from the tip, there are two *accessory* (bacterio)chlorophylls of the same sort as in P. They are called by letter 'B'. In another tier higher, there are located either modified Chl*a* in case of FeS type of RC, or otherwise, in case of Q type, it is a demetallated pigment (i.e. (bacterio)pheophytine) of once again identical type as in P and B. Sometimes these positions are denoted by letter 'H'. In the last level are usually located binding pockets for quinones. In Q type of RC, one pocket (called Q_B) is freely opened into the inner membranous space where quinones move freely. Quinone Q_A is trapped in the protein (Wraight and Gunner, 2009; Orf et al., 2018). Permanently bound phylloquinones can be present even in FeS type but only as secondary electron acceptors, not the terminal (Heathcote and Jones, 2012).

The letters 'P' and 'B', which are standing for special pair and accessory pigments respectively, are always followed by a suffix of their characteristic Q_y spectral band location. For example, the presumably best-known P700 and P680 stand for the special pairs of land plants' RC PSI and PSII respectively. Besides, molecules of carotenoids or a single non-heme metallic atom, laying in the main axis of symmetry, can occur as well (Blankenship, 2014).

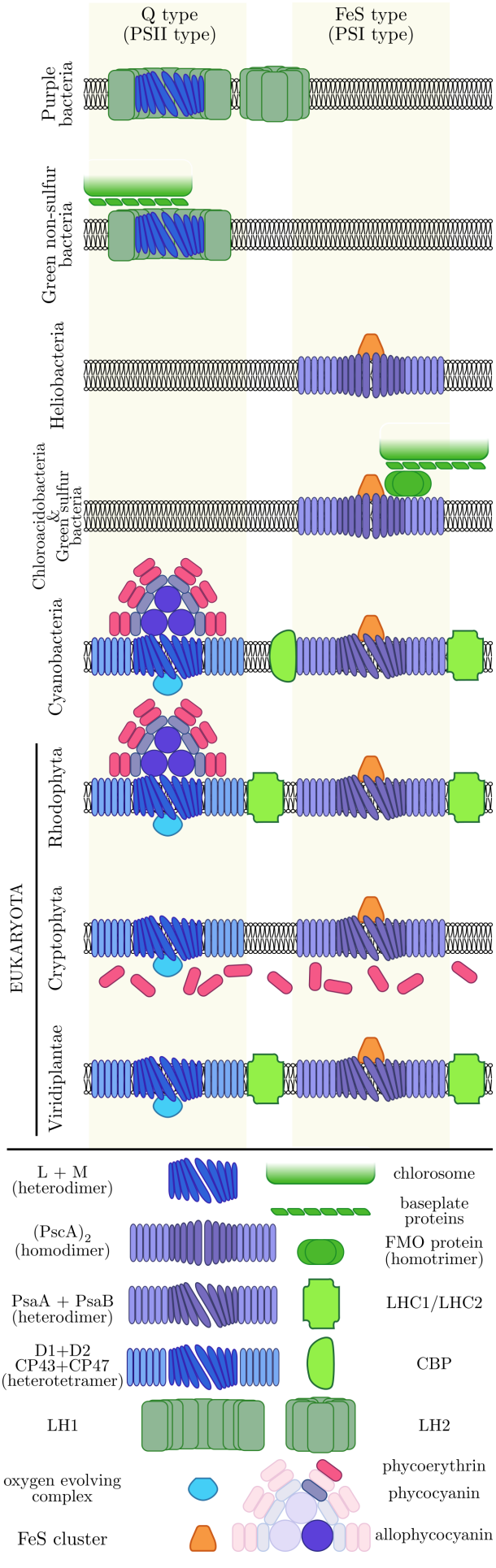

Figure 3.1: Scheme of RC types and characteristic antenna complexes present in various taxonomic groups. Upper side of membrane is cytosolic/stromal, bottom is periplasmic/lumenal. Based on nomenclature of Schubert et al. (1998) and on figures of Hohmann-Marriott and Blankenship (2011, 2012); Blankenship (2014); Mirkovic and Scholes (2015); Mirkovic et al. (2017).

The excitation energy from LH antennas can theoretically arrive at any pigment of compatible optical properties and it's then directed towards the special pair. The states of P molecules lays on the bottom of the energy scale. Once the special pair is excited, the excited electron itself leaves the pair and pursue its pathway towards the terminal acceptor—either over a FeS cluster to a mobile ferredoxin soluted in cytoplasm (FeS type), or to a mobile quinone Q_B in cytoplasmic/thylakoid membrane (Q type)—using one of the available branches[4] of pigments (Blankenship, 2014).

3.2 Purple Bacterium *Rhodobacter sphaeroides* as a Model Example

Reaction centres of gram-negative purple non-sulfur photoheterotrophic bacteria (pbRC) have one of the simplest structures of all of the other RC types, see Figure 3.1. The core transmembrane protein dimer is structurally independent on the surrounding antennas and can be thus easily purified and analysed (Cogdell et al., 2006). The photosynthetic complexes are located at the cytoplasmic membrane where they may form specialised spherical vesicle-like membrane protrusions into the cytoplasm[5]. It's a reasonable example of the ongoing process of compartmentalisation, alike the Cyanobacterial and chloroplastidal thylakoids (Sawicki and Chen, 2020).

The LH apparatus of purple bacteria—here I focus on the *Rb. sphaeroides* only but most of the structure can be found in different purple bacteria as well, just the protein nomenclature will differ—basically consists of three basic units: two antenna complexes named LH1 and LH2, and one RC complex (pbRC)[6]. LH2 is the most peripheral antenna complex since it absorbs the shortest wavelengths. It is a circularly shaped multimer of nine subunits[7]—heterodimers of α and β polypeptides (Gabrielsen et al., 2009). On the other hand, the LH1 antenna is closely adjacent to the RC and forms the LH1-RC complex. Depending on the species and also on the environment, LH1 can either completely encircle a single pbRC, or it can associate two pbRCs together while adopting the shape of letter 'S' (see Figure 3.2c). Its structural composition has similar arrangement as the LH2, with a single exception. A lone α-helix of polypeptide PufX is always[8] intercalated into the structure of LH1, which is embedding the RC. It partially ensures the flow of quinones and quinols between the RC and the membranous space (Farchaus et al., 1992; Lilburn et al., 1992), and also helps to colocalise the LH1-RC complexes together while increasing the local concentrations of quinones (Comayras et al., 2005). Bullough et al. (2009) went into much more details about LH1-RC complexes of various species.

More interesting are the pigments inside the antennas. LH2 contains arrangements of two distinct rings of BChl*a* interlinked by a similar ring of carotenoids. One ring called B800 consists of 9 BChl*a* (i.e. 1 molecule of BChl*a* per an $\alpha\beta$ subunit) and is located close to the cytoplasmic side of the membrane. The second ring is dubbed B850. It consists of 18 BChl*a* molecules (i.e. 2 molecules per $\alpha\beta$ subunit) and can be found on the outer part of complex near periplasm. Nine molecules of carotenoids are then placed in-between and perpendicular to both rings. Apparently the intermolecular distance within molecules of B850 ring is necessarily much smaller than in B800 what results in formation of

[4] Despite the two fold symmetry, both branches don't have to be necessarily involved in the electron transfer. In Q type of RCs, only the branch A is actually used. However, the spatial distribution of the unpaired electron of the special pair after the charge separation seems to be always uneven, see Lendzian et al. (1993); Heathcote and Jones (2012).

[5] Analogous membrane invaginations can be found in many other bacterial species, adopting wide variety of shapes (Jones, 2009).

[6] The reality is that more kinds of peripheral antenna complexes can be present in *Rb. sphaeroides* and all other purple bacteria besides just LH2. They usually appear as a low-light adaptation of the normal antennas. Scheuring (2006) names them LH3, LH4, etc., although Gabrielsen et al. (2009) persist on using names LH1 and LH2 only together with specifying notation.

[7] The exact number is species-specific and can be either eight or nine. An overview can be found in Mothersole et al. (2018).

[8] Always in terms of *Rb. sphaeroides*. For example LH1-RC complex of related purple bacterium *Thermochromatium tepidum* is completely PufX-analogue free, forming perfect circle around core pbRC dimer (Niwa et al., 2014).

one large exciton state. That's the reason for 50 nm shift of their lowest absorption peaks even though the molecules of both rings are chemically identical (Novoderezhkin and van Grondelle, 2018).

The number of BChl*a* molecules in LH1 can be even larger; for dimeric form usually present in *Rb. sphaeroides* it is 56 (Qian et al., 2014). Since their separation is also short, the exciton complex is formed as well. Due to the larger size, though, the absorption peak is shifted even further to ca 875 nm. Thus the exciton is named B875 (Nagarajan and Parson, 1997).

The RC of *Rb. sphaeroides* is a good archetype of Q type RC. A comprehensive scrutiny of the pbRC structure was done by Roy et al. (1995); Roy and Lancaster (2008). Here, I mention just the most pertinent features. To start with, the core of *Rb. sphaeroides* and few other purple bacteria is in fact a heterotrimer of polypeptides L, M, and H (abbreviations for light, medium, and heavy; as they were firstly characterised by SDS-PAGE; Clayton and Haselkorn, 1972; Okamura et al., 1974). L and M share the twofold (pseudo)symmetry and both have five TMH, as expected. The H subunit (sometimes also called PuhA) has only one TMH and a globular part with β-sheet motifs on the cytoplasmic side of the membrane (Allen et al., 1987). The thing is, the names of polypeptides don't correspond to reality since their true size and molecular weight wasn't measured right by Clayton and Haselkorn (1972); Okamura et al. (1974). The largest is M (34 kDa, 307 AA), then L (31 kDa, 281 AA), and finally the actually lightest H (28 kDa, 260 AA) (Allen et al., 1987). Despite the names are misleading, they are still normally used.

Only the polypeptides L and M contribute to the cofactors organisation, binding them non-covalently. There are ten cofactors located in the pbRC (Heathcote and Jones, 2012). The special pair (P_A, P_B) as well as the accessory pigments (B_A, B_B) of *Rb. sphaeroides* always consist of BChl*a* molecules. The H position of pigments (H_A, H_B) belongs to bacteriopheophytines *a*, i.e. demetallated BChl*a*. Ubiquinone-10 as Q_A is bound permanently in a hydrophobic pocket of the protein M. The site for second ubiquinone-10 called Q_B is in fact rather a tunnel through the M protein than just a pocket. It enables oxidised ubiquinones to enter the Q_B site, be reduced to ubiquinols, and then leave the RC and be replaced by a new ubiquinone. Wraight and Gunner (2009) dedicated a whole review to quinones of purple bacteria only.

Additionally, one molecule of carotenoid bound by protein M, located nearby the accessory pigment B_B can be found in pbRC. Its exact chemical nature depends on the aerobicity of the environment (Heathcote and Jones, 2012). It's either *spheroidene* (in dark or semiaerobic env.) or *spheriodenone* (in illuminated or anaerobic env.). Finally, one non-heme ferrous iron atom[9] is located directly on the main axis of symmetry, and at the middle point between Q_A and Q_B sites. It is bound covalently to four histidines (L-His190, L-His230, M-His219, M-His266) and one glutamate (M-Glu234) (Schieferstein et al., 2014). It has thus mainly structural function since it binds both proteins together (Heathcote and Jones, 2012).

3.2.1 Structure and Optical Properties

The optical properties are closely related to the molecular structure. Figure 3.2a,b shows the arrangement of pbRC cofactors as reported by Schieferstein et al. (2014); Khvostichenko et al. (2014) using x-ray crystallography at room temperature in 2.5 Å resolution. The distances between molecules were measured centre-to-centre.

The distances between molecules along with their individual environment affect the strength of intermolecular coupling, see subsection 2.1.2. It's then the ratio of intermolecular coupling $V_{\alpha\alpha'}$ and the reorganisation energy λ_r what influences the observable optical spectra as well as the way in which EET occurs (see section 2.2)

[9] Certain strains of *Rb. sphaeroides* may bind manganese atom instead (Blankenship, 2014).

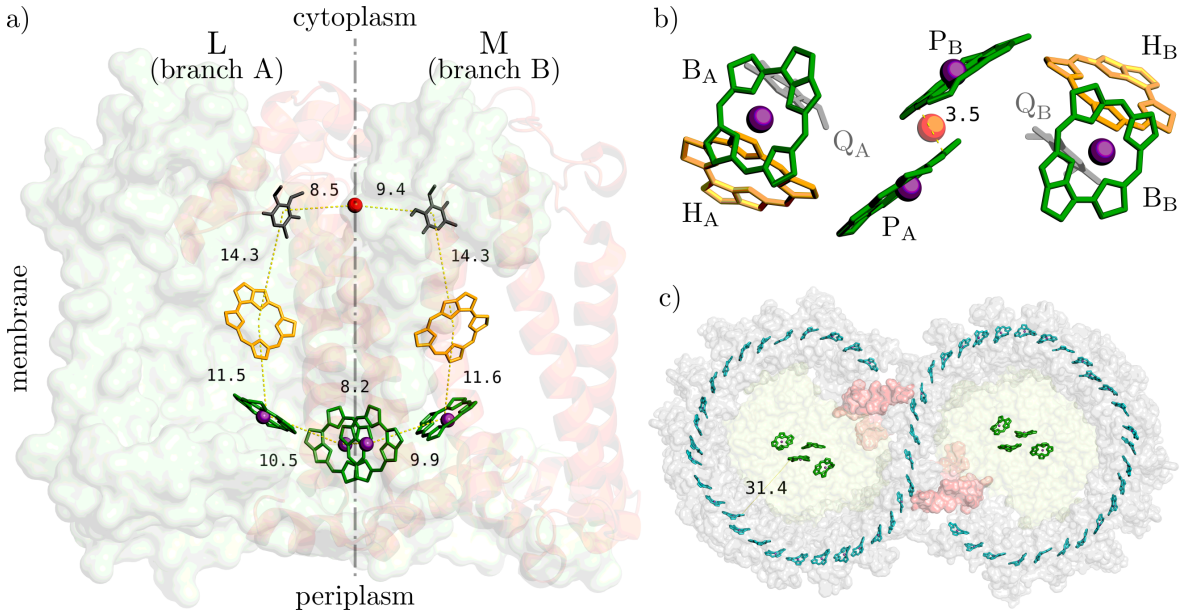

Figure 3.2: RC of *Rb. sphaeroides*. (a) Core heterodimeric complex consisting of protein subunits L (left) and M (right). L is depicted in terms of vdW surface while in M is emphasised the common secondary structure of 5 TMH. Distances between cofactors were measured center-to-center in ångströms. BChl*a* are shown in dark green with heme Mg atom in purple; BPhe*a* in orange; ubiquinones in dark grey; ferrous non-heme iron in red. The main axis of twofold symmetry is shown as well. (b) View from the bottom periplasmic side of picture (a). Names of cofactors are included. The interplanar distance between molecules of special pair (P_A and P_B) is emphasised in the middle. (c) Bottom view on the whole LH1-RC-PufX dimer where only molecules of BChl*a* remained explicitly visible. The LH1 complex is encircling two core pbRC heterodimers and it contains an 'S'-shaped line of BChl*a* (in cyan). Two PufX subunits are highlighted in red. The other colouration correspond to (a,b). The distance between LH1 and RC special pair is noted on the left side in ångströms. Only the main backbones of porphyrin rings are shown in all cases; hydrophobic chains of ubiquinones were also omitted.
Figure was generated with PyMOL (Molecular Graphics System, Version 2.3, Schrödinger, LLC.) using PDB files (a,b) `4tqq` (Schieferstein et al., 2014; Khvostichenko et al., 2014) and (c) `4v9g` (Qian et al., 2013, 2014).

The uniquely close proximity of the special pair molecules visible on Figure 3.2b necessarily includes orbital overlap and strong interaction. Although this overlap would need to be treated separately and with much more attention because it disrupts most of the initial assumptions, see chapter 2, for general purposes, it can be still approximated and described as a simple delocalised Frenkel exciton (see subsection 2.1.3). Both molecules thus behave as a single photochemical entity. The lower absorbance peak (Q_y)—normally located at wavelength of about 800–815 nm for a lone BChl*a* in protein environment—is thus split into two peaks (analogously to Figure 2.2). The lower gives the molecules of special pair their alternative name, P870 [10] (also called P_-). The second and energetically higher peak is called P_+ and it stays nearby the above mentioned range of monomers near and can be sometimes observed as a little shoulder on the absorbance spectra. Absorbance peak of monomeric and weakly coupled accessory BChl*a* B_A and B_B are there located as well, for obvious reasons (see Jordanides et al., 2001; Renger et al., 2013). The BPhe*a* differs from the previous by the magnesium atom. Its absence results in a shift to ca 760 nm. The sequential movement of absorption peaks to the far-IR part of spectra as approaching the P870 is illustrated on Figure 3.3.

The strength of intermolecular coupling along with the site energies (i.e. values of Q_y transition in case of chlorophylls) can be obtained either by fitting theoretical model on experimental data, or by *ab initio* QCh methods (see Renger and Müh, 2013). Such pieces of information can then be used to calculate the transfer rates between molecules or to determine the spectra of linear absorbance, circular dichroism, polarisation etc. (e.g. Kramer et al., 2018).

[10] Close values can be found in literature sometimes (e.g. P865) as a result of dependency on the environment while being measured (Heathcote and Jones, 2012).

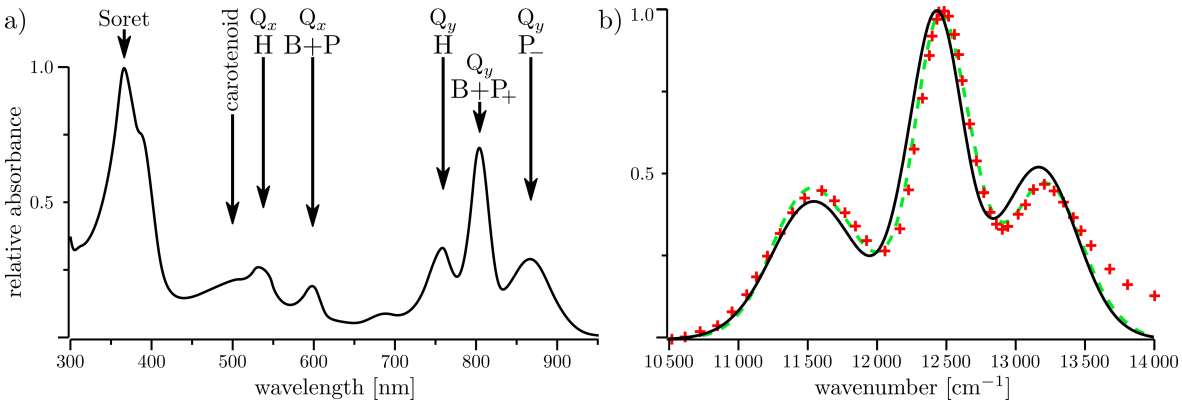

Figure 3.3: Absorption spectra of RC of *Rb. sphaeroides* at 300 K. (a) Experimentally obtained spectrum (taken from Jones, 2018; Leonova et al., 2011). Names of electronic transitions (Q_x, Q_y) of individual RC pigments (P, B, H, carotenoid) that dominates in particular spectral peaks are written above them. (b) Examples of theoretical modelling of absorption spectra expressed as a function of wavenumber (see List of Physical Constants and Used Notations). Red crosses stand for the experimental data (taken from Cherepy et al., 1997); green dashed line was calculated by Strümpfer and Schulten (2012a) using HEOM (see subsection 2.2.3); black solid line was calculated with Python package QUANTArhei (Mančal et al., 2020) and with a PDB file `4tqq` (Schieferstein et al., 2014), based on data used by Strümpfer and Schulten (2012a)[11]. All the spectra are normalised to one.

3.2.2 Excitation Energy Transfer Dynamics

Since the beginning of photosynthesis research, scientist are captivated by the high quantum yields and transfer efficiency. Measurements of such optical properties offered valuable insight into the EET dynamics. The true turmoil have begun after the development of femtosecond[12] laser technology and spread of femtosecond spectroscopy (for review see Vos and Martin, 1999). The individual steps of EET occur on exactly such short timescale and this technology made them directly observable.

The improving accuracy of spectroscopy and molecular structure analysis is enabling researchers to further develop the theoretical models. The variable which is frequently sought is the transfer rate of EET. It expresses the time of moving excitation from one state to another. Several theories and models how the rates can be calculated were presented in previous chapter 2. It should be clear that such state doesn't always include just one molecule; it can be a whole aggregate of molecules. The transfer rates are thus basis dependent. Usually, as long as it is possible, the site basis is preferred due to its straightforward interpretation. However, the presence of strong intermolecular interactions leading to completely delocalised excitons disables this option.

The LH1-RC-PufX complex of *Rb. sphaeroides* is again a great example. The molecules of BChl*a* in LH1 antenna form a delocalised exciton states. The transfer time between individual exciton states is fairly fast, reaching 80 fs. On the contrary, the energy transfer from LH1 to the RC is much longer, about 35 ps (Fleming and van Grondelle, 1997). This step represents even the total rate-limiting step of the light-harvesting process (Valkunas et al., 1992; Beekman et al., 1994). Under physiological conditions, the energy is transferred directly to the special pair P870 (Damjanović et al., 2000; Paleček, 2016). The exceptional spectral overlap of LH1 and P− state of the special pair—both centered around ca 870 nm—favors FRET and it stands behind the great transfer efficiency there (Jones, 2018). Nevertheless, even the B and H pigments are obviously capable of accepting the excitation from LH1, and also of the direct photon capture. These cases of EET within the pbRC were investigated both experimentally and theoretically, for overview of selected works please see Table 3.1.

[11] The numerical values of site energies, damping times, reorganisation energies, and width of Gaussian distributions used for description of the so-called *static disorder* were taken directly from Strümpfer and Schulten (2012a), parameter set 2. Therein written intermolecular couplings were complemented by Coulombic couplings in dipole-dipole approximation. The static disorder was simulated by assuming Gaussian distribution of site energies and consequent averaging over 15 000 (instead of 1 000 used by Strümpfer and Schulten) random realisations in Monte-Carlo-like procedure. Insight into the calculation can offer Jordanides et al. (2001) or Valkunas et al. (2013).

[12] 1 femtosecond [fs] = 10^{-15} second

Once the excitation reaches the special pair, the charge separation happens shortly. The excited electron itself moves to molecule B_A (3 ps) and subsequently to H_A (0.9 ps). The spatial separation, which prevents charge recombination with P^+, is completed by a transfer to ubiquinones (> 200 ps). The thing is, all these steps take place on more than one order longer timescale than EET. With a single exception of the EET between LH1 and RC, as mentioned above (> 35 ps) (see Renger, 2018).

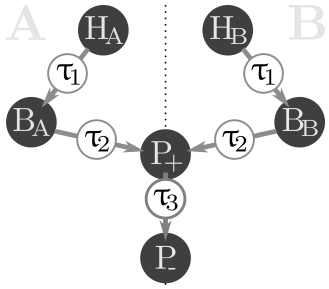

Figure 3.4: Diagram of excitation energy flow within the main RC cofactors (H, B, P). Times τ represents the transfer times, see Table 3.1. P_+ and P_- stands for the exciton energy levels formed by P_A and P_B.

Table 3.1: Excitation energy transfer rates within the pbRC of *Rb. sphaeroides* were measured and calculated by various authors. Results of computer simulations performed as a part of this thesis were obtained by using the QUANTArhei package (Mančal et al., 2020). They are presented in the last right column of the table[a].

		King et al. (1997)	Vos et al. (1997)	Jordanides et al. (2001)†	Niedringhaus et al. (2018)[b]	QUANTArhei†
τ_1	A	160 fs[c]	< 100 fs	165 fs	50 fs	837 fs
	B			371 fs	99 fs	1 405 fs
τ_2	A	163 ± 54 fs	≈ 200 fs	189 fs	164 fs	161 fs
	B			320 fs	156 fs	146 fs
τ_3		71 ± 24 fs	50–100 fs	-	25 fs	11 fs

† These data are based on computer simulations and computations.
[a] The structural data were taken from Schieferstein et al. (2014) (PDB file `4tqq`) and parameters from Strümpfer and Schulten (2012a); see also footnote 11.
[b] *Rb. capsulatus* instead of *Rb. sphaeroides* was measured by the authors. Also the temperature was different, 77 K.
[c] This value was just roughly calculated by the authors since only H to P transfer was measured in their experiment.

Absorption spectrum

EET dynamics

Figure 3.5: In these QR codes are encoded the Python scripts of the linear absorption spectrum (Figure 3.3) and EET times (Table 3.1) calculations. For reading the QR code, you can use your smartphone (various applications were tested, e.g. Kaspersky™QR Scanner) or upload the QR code image into some online application, e.g. `online-barcode-reader.inliteresearch.com`. Once the file is saved with the `.py` extension, it can be launched by Python 3.7+ with installed package QUANTArhei (Mančal et al., 2020) along with its own requirements. Alternatively, some online Python compiler can be used too, e.g. `repl.it`. The needed PDB file would be downloaded automatically from the Protein Data Bank after running the script.

Discussion

The chlorophylls of LH antennas tremendously outnumber the RC cofactors. In case of *Rb. sphaeroides* it's by a factor of ca 17–40 (see Sener et al., 2007). Moreover, since the excitation energy is transferred directly from the LH1 antenna to the special pair of RC, the contribution of the other RC cofactors to the light-harvesting is fairly questionable (Heathcote and Jones, 2012). However, their main and indisputable function is the electron transfer after the charge separation event.

Notwithstanding, RCs are a great subject of study. As was implied in section 3.1, the conserved structure of RCs clearly reflects the evolutionary relations between organisms and enlightens the ways in which endosymbiotic processes occurred. RCs are also very useful and valuable models for the study of EET mechanisms. Their rather simple structure invites the application of even the most computationally costly methods what reveals their accuracy.

Computer modelling and simulations are recently the only way of theoretical investigation due to the enormous complexity of the biological systems. Several steps have to be achieved before the simulation can be performed. (i) It is mandatory to know the atomic structure of the system, e.g. from x-ray crystallography or cryo-electron microscopy. (ii) Secondly, the electron densities, site energies, and intermolecular Coulombic interactions have to be determined, e.g. by the recent QCh methods. (iii) Then it is necessary to properly describe the dynamics of the system and the influence of the bath. (iv) Finally, the optical properties of the system, EET dynamics, or the lifetimes of particular states can be determined (Renger et al., 2013).

In each of these points, some useful approximations can be introduced. However, one has to always ponder on the most suitable choice of models, methods, and used approximation since it is necessary to balance the computational cost with the potentially introduced errors. For example, Figure 3.3b shows the comparison of two calculated absorption spectra with an experimental one. Although both theoretically determined spectra are pretty similar, their calculation times differ significantly. The HEOM method adopted by the authors of the original article (Strümpfer and Schulten, 2012a) takes generally tens of hours (Kramer et al., 2018). But by adopting less exact method, the computation performed herein with QUANTArhei (Mančal et al., 2020) took merely few minutes[13].

Apparently, noticeable differences come to light when the energy transfer times are evaluated, see Table 3.1. The values given by QUANTArhei correspond only partially; especially the times of τ_1 deviate greatly. This is primarily caused by the selected approximative treatment. While the strongly coupled special pair ($V_{P,P} = 500\,\mathrm{cm}^{-1}$; $\lambda_{\mathrm{r,H}} = 80\,\mathrm{cm}^{-1}$) was treated with the suitable SRT, for the RC as a whole was then adopted the (generalised) FRET. Even though the coupling between pigments H and B was far from being negligible with respect to the reorganisation energy ($V_{\mathrm{H,B}} = 130\,\mathrm{cm}^{-1}$; $\lambda_{\mathrm{r,H}} = 50\,\mathrm{cm}^{-1}$). Besides, the theoretical model also didn't take into account all the electronic states present. The thing is, the charge separated pairs of molecules should also contribute to it. For the sake of better results, a much more advanced model and theoretical approach would need to be adopted.

The prospects of photosynthesis research are auspicious. Because of the immense degree of interdisciplinarity, every advance has a potential to find application in various different fields, and *vice versa*. Probably the highest attention is recently paid to the artificial photosynthesis and to the research of organic solar cells. By and large, three approaches are currently made. It's either enhancing the already existing complexes of natural origin, or inventing completely new photochemical systems

[13]The calculation of lifetime broadening (relaxation tensor) was omitted, and, in fact, replaced by inhomogeneous broadening in Monte-Carlo-like algorithm.

from scratch. Besides, somewhere in-between these two is the so-called *semi-artificial photosynthesis*.

The first approach generally aims to broaden the exploited part of light spectra and increase the efficiency of natural LH complexes (see Chen and Blankenship, 2011; Blankenship et al., 2011). Additionally, it also tries to link the EET directly with other enzymatic reactions so the excitation energy could be used in novel ways. The second approach is rather a matter of material science. It's mostly interested in inorganic catalysts capable of e.g. light-driven water oxidation in a robust scale. The semi-artificial photosynthesis is then interested in wiring natural LH complexes with metallic electrodes for the sake of minimising losses during the electron transport between individual complexes. This concept is also called bio-photoelectrochemistry (for more information see Zhang and Reisner, 2020).

In all these cases, the theoretical understanding of the processes, which are being designed, as well as their structural description is obviously necessary. Moreover, adopting computer simulations before the experiments can be by far faster, cheaper, and easier alternative of doing the initial research.

Summary

The photosynthetic reaction centres (RCs) represent the actual place where the energy carried by photons is turned into a charge-separated states which then enable establishment of the electrochemical H^+ transmembrane gradient used by ATP synthases. In general, the cores of RCs of all photosynthetic organisms have similar, conserved structure (see section 3.1). The complexes are (pseudo)symmetric dimers of at least two protein subunits embedding non-covalently bound molecules of pigments, mostly various types of chlorophylls. The pigments always form two distinct branches with the so-called special pair located in the middle. The special pair—two rather closely separated chromophores—is the place where all the excitation energy flows into, where the charge separation occurs, and also where the electron transfer begins.

In chapter 2 an introduction to the quantum mechanical description of the whole excitation energy transfer process was presented . Two still frequently used approximate methods were discussed. Generally, Förster theory operates on the limit of weak intermolecular coupling when each molecule retains its individuality. Redfield theory, on the other hand, assumes weak molecule-environment interaction, which results in formation of delocalised Frenkel exciton states. Besides, one state-of-the-art formally exact method—HEOM—was introduced. RCs serve as a valuable model for evaluation of the computational methods due to their structural simplicity as well as their functional importance.

As a model example, that was scrutinised in detail, the RC of purple photosynthetic bacterium *Rhodobacter sphaeroides*—one of the first model organisms in the research of photosynthesis (section 3.2)—was selected. The molecular structure, optical properties, and the excitation energy transfer dynamics of pbRC were described. Data based on both experimental measurements as well as theoretical calculations and simulations were presented. Own results, which were calculated for the PDB file `4tqq` (Schieferstein et al., 2014; Khvostichenko et al., 2014), with data provided by Strümpfer and Schulten (2012a), and by using the QUANTArhei package (Mančal et al., 2020) for Python, were also included (subsection 3.2.2). Despite the absorption spectrum is fairly similar to the one calculated by Strümpfer and Schulten (2012a) using HEOM, the EET transfer times are not in a very good agreement with other authors. That has been caused primarily by the approximate nature of the adopted methods as well as by the simplified theoretical model. For example, the influence of charge-separated states was completely omitted here (see Discussion).

The development of theoretical and computational methods is crucial, for example, for the research of artificial light-harvesting systems where understanding of the processes is obviously necessary.

References

Abramavicius, D., Palmieri, B., Voronine, D. V., Šanda, F., and Mukamel, S. (2009). Coherent Multidimensional Optical Spectroscopy of Excitons in Molecular Aggregates; Quasiparticle versus Supermolecule Perspectives. *Chem. Rev.*, 109(6):2350–2408. https://doi.org/10.1021/cr800268n.

Abramavicius, D., Butkus, V., and Valkunas, L. (2011). Interplay of Exciton Coherence and Dissipation in Molecular Aggregates. In Würfel, U., Thorwart, M., and Weber, E. R., editors, *Quantum Effic. complex Syst. Part II From Mol. Aggregates to Org. Sol. Cells*, Semiconductors and Semimetals, chapter 1, pages 3–46. Elsevier, 1st edition. ISBN 978-0-12-391060-8. https://doi.org/10.1016/B978-0-12-391060-8.00001-0.

Agranovich, V. M. and Basko, D. M. (2000). Frenkel excitons beyond the Heitler-London approximation. *J. Chem. Phys.*, 112(18):8156–8162. https://doi.org/10.1063/1.481416.

Al-Khalili, J. and McFadden, J. (2014). *Life on the Edge: The Coming of Age of Quantum Biology*. Bantam Press. ISBN 978-0593069325.

Allen, J. and Williams, J. (1998). Photosynthetic reaction centers. *FEBS Lett.*, 438(1-2):5–9. https://doi.org/10.1016/S0014-5793(98)01245-9.

Allen, J. P., Feher, G., Yeates, T. O., Komiya, H., and Rees, D. C. (1987). Structure of the reaction center from *Rhodobacter sphaeroides* R-26: the protein subunits. *Proc. Natl. Acad. Sci.*, 84(17):6162–6166. https://doi.org/10.1073/pnas.84.17.6162.

Andrews, D. L. (1989). A unified theory of radiative and radiationless molecular energy transfer. *Chem. Phys.*, 135(2): 195–201. https://doi.org/10.1016/0301-0104(89)87019-3.

Andrews, D. L. and Bradshaw, D. S. (2004). Virtual photons, dipole fields and energy transfer: a quantum electrodynamical approach. *Eur. J. Phys.*, 25(6):845–858. https://doi.org/10.1088/0143-0807/25/6/017.

Beekman, L. M. P., van Mourik, F., Jones, M. R., Visser, H. M., Hunter, C. N., and van Grondelle, R. (1994). Trapping Kinetics in Mutants of the Photosynthetic Purple Bacterium *Rhodobacter sphaeroides*: Influence of the Charge Separation Rate and Consequences for the Rate-Limiting Step in the Light-Harvesting Process. *Biochemistry*, 33 (11):3143–3147. https://doi.org/10.1021/bi00177a001.

Bell, R. J. and Dean, P. (1970). Atomic vibrations in vitreous silica. *Discuss. Faraday Soc.*, 50:55. https://doi.org/10.1039/df9705000055.

Björn, L. O. (2015). The Nature of Light and Its Interaction with Matter. In *Photobiology*, chapter 1, pages 1–20. Springer New York, New York, NY. https://doi.org/10.1007/978-1-4939-1468-5_1.

Björn, L. O. and Ghiradella, H. (2015). Spectral Tuning in Biology I: Pigments. In *Photobiology*, pages 97–117. Springer New York, New York, NY. https://doi.org/10.1007/978-1-4939-1468-5_9.

Björn, L. O., Papageorgiou, G. C., Blankenship, R. E., and Govindjee (2009). A viewpoint: Why chlorophyll *a*? *Photosynth. Res.*, 99(2):85–98. https://doi.org/10.1007/s11120-008-9395-x.

Blankenship, R. E. (1992). Origin and early evolution of photosynthesis. *Photosynth. Res.*, 33(2):91–111. https://doi.org/10.1007/BF00039173.

Blankenship, R. E. (2014). *Molecular Mechanisms of Photosynthesis*. Wiley Blackwell, second edition. ISBN 978-1-405-18976-7.

Blankenship, R. E. and Matsuura, K. (2003). Antenna Complexes from Green Photosynthetic Bacteria. In Green, B. R. and Parson, W. W., editors, *Light. Antennas*, volume 13 of *Advances in Photosynthesis and Respiration*, chapter 6, pages 195–217. Springer, Dordrecht. ISBN 978-90-481-5468-5. https://doi.org/10.1007/978-94-017-2087-8_6.

Blankenship, R. E., Tiede, D. M., Barber, J., Brudvig, G. W., Fleming, G., Ghirardi, M., Gunner, M. R., Junge, W., Kramer, D. M., Melis, A., Moore, T. A., Moser, C. C., Nocera, D. G., Nozik, A. J., Ort, D. R., Parson, W. W., Prince, R. C., and Sayre, R. T. (2011). Comparing Photosynthetic and Photovoltaic Efficiencies and Recognizing the Potential for Improvement. *Science*, 332(6031):805–809. https://doi.org/10.1126/science.1200165.

Bondarenko, A. S., Knoester, J., and Jansen, T. L. (2020). Comparison of methods to study excitation energy transfer in molecular multichromophoric systems. *Chem. Phys.*, 529:1–12. https://doi.org/10.1016/j.chemphys.2019.110478.

Braslavsky, S. E. (2007). Glossary of terms used in photochemistry 3rd edition. *Pure Appl. Chem.*, 79(3):293–465. https://doi.org/10.1351/pac200779030293.

Braslavsky, S. E., Fron, E., Rodríguez, H. B., Román, E. S., Scholes, G. D., Schweitzer, G., Valeur, B., and Wirz, J. (2008). Pitfalls and limitations in the practical use of Förster's theory of resonance energy transfer. *Photochem. Photobiol. Sci.*, 7(12):1444–1448. https://doi.org/10.1039/b810620g.

Breuer, H.-P. and Petruccione, F. (2007). *The Theory of Open Quantum Systems*. Oxford University Press. ISBN 9780199213900. https://doi.org/10.1093/acprof:oso/9780199213900.001.0001.

Brune, D. C. (1989). Sulfur oxidation by phototrophic bacteria. *BBA - Bioenerg.*, 975(2):189–221. https://doi.org/10.1016/S0005-2728(89)80251-8.

Bryant, D. A., Costas, A. M. G., Maresca, J. A., Chew, A. G. M., Klatt, C. G., Bateson, M. M., Tallon, L. J., Hostetler, J., Nelson, W. C., Heidelberg, J. F., and Ward, D. M. (2007). *Candidatus* Chloracidobacterium thermophilum: An Aerobic Phototrophic Acidobacterium. *Science*, 317(5837):523–526. https://doi.org/10.1126/science.1143236.

Buchanan, B. B., Gruissem, W., and Jones, R. L., editors (2015). *Biochemistry & molecular biology of plants*. John Wiley & Sons, Ltd., first edition. ISBN 9780470714218.

Bullough, P. A., Qian, P., and Hunter, C. N. (2009). Reaction Center-Light-Harvesting Core Complexes of Purple Bacteria. In Hunter, C. N., Daldal, F., Thurnauer, M. C., and Beatty, J. T., editors, *Purple Phototrophic Bact.*, Advances in Photosynthesis and Respiration, pages 155–179. Springer. https://doi.org/10.1007/978-1-4020-8815-5_9.

Calhoun, T. R., Ginsberg, N. S., Schlau-Cohen, G. S., Cheng, Y.-C., Ballottari, M., Bassi, R., and Fleming, G. R. (2009). Quantum Coherence Enabled Determination of the Energy Landscape in Light-Harvesting Complex II. *J. Phys. Chem. B*, 113(51):16291–16295. https://doi.org/10.1021/jp908300c.

Cao, J., Cogdell, R. J., Coker, D. F., Duan, H. G., Hauer, J., Kleinekathöfer, U., Jansen, T. L., Mančal, T., Dwayne Miller, R. J., Ogilvie, J. P., Prokhorenko, V. I., Renger, T., Tan, H. S., Tempelaar, R., Thorwart, M., Thyrhaug, E., Westenhoff, S., and Zigmantas, D. (2020). Quantum biology revisited. *Sci. Adv.*, 6(14):1–12. https://doi.org/10.1126/sciadv.aaz4888.

Caruso, F., Chin, A. W., Datta, A., Huelga, S. F., and Plenio, M. B. (2009). Highly efficient energy excitation transfer in light-harvesting complexes: The fundamental role of noise-assisted transport. *J. Chem. Phys.*, 131(10). https://doi.org/10.1063/1.3223548. `arXiv:0901.4454 [quant-ph]`.

Chen, M. and Blankenship, R. E. (2011). Expanding the solar spectrum used by photosynthesis. *Trends Plant Sci.*, 16 (8):427–431. https://doi.org/10.1016/j.tplants.2011.03.011.

Cheng, Y.-C. and Fleming, G. R. (2009). Dynamics of Light Harvesting in Photosynthesis. *Annu. Rev. Phys. Chem.*, 60(1):241–262. https://doi.org/10.1146/annurev.physchem.040808.090259.

Chenu, A. and Scholes, G. D. (2015). Coherence in Energy Transfer and Photosynthesis. *Annu. Rev. Phys. Chem.*, 66 (1):69–96. https://doi.org/10.1146/annurev-physchem-040214-121713.

Cherepy, N. J., Shreve, A. P., Moore, L. J., Boxer, S. G., and Mathies, R. A. (1997). Temperature Dependence of the Q_y Resonance Raman Spectra of Bacteriochlorophylls, the Primary Electron Donor, and Bacteriopheophytins in the Bacterial Photosynthetic Reaction Center. *Biochemistry*, 36(28):8559–8566. https://doi.org/10.1021/bi970024r.

Chin, A. W., Rivas, Á., Huelga, S. F., and Plenio, M. B. (2010). Exact mapping between system-reservoir quantum models and semi-infinite discrete chains using orthogonal polynomials. *J. Math. Phys.*, 51(9):092109. https://doi.org/10.1063/1.3490188. `arXiv:1006.4507 [quant-ph]`.

Cho, M. (2009). *Two-Dimensional Optical Spectroscopy*. CRC Press. ISBN 9780429189258. https://doi.org/10.1201/9781420084306.

Clayton, R. K. and Haselkorn, R. (1972). Protein components of bacterial photosynthetic membranes. *J. Mol. Biol.*, 68(1):97–105. https://doi.org/10.1016/0022-2836(72)90265-3.

Clegg, R. M. (2006). The history of FRET : From conception through the labors of birth. *Rev. Fluoresc.*, 3:1–45. https://doi.org/10.1007/0-387-33016-X_1.

Cogdell, R. J., Gall, A., and Köhler, J. (2006). The architecture and function of the light-harvesting apparatus of purple bacteria: From single molecules to *in vivo* membranes. *Q. Rev. Biophys.*, 39(3):227–324. https://doi.org/10.1017/S0033583506004434.

Collini, E., Curutchet, C., Mirkovic, T., and Scholes, G. D. (2009). Electronic Energy Transfer in Photosynthetic Antenna Systems. In Burghardt, I., Volkhard, M., Micha, D. A., and Bittner, E. R., editors, *Energy Transf. Dyn. Biomol. Syst.*, Chemical physics, pages 3–34. Springer, Berlin, 1st edition. ISBN 978-3-642-02306-4. https://doi.org/10.1007/978-3-642-02306-4.

Collini, E., Wong, C. Y., Wilk, K. E., Curmi, P. M. G., Brumer, P., and Scholes, G. D. (2010). Coherently wired light-harvesting in photosynthetic marine algae at ambient temperature. *Nature*, 463(7281):644–647. https://doi.org/10.1038/nature08811.

Comayras, F., Jungas, C., and Lavergne, J. (2005). Functional Consequences of the Organization of the Photosynthetic Apparatus in *Rhodobacter sphaeroides*: I. QUINONE DOMAINS AND EXCITATION TRANSFER IN CHROMATOPHORES AND REACTION CENTER-ANTENNA COMPLEXES. *J. Biol. Chem.*, 280(12):11203–11213. https://doi.org/10.1074/jbc.M412088200.

Croce, R., van Grondelle, R., van Amerongen, H., and van Stokkum, I. (2018). *Light harvesting in photosynthesis*. Taylor & Francis/CRC Press. ISBN 9781482218350.

Curutchet, C. and Mennucci, B. (2017). Quantum chemical studies of light harvesting. *Chem. Rev.*, 117(2):294–343. https://doi.org/10.1021/acs.chemrev.5b00700.

Curutchet, C. and Mennucci, B. (2018). Chlorophylls in a protein environment: How to calculate their spectral and redox properties (from MO to DFT). In Croce, R., van Grondelle, R., van Amerongen, H., and van Stokkum, I., editors, *Light Harvest. Photosynth.*, chapter 2, pages 21–36. Taylor & Francis/CRC Press, Boca Raton. https://doi.org/10.1201/9781351242899-2.

Damjanović, A., Ritz, T., and Schulten, K. (2000). Excitation Energy Trapping by the Reaction Center of *Rhodobacter sphaeroides*. *Int. J. Quantum Chem.*, 77(1):139–151. https://doi.org/10.1002/(SICI)1097-461X(2000)77:13.0.CO;2-S.

Davydov, A. S. (1948). Theory of absorption spectra of molecular crystals. *Zhurnal Eksp. I Teor. Fiz.*, 18(2):210–218.

Davydov, A. S. (1971). *Theory of molecular excitons*. Springer, 2 edition. ISBN 978-1-4899-5171-7. https://doi.org/10.1007/978-1-4899-5169-4.

Davydov, A. S. (2008). Theory of absorption spectra of molecular crystals. *Ukr. J. Phys.*, 53(Special Issue):65–70. `http://archive.ujp.bitp.kiev.ua/files/journals/53/si/53SI14p.pdf`.

Deisenhofer, J. and Norris, J. R. (1993). *Photosynthetic Reaction Center*, volume 1. Elsevier. ISBN 978-0-12-208661-8. https://doi.org/10.1016/C2009-0-02600-2.

Dexter, D. L. (1953). A theory of sensitized luminescence in solids. *J. Chem. Phys.*, 21(5):836–850. https://doi.org/10.1063/1.1699044.

Dirac, P. A. M. (1927). The quantum theory of the emission and absorption of radiation. *Proc. R. Soc. Lond. A*, 114 (767):243–265. https://doi.org/10.1098/rspa.1927.0039.

Dronamraju, K. R. (1999). Erwin Schrödinger and the origins of molecular biology. *Genetics*, 153(3):1071–1076. `http://www.ncbi.nlm.nih.gov/pubmed/10545442`.

Duan, H.-G., Prokhorenko, V. I., Cogdell, R., Ashraf, K., Stevens, A. L., Thorwart, M., and Miller, R. J. D. (2016). Nature does not rely on long-lived electronic quantum coherence for photosynthetic energy transfer. *Proc. Natl. Acad. Sci.*, 114(32):8493–8498. https://doi.org/10.1073/pnas.1702261114. `arXiv:1610.08425 [physics.bio-ph]`.

Dutton, P. L. (1986). Energy Transduction in Anoxygenic Photosynthesis. In *Photosynth. III*, pages 197–237. Springer Berlin Heidelberg, Berlin, Heidelberg. https://doi.org/10.1007/978-3-642-70936-4_5.

Engel, G. S., Calhoun, T. R., Read, E. L., Ahn, T. K., Mančal, T., Cheng, Y. C., Blankenship, R. E., and Fleming, G. R. (2007). Evidence for wavelike energy transfer through quantum coherence in photosynthetic systems. *Nature*, 446(7137):782–786. https://doi.org/10.1038/nature05678.

Farchaus, J., Barz, W., Grünberg, H., and Oesterhelt, D. (1992). Studies on the expression of the *pufX* polypeptide and its requirement for photoheterotrophic growth in *Rhodobacter sphaeroides*. *EMBO J.*, 11(8):2779–2788. https://doi.org/10.1002/j.1460-2075.1992.tb05345.x.

Fassioli, F., Dinshaw, R., Arpin, P. C., and Scholes, G. D. (2014). Photosynthetic light harvesting: Excitons and coherence. *J. R. Soc. Interface*, 11(92):1–22. https://doi.org/10.1098/rsif.2013.0901.

Feynman, R. P. (1948). Space-Time Approach to Non-Relativistic Quantum Mechanics. *Rev. Mod. Phys.*, 20(2):367–387. https://doi.org/10.1103/RevModPhys.20.367.

Fleming, G. R. and van Grondelle, R. (1997). Femtosecond spectroscopy of photosynthetic light-harvesting systems. *Curr. Opin. Struct. Biol.*, 7(5):738–748. https://doi.org/10.1016/S0959-440X(97)80086-3.

Förster, T. (1946). Energiewanderung und Fluoreszenz. *Naturwissenschaften*, 33(6):166–175. https://doi.org/10.1007/BF00585226.

Förster, T. (1948). Zwischenmolekulare Energiewanderung und Konzentrationsdepolarisation der Fluoreszenz. *Ann. Phys.*, 463(2):55–75. https://doi.org/10.1002/andp.19614630112.

Förster, T. (1967). Mechanisms of Energy Transfer. *Compr. Biochem.*, 22:61–80. https://doi.org/10.1016/B978-1-4831-9712-8.50010-2.

Förster, T. (1993). Intermolecular energy migration and fluorescence. In Mielczarek, E. V., Greenbaum, E., and Knox, R. S., editors, *Biol. Phys.*, pages 148–160. American Institute of Physics. ISBN 0-88318-855-4.

Förster, T. (2012). Energy migration and fluorescence. *J. Biomed. Opt.*, 17(1):011002. https://doi.org/10.1117/1.jbo.17.1.011002.

Frank, H. A. and Cogdell, R. J. (2012). *Light capture in photosynthesis*, volume 8. Elsevier Ltd. ISBN 9780080957180. https://doi.org/10.1016/B978-0-12-374920-8.00808-0.

Frenkel, J. (1931). On the transformation of light into heat in solids. i. *Phys. Rev.*, 37(1):17–44. https://doi.org/10.1103/PhysRev.37.17.

Gabrielsen, M., Gardiner, A. T., and Cogdell, R. J. (2009). Peripheral Complexes of Purple Bacteria. In Hunter, C. N., Daldal, F., Thurnauer, M. C., and Beatty, J. T., editors, *Purple Phototrophic Bact.*, Advances in Photosynthesis and Respiration, chapter 8, pages 135–153. Springer. https://doi.org/10.1007/978-1-4020-8815-5_8.

Gelzinis, A., Augulis, R., Butkus, V., Robert, B., and Valkunas, L. (2019). Two-dimensional spectroscopy for non-specialists. *Biochim. Biophys. Acta - Bioenerg.*, 1860(4):271–285. https://doi.org/10.1016/j.bbabio.2018.12.006.

Golbeck, J. H. and van der Est, A. (2014). *The Biophysics of Photosynthesis*. Biophysics for Life Sciences. Springer. ISBN 978-1-4939-1148-6. https://doi.org/10.1007/978-1-4939-1148-6.

Gouterman, M. (1961). Spectra of porphyrins. *J. Mol. Spectrosc.*, 6(4):138–163. https://doi.org/10.1016/0022-2852(61)90236-3.

Govorov, A., Hernández Martínez, P. L., and Demir, H. V. (2016). *Understanding and Modeling Förster-type Resonance Energy Transfer (FRET): Introduction to FRET*, volume 1 of *SpringerBriefs in Applied Sciences and Technology*. Springer Singapore, Singapore, 1 edition. ISBN 978-981-287-377-4. https://doi.org/10.1007/978-981-287-378-1.

Green, B. R. (2003). The Evolution of Light-harvesting Antennas. In Green, B. R. and Parson, W. W., editors, *Light. Antennas*, volume 13 of *Advances in Photosynthesis and Respiration*, chapter 4, pages 129–168. Springer. ISBN 978-90-481-5468-5. https://doi.org/10.1007/978-94-017-2087-8_4.

Hamm, P. (2005). Principles of Nonlinear Optical Spectroscopy: A Practical Approach. `http://www.mitr.p.lodz.pl/evu/lectures/Hamm.pdf`.

Harcourt, R. D., Scholes, G. D., and Ghiggino, K. P. (1994). Rate expressions for excitation transfer. II. Electronic considerations of direct and through-configuration exciton resonance interactions. *J. Chem. Phys.*, 101(12):10521–10525. https://doi.org/10.1063/1.467869.

Harrop, S. J., Wilk, K. E., Dinshaw, R., Collini, E., Mirkovic, T., Teng, C. Y., Oblinsky, D. G., Green, B. R., Hoef-Emden, K., Hiller, R. G., Scholes, G. D., and Curmi, P. M. (2014). Single-residue insertion switches the quaternary structure and exciton states of cryptophyte light-harvesting proteins. *Proc. Natl. Acad. Sci. U. S. A.*, 111(26). https://doi.org/10.1073/pnas.1402538111.

Hassani, S. (2009). *Mathematical Methods for students of physics and related fields*. Springer. ISBN 978-0-387-09503-5. https://doi.org/10.1007/978-0-387-09504-2.

Heathcote, P. and Jones, M. R. (2012). The structure-function relationships of photosynthetic reaction centers. In *Compr. Biophys.*, chapter Chapter 8., pages 115–144. Elsevier B.V. ISBN 9780080957180. https://doi.org/10.1016/B978-0-12-374920-8.00809-2.

Hohmann-Marriott, M. F. and Blankenship, R. E. (2011). Evolution of Photosynthesis. *Annu. Rev. Plant Biol.*, 62(1):515–548. https://doi.org/10.1146/annurev-arplant-042110-103811.

Hohmann-Marriott, M. F. and Blankenship, R. E. (2012). The Photosynthetic World. In *Photosynthesis*, volume 34 of *Advances in Photosynthesis and Respiration*, chapter 1, pages 3–32. Springer. ISBN 978-94-007-1578-3. https://doi.org/10.1007/978-94-007-1579-0_1.

Hwang-Fu, Y. H., Chen, W., and Cheng, Y.-C. (2015). A coherent modified Redfield theory for excitation energy transfer in molecular aggregates. *Chem. Phys.*, 447:46–53. https://doi.org/10.1016/j.chemphys.2014.11.026.

Ishizaki, A. and Fleming, G. R. (2009). Unified treatment of quantum coherent and incoherent hopping dynamics in electronic energy transfer: Reduced hierarchy equation approach. *J. Chem. Phys.*, 130(23). https://doi.org/10.1063/1.3155372.

Ishizaki, A. and Fleming, G. R. (2012). Quantum Coherence in Photosynthetic Light Harvesting. *Annu. Rev. Condens. Matter Phys.*, 3(1):333–361. https://doi.org/10.1146/annurev-conmatphys-020911-125126.

Jang, S. (2020). *Dynamics of Molecular Excitons*. Nanophotonics. Elsevier, first edition. ISBN 9780081023358.

Jang, S., Newton, M. D., and Silbey, R. J. (2004). Multichromophoric Förster Resonance Energy Transfer. *Phys. Rev. Lett.*, 92(21):218301. https://doi.org/10.1103/PhysRevLett.92.218301.

Jaschke, P. R., Hardjasa, A., Digby, E. L., Hunter, C. N., and Beatty, J. T. (2011). A *bchD* (Magnesium Chelatase) Mutant of *Rhodobacter sphaeroides* Synthesizes Zinc Bacteriochlorophyll through Novel Zinc-containing Intermediates. *J. Biol. Chem.*, 286(23):20313–20322. https://doi.org/10.1074/jbc.M110.212605.

Jones, M. R. (2009). The petite purple photosynthetic powerpack. *Biochem. Soc. Trans.*, 37(2):400–407. https://doi.org/10.1042/BST0370400.

Jones, M. R. (2018). Reaction centers: Structure and mechanism. In Croce, R., van Grondelle, R., van Amerongen, H., and van Stokkum, I., editors, *Light Harvest. Photosynth.*, chapter 9, pages 181–205. Taylor & Francis/CRC Press, Boca Raton. https://doi.org/10.1201/9781351242899-9.

Jordanides, X. J., Scholes, G. D., and Fleming, G. R. (2001). The mechanism of energy transfer in the bacterial photosynthetic reaction center. *J. Phys. Chem. B*, 105(8):1652–1669. https://doi.org/10.1021/jp003572e.

Kasha, M. (1963). Energy Transfer Mechanisms and the Molecular Exciton Model for Molecular Aggregates. *Radiat. Res.*, 20(1):55. https://doi.org/10.2307/3571331.

Kasha, M., Rawls, H. R., and El-Bayoumi, M. A. (1965). The Exciton Model In Molecular Spectroscopy. *Pure Appl. Chem.*, 11(3-4):371–392. https://doi.org/10.1351/pac196511030371.

Kassal, I., Yuen-Zhou, J., and Rahimi-Keshari, S. (2013). Does Coherence Enhance Transport in Photosynthesis? *Phys. Chem. Lett.*, 4:362–367. https://doi.org/doi.org/10.1021/jz301872b.

Khvostichenko, D. S., Schieferstein, J. M., Pawate, A. S., Laible, P. D., and Kenis, P. J. A. (2014). X-ray Transparent Microfluidic Chip for Mesophase-Based Crystallization of Membrane Proteins and On-Chip Structure Determination. *Cryst. Growth Des.*, 14(10):4886–4890. https://doi.org/10.1021/cg5011488.

Kiang, N. Y., Siefert, J., Govindjee, and Blankenship, R. E. (2007). Spectral signatures of photosynthesis. I. Review of Earth organisms. *Astrobiology*, 7(1):222–251. https://doi.org/10.1089/ast.2006.0105.

King, B. A., Stanley, R. J., and Boxer, S. G. (1997). Excited state energy transfer pathways in photosynthetic reaction centers. 2. Heterodimer special pair. *J. Phys. Chem. B*, 101(18):3644–3648. https://doi.org/10.1021/jp964025p.

König, C. and Neugebauer, J. (2012). Quantum chemical description of absorption properties and excited-state processes in photosynthetic systems. *ChemPhysChem*, 13(2):386–425. https://doi.org/10.1002/cphc.201100408.

Kramer, T., Noack, M., Reinefeld, A., Rodriguez, M., and Zelinskyy, Y. (2018). Efficient calculation of open quantum system dynamics and time-resolved spectroscopy with Distributed Memory HEOM (DM-HEOM). *J. Comput. Chem.*, 39(22):1779–1794. https://doi.org/10.1002/jcc.25354. `arXiv:1803.03498 [physics.chem-ph]`.

Kreisbeck, C. and Kramer, T. (2012). Long-Lived Electronic Coherence in Dissipative Exciton Dynamics of Light-Harvesting Complexes. *J. Phys. Chem. Lett.*, 3(19):2828–2833. https://doi.org/10.1021/jz3012029.

Kreisbeck, C., Kramer, T., Rodríguez, M., and Hein, B. (2011). High-Performance Solution of Hierarchical Equations of Motion for Studying Energy Transfer in Light-Harvesting Complexes. *J. Chem. Theory Comput.*, 7(7):2166–2174. https://doi.org/10.1021/ct200126d.

Krueger, B. P., Scholes, G. D., and Fleming, G. R. (1998). Calculation of couplings and energy-transfer pathways between the pigments of LH2 by the *ab initio* transition density cube method. *J. Phys. Chem. B*, 102(27):5378–5386. https://doi.org/10.1021/jp983589l.

Küpper, H., Küpper, F., and Spiller, M. (1998). *In situ* detection of heavy metal substituted chlorophylls in water plants. *Photosynth. Res.*, 58(2):123–133. https://doi.org/10.1023/A:1006132608181.

Lambert, N., Chen, Y. N., Cheng, Y.-C., Li, C. M., Chen, G. Y., and Nori, F. (2013). Quantum biology. *Nat. Phys.*, 9 (1):10–18. https://doi.org/10.1038/nphys2474.

Lee, H., Cheng, Y.-C., and Fleming, G. R. (2007). Coherence Dynamics in Photosynthesis: Protein Protection of Excitonic Coherence. *Science*, 316(5830):1462–1465. https://doi.org/10.1126/science.1142188.

Lendzian, F., Huber, M., Isaacson, R., Endeward, B., Plato, M., Bönigk, B., Möbius, K., Lubitz, W., and Feher, G. (1993). The electronic structure of the primary donor cation radical in *Rhodobacter sphaeroides* R-26: ENDOR and TRIPLE resonance studies in single crystals of reaction centers. *Biochim. Biophys. Acta - Bioenerg.*, 1183(1): 139–160. https://doi.org/10.1016/0005-2728(93)90013-6.

Leonova, M. M., Fufina, T. Y., Vasilieva, L. G., and Shuvalov, V. A. (2011). Structure-function investigations of bacterial photosynthetic reaction centers. *Biochem.*, 76(13):1465–1483. https://doi.org/10.1134/S0006297911130074.

Li, H. and Cundiff, S. T. (2017). 2D Coherent Spectroscopy of Electronic Transitions. In *Adv. At. Mol. Opt. Phys.*, volume 66, pages 1–48. Elsevier Inc., 1 edition. https://doi.org/10.1016/bs.aamop.2017.03.004.

Lilburn, T. G., Haith, C. E., Prince, R. C., and Beatty, J. T. (1992). Pleiotropic effects of *pufX* gene deletion on the structure and function of the photosynthetic apparatus of *Rhodobacter capsulatus*. *Biochim. Biophys. Acta - Bioenerg.*, 1100(2):160–170. https://doi.org/10.1016/0005-2728(92)90077-F.

Linnanto, J. and Korppi-Tommola, J. (2006). Quantum chemical simulation of excited states of chlorophylls, bacteriochlorophylls and their complexes. *Phys. Chem. Chem. Phys.*, 8(6):663–687. https://doi.org/10.1039/B513086G.

Madigan, M. T. and Jung, D. O. (2009). An Overview of Purple Bacteria: Systematics, Physiology, and Habitats. In Hunter, C. N., Daldal, F., Thurnauer, M. C., and Beatty, J. T., editors, *Purple Phototrophic Bact.*, volume 28 of *Advances in Photosynthesis and Respiration*, chapter 1, pages 1–15. Springer. https://doi.org/10.1007/978-1-4020-8815-5_1.

Madjet, M. E., Abdurahman, A., and Renger, T. (2006). Intermolecular coulomb couplings from *ab initio* electrostatic potentials: Application to optical transitions of strongly coupled pigments in photosynthetic antennae and reaction centers. *J. Phys. Chem. B*, 110(34):17268–17281. https://doi.org/10.1021/jp0615398.

Madjet, M. E. A., Müh, F., and Renger, T. (2009). Deciphering the influence of short-range electronic couplings on optical properties of molecular dimers: Application to "special pairs" in photosynthesis. *J. Phys. Chem. B*, 113(37): 12603–12614. https://doi.org/10.1021/jp906009j.

Makarov, D. E. and Makri, N. (1994). Path integrals for dissipative systems by tensor multiplication. Condensed phase quantum dynamics for arbitrarily long time. *Chem. Phys. Lett.*, 221(5-6):482–491. https://doi.org/10.1016/0009-2614(94)00275-4.

Mäkelä, H. and Möttönen, M. (2013). Effects of the rotating wave and secular approximations on non-Markovianity. *Phys. Rev. A - At. Mol. Opt. Phys.*, 88(5):1–10. https://doi.org/10.1103/PhysRevA.88.052111. `arXiv:1306.6301 [quant-ph]`.

Makri, N. and Makarov, D. E. (1995a). Tensor propagator for iterative quantum time evolution of reduced density matrices. I. Theory. *J. Chem. Phys.*, 102(11):4600–4610. https://doi.org/10.1063/1.469508.

Makri, N. and Makarov, D. E. (1995b). Tensor propagator for iterative quantum time evolution of reduced density matrices. II. Numerical methodology. *J. Chem. Phys.*, 102(11):4611–4618. https://doi.org/10.1063/1.469509.

Mančal, T. (2013). Excitation energy transfer in a classical analogue of photosynthetic antennae. *J. Phys. Chem. B*, 117(38):11282–11291. https://doi.org/10.1021/jp402101z.

Mančal, T., Nothling, T., Malý, P., Sláma, V., and Herman, D. (2020). QUANTArhei. version: 0.0.59. `https://github.com/tmancal74/quantarhei`.

Marx, A., David, L., and Adir, N. (2014). Piecing Together the Phycobilisome. In Hohmann-Marriott, M. F., editor, *Struct. Basis Biol. Energy Gener.*, Advances in Photosynthesis and Respiration, chapter 4, pages 59–76. Springer Netherlands. ISBN 978-94-017-8741-3. https://doi.org/10.1007/978-94-017-8742-0_4.

Masters, B. R. (2014). Paths to Förster's resonance energy transfer (FRET) theory. *Eur. Phys. J. H*, 39(1):87–139. https://doi.org/10.1140/epjh/e2013-40007-9.

May, V. and Kühn, O. (2011). *Charge and Energy Transfer Dynamics in Molecular Systems*. Wiley-VCH Verlag GmbH & Co. KGaA, Weinheim, Germany, third edition. ISBN 9783527633791. https://doi.org/10.1002/9783527633791.

Mirkovic, T. and Scholes, G. D. (2015). Photosynthetic Light Harvesting. In Björn, L. O., editor, *Photobiology*, chapter 17, pages 231–241. Springer New York, New York, NY. https://doi.org/10.1007/978-1-4939-1468-5_17.

Mirkovic, T., Ostroumov, E. E., Anna, J. M., van Grondelle, R., Govindjee, and Scholes, G. D. (2017). Light absorption and energy transfer in the antenna complexes of photosynthetic organisms. *Chem. Rev.*, 117(2):249–293. https://doi.org/10.1021/acs.chemrev.6b00002.

Mohseni, M., Rebentrost, P., Lloyd, S., and Aspuru-Guzik, A. (2008). Environment-assisted quantum walks in photosynthetic energy transfer. *J. Chem. Phys.*, 129(17):174106. https://doi.org/10.1063/1.3002335. `arXiv:0805.2741`.

Mohseni, M., Omar, Y., Engel, G. S., and Plenio, M. B. (2014). *Quantum Effects in Biology*. Cambridge University Press. ISBN 978-1-107-01080-2.

Mothersole, D. J., Farmer, D. A., Hitchcock, A., and Hunter, C. N. (2018). Photosynthetic apparatus in purple bacteria. In Croce, R., van Grondelle, R., van Amerongen, H., and van Stokkum, I., editors, *Light Harvest. Photosynth.*, chapter 6, pages 95–120. Taylor & Francis/CRC Press, Boca Raton. https://doi.org/10.1201/9781351242899-6.

Müh, F. and Renger, T. (2014). Structure-Based Calculation of Pigment–Protein and Excitonic Pigment–Pigment Coupling in Photosynthetic Light-Harvesting Complexes. In Golbeck, J. H. and van der Est, A., editors, *Biophys. Photosynth.*, chapter 1, pages 3–44. Springer. ISBN 978-1-4939-1148-6. https://doi.org/10.1007/978-1-4939-1148-6_1.

Mukai, K., Abe, S., and Sumi, H. (1999). Theory of Rapid Excitation-Energy Transfer from B800 to Optically-Forbidden Exciton States of B850 in the Antenna System LH2 of Photosynthetic Purple Bacteria. *J. Phys. Chem. B*, 103(29): 6096–6102. https://doi.org/10.1021/jp984469g.

Mukamel, S. (1995). *Principles of Nonlinear Optical Spectroscopy*. Oxford University Press. ISBN 0-19-509278-3.

Nagarajan, V. and Parson, W. W. (1997). Excitation energy transfer between the b850 and b875 antenna complexes of *Rhodobacter sphaeroides*. *Biochemistry*, 36(8):2300–2306. https://doi.org/10.1021/bi962534b.

Nakajima, S. (1958). On Quantum Theory of Transport Phenomena. *Prog. Theor. Phys.*, 20(6):948–959. https://doi.org/10.1143/ptp.20.948.

Nelson, D. L. and Cox, M. M. (2013). *Principles of Biochemistry Lehninger Sixth edition*. W. H. Freeman and Company, sixth edition. ISBN 978-1-4641-0962-1.

Niedringhaus, A., Policht, V. R., Sechrist, R., Konar, A., Laible, P. D., Bocian, D. F., Holten, D., Kirmaier, C., and Ogilvie, J. P. (2018). Primary processes in the bacterial reaction center probed by two-dimensional electronic spectroscopy. *Proc. Natl. Acad. Sci. U. S. A.*, 115(14):3563–3568. https://doi.org/10.1073/pnas.1721927115.

Niwa, S., Yu, L.-J., Takeda, K., Hirano, Y., Kawakami, T., Wang-Otomo, Z.-Y., and Miki, K. (2014). Structure of the LH1–RC complex from *Thermochromatium tepidum* at 3.0 Å. *Nature*, 508(7495):228–232. https://doi.org/10.1038/nature13197.

Novoderezhkin, V. I. and van Grondelle, R. (2018). Modeling of energy transfer in photosynthetic light harvesting. In Croce, R., van Amerongen, H., and van Stokkum, I., editors, *Light Harvest. Photosynth.*, chapter 13, pages 269–303. Taylor & Francis/CRC Press, Boca Raton. https://doi.org/10.1201/9781351242899-13.

Oelze, J. (1985). Analysis of Bacteriochlorophylls. In Gottschalk, G., editor, *Methods Microbiol.*, volume 18, chapter 9, pages 257–284. Elsevier. ISBN 978-0-12-521518-3. https://doi.org/10.1016/S0580-9517(08)70478-1.

Okamura, M. Y., Steiner, L. A., and Feher, G. (1974). Characterization of reaction centers from photosynthetic bacteria. I. Subunit structure of the protein mediating the primary photochemistry in *Rhodopseudomonas spheroides* R-26. *Biochemistry*, 13(7):1394–1403. https://doi.org/10.1021/bi00704a013.

Olaya-Castro, A. and Scholes, G. D. (2011). Energy transfer from Förster-Dexter theory to quantum coherent light-harvesting. *Int. Rev. Phys. Chem.*, 30(1):49–77. https://doi.org/10.1080/0144235X.2010.537060.

Orf, G. S. and Blankenship, R. E. (2013). Chlorosome antenna complexes from green photosynthetic bacteria. *Photosynth. Res.*, 116(2-3):315–331. https://doi.org/10.1007/s11120-013-9869-3.

Orf, G. S., Tank, M., Vogl, K., Niedzwiedzki, D. M., Bryant, D. A., and Blankenship, R. E. (2013). Spectroscopic insights into the decreased efficiency of chlorosomes containing bacteriochlorophyll *f*. *Biochim. Biophys. Acta - Bioenerg.*, 1827(4):493–501. https://doi.org/10.1016/j.bbabio.2013.01.006.

Orf, G. S., Gisriel, C., and Redding, K. E. (2018). Evolution of photosynthetic reaction centers: insights from the structure of the heliobacterial reaction center. *Photosynth. Res.*, 138(1):11–37. https://doi.org/10.1007/s11120-018-0503-2.

Paleček, D. (2016). *Quantum Coherence for Light Harvesting*. Doctoral dissertation; Supervisors: Roman Dědic, Donatas Zigmantas, Lund University.

Paleček, D., Edlund, P., Westenhoff, S., and Zigmantas, D. (2017). Quantum coherence as a witness of vibronically hot energy transfer in bacterial reaction center. *Sci. Adv.*, 3(9):e1603141. https://doi.org/10.1126/sciadv.1603141.

Panitchayangkoon, G., Hayes, D., Fransted, K. A., Caram, J. R., Harel, E., Wen, J., Blankenship, R. E., and Engel, G. S. (2010). Long-lived quantum coherence in photosynthetic complexes at physiological temperature. *Proc. Natl. Acad. Sci. U. S. A.*, 107(29):12766–12770. https://doi.org/10.1073/pnas.1005484107.

Parson, W. W. (2015). *Modern Optical Spectroscopy*. Springer. ISBN 9783662467763. https://doi.org/10.1007/978-3-662-46777-0.

Pinnola, A., Kirilovsky, D., and Bassi, R. (2018). Photoprotective excess energy dissipation. In Croce, R., van Grondelle, R., van Amerongen, H., and van Stokkum, I., editors, *Light Harvest. Photosynth.*, chapter 11, pages 219–245. Taylor & Francis/CRC Press, Boca Raton. https://doi.org/10.1201/9781351242899-11.

Plenio, M. B. and Huelga, S. F. (2008). Dephasing-assisted transport: quantum networks and biomolecules. *New J. Phys.*, 10(11):113019. https://doi.org/10.1088/1367-2630/10/11/113019. `arXiv:0807.4902`.

Prior, J., Chin, A. W., Huelga, S. F., and Plenio, M. . B. (2010). Efficient simulation of strong system-environment interactions. *Phys. Rev. Lett.*, 105(5):050404. https://doi.org/10.1103/PhysRevLett.105.050404. `arXiv:1003.5503 [quant-ph]`.

Pšenčík, J., Butcher, S. J., and Tuma, R. (2014). Chlorosomes: Structure, Function and Assembly. In Hohmann-Marriott, M. F., editor, *Struct. Basis Biol. Energy Gener.*, Advances in Photosynthesis and Respiration, chapter 5, pages 77–109. Springer Netherlands. ISBN 978-94-017-8741-3. https://doi.org/10.1007/978-94-017-8742-0_5.

Qian, P., Papiz, M. Z., Jackson, P. J., Brindley, A. A., Ng, I. W., Olsen, J. D., Dickman, M. J., Bullough, P. A., and Hunter, C. N. (2013). Three-Dimensional Structure of the *Rhodobacter sphaeroides* RC-LH1-PufX Complex: Dimerization and Quinone Channels Promoted by PufX. *Biochemistry*, 52(43):7575–7585. https://doi.org/10.1021/bi4011946.

Qian, P., Papiz, M. Z., Jackson, P. J., Brindley, A. A., Ng, I. W., Olsen, J. D., Dickman, M. J., Bullough, P. A., and Hunter, C. N. (2014). RC-LH1-PufX dimer complex from *Rhodobacter sphaeroides*. https://doi.org/10.2210/pdb4v9g/pdb.

Rathbone, H. W., Davis, J. A., Michie, K. A., Goodchild, S. C., Robertson, N. O., and Curmi, P. M. G. (2018a). Coherent phenomena in photosynthetic light harvesting: part one—theory and spectroscopy. *Biophys. Rev.*, 10(5): 1427–1441. https://doi.org/10.1007/s12551-018-0451-2.

Rathbone, H. W., Davis, J. A., Michie, K. A., Goodchild, S. C., Robertson, N. O., and Curmi, P. M. G. (2018b). Coherent phenomena in photosynthetic light harvesting: part two—observations in biological systems. *Biophys. Rev.*, 10(5):1443–1463. https://doi.org/10.1007/s12551-018-0456-x.

Rebentrost, P., Mohseni, M., Kassal, I., Lloyd, S., and Aspuru-Guzik, A. (2009). Environment-assisted quantum transport. *New J. Phys.*, 11(3):033003. https://doi.org/10.1088/1367-2630/11/3/033003. `arXiv:0807.0929`.

Redfield, A. G. (1957). On the Theory of Relaxation Processes. *IBM J. Res. Dev.*, 1(1):19–31. https://doi.org/10.1147/rd.11.0019.

Redfield, A. G. (1965). The Theory of Relaxation Processes. In *Adv. Magn. Opt. Reson.*, volume 1, pages 1–32. Academic Press Inc. ISBN 978-1-4832-3114-3. https://doi.org/10.1016/B978-1-4832-3114-3.50007-6.

Renger, T. (2018). Photoinduced electron transfer in the reaction centers. In Croce, R., van Grondelle, R., van Amerongen, H., and van Stokkum, I., editors, *Light Harvest. Photosynth.*, chapter 15, pages 327–357. Taylor & Francis/CRC Press.

Renger, T. and Holzwarth, A. R. (2008). Theory of Excitation Energy Transfer and Optical Spectra of Photosynthetic Systems. In *Biophys. Tech. Photosynth.*, chapter 21, pages 421–443. Springer. https://doi.org/10.1007/978-1-4020-8250-4_21.

Renger, T. and Müh, F. (2013). Understanding photosynthetic light-harvesting: a bottom up theoretical approach. *Phys. Chem. Chem. Phys.*, 15:3348–3371. https://doi.org/10.1039/c3cp43439g.

Renger, T., May, V., and Kühn, O. (2001). Ultrafast excitation energy transfer dynamics in photosynthetic pigment–protein complexes. *Phys. Rep.*, 343(3):137–254. https://doi.org/10.1016/S0370-1573(00)00078-8.

Renger, T., Madjet, M. E.-A., Schmidt am Busch, M., Adolphs, J., and Müh, F. (2013). Structure-based modeling of energy transfer in photosynthesis. *Photosynth. Res.*, 116(2-3):367–388. https://doi.org/10.1007/s11120-013-9893-3.

Roy, C. and Lancaster, D. (2008). Structures of Reaction Centers in Anoxygenic Bacteria. In Renger, G., editor, *Prim. Process. Photosynth. - Part 2*, chapter Chapter 11, pages 5–56. RSC Publishing. ISBN 978-0-85404-236-4. https://doi.org/10.1039/9781847558169.

Roy, C., Lancaster, D., Ermler, U., and Michel, H. (1995). The Structures of Photosynthetic Reaction Centers from Purple Bacteria as Revealed by X-Ray Crystallography. In *Anoxygenic Photosynth. Bact.*, volume 2 of *Advances in Photosynthesis and Respiration*, chapter 23, pages 503–526. Kluwer Academic Publishers, Dordrecht. https://doi.org/10.1007/0-306-47954-0_23.

Savikhin, S., Buck, D. R., and Struve, W. S. (1997). Oscillating anisotropies in a bacteriochlorophyll protein: Evidence for quantum beating between exciton levels. *Chem. Phys.*, 223(2-3):303–312. https://doi.org/10.1016/S0301-0104(97)00223-1.

Sawicki, A. and Chen, M. (2020). Molecular Mechanism of Photosynthesis Driven by Red-Shifted Chlorophylls. In Wang, Q., editor, *Microb. Photosynth.*, chapter 1, pages 3–42. Springer Singapore, Singapore. https://doi.org/10.1007/978-981-15-3110-1_1.

Scheer, H. (2003). The Pigments. In *Light. Antennas*, volume 13 of *Advances in Photosynthesis and Respiration*, chapter 2, pages 29–81. Springer. ISBN 978-90-481-5468-5. https://doi.org/10.1007/978-94-017-2087-8_2.

Scheer, H. (2008). Chlorophylls. In Renger, G., editor, *Prim. Process. Photosynth. - Part 1*, chapter Chapter 3, pages 101–149. RSC Publishing. ISBN 978-0-85404-369-9. https://doi.org/10.1039/9781847558152.

Scheuring, S. (2006). AFM studies of the supramolecular assembly of bacterial photosynthetic core-complexes. *Curr. Opin. Chem. Biol.*, 10(5):387–393. https://doi.org/10.1016/j.cbpa.2006.08.007.

Schieferstein, J. M., Khvostichenko, D. S., Pawate, A. S., and Kenis, P. J. A. (2014). Photosynthetic Reaction Center from *R. sphaeroides* Analyzed at Room Temperature on an X-ray Transparent Microfluidic Chip. https://doi.org/10.2210/pdb4TQQ/pdb.

Schlau-Cohen, G. S., Ishizaki, A., and Fleming, G. R. (2011). Two-dimensional electronic spectroscopy and photosynthesis: Fundamentals and applications to photosynthetic light-harvesting. *Chem. Phys.*, 386(1-3):1–22. https://doi.org/10.1016/j.chemphys.2011.04.025.

Scholes, G. D. (2020). Limits of exciton delocalization in molecular aggregates. *Faraday Discuss.*, 221:265–280. https://doi.org/10.1039/C9FD00064J.

Scholes, G. D. and Fleming, G. R. (2000). On the Mechanism of Light Harvesting in Photosynthetic Purple Bacteria: B800 to B850 Energy Transfer. *J. Phys. Chem. B*, 104(8):1854–1868. https://doi.org/10.1021/jp9934351.

Scholes, G. D., Harcourt, R. D., and Ghiggino, K. P. (1995). Rate expressions for excitation transfer. III. An *ab initio* study of electronic factors in excitation transfer and exciton resonance interactions. *J. Chem. Phys.*, 102(24): 9574–9581. https://doi.org/10.1063/1.468773.

Scholes, G. D., Gould, I. R., Cogdell, R. J., and Fleming, G. R. (1999). *Ab initio* molecular orbital calculations of electronic couplings in the LH2 bacterial light-harvesting complex of *Rps. acidophila*. *J. Phys. Chem. B*, 103(13): 2543–2553. https://doi.org/10.1021/jp9839753.

Scholes, G. D., Jordanides, X. J., and Fleming, G. R. (2001). Adapting the Förster Theory of Energy Transfer for Modeling Dynamics in Aggregated Molecular Assemblies. *J. Phys. Chem. B*, 105(8):1640–1651. https://doi.org/10.1021/jp003571m.

Scholes, G. D., Curutchet, C., Mennucci, B., Cammi, R., and Tomasi, J. (2007). How Solvent Controls Electronic Energy Transfer and Light Harvesting. *J. Phys. Chem. B*, 111(25):6978–6982. https://doi.org/10.1021/jp072540p.

Scholes, G. D., Fleming, G. R., Chen, L. X., Aspuru-Guzik, A., Buchleitner, A., Coker, D. F., Engel, G. S., van Grondelle, R., Ishizaki, A., Jonas, D. M., Lundeen, J. S., McCusker, J. K., Mukamel, S., Ogilvie, J. P., Olaya-Castro, A., Ratner, M. A., Spano, F. C., Whaley, K. B., and Zhu, X. (2017). Using coherence to enhance function in chemical and biophysical systems. *Nature*, 543(7647):647–656. https://doi.org/10.1038/nature21425.

Schrödinger, E. (1944). *What Is Life?* Cambridge University Press. ISBN 0-521-42708-8.

Schubert, W.-D., Klukas, O., Saenger, W., Witt, H. T., Fromme, P., and Krauß, N. (1998). A common ancestor for oxygenic and anoxygenic photosynthetic systems. *J. Mol. Biol.*, 280(2):297–314. https://doi.org/10.1006/jmbi.1998.1824.

Sener, M. K., Olsen, J. D., Hunter, C. N., and Schulten, K. (2007). Atomic-level structural and functional model of a bacterial photosynthetic membrane vesicle. *Proc. Natl. Acad. Sci. U. S. A.*, 104(40):15723–15728. https://doi.org/10.1073/pnas.0706861104.

Sener, M. K., Strümpfer, J., Hsin, J., Chandler, D., Scheuring, S., Hunter, C. N., and Schulten, K. (2011). Förster energy transfer theory as reflected in the structures of photosynthetic light-harvesting systems. *ChemPhysChem*, 12 (3):518–531. https://doi.org/10.1002/cphc.201000944.

Stomp, M., Huisman, J., Stal, L. J., and Matthijs, H. C. (2007). Colorful niches of phototrophic microorganisms shaped by vibrations of the water molecule. *ISME J.*, 1(4):271–282. https://doi.org/10.1038/ismej.2007.59.

Strümpfer, J. and Schulten, K. (2012a). Excited state dynamics in photosynthetic reaction center and light harvesting complex 1. *J. Chem. Phys.*, 137(6). https://doi.org/10.1063/1.4738953.

Strümpfer, J. and Schulten, K. (2012b). Open quantum dynamics calculations with the hierarchy equations of motion on parallel computers. *J. Chem. Theory Comput.*, 8(8):2808–2816. https://doi.org/10.1021/ct3003833.

Sumi, H. (1999). Theory on rates of excitation-energy transfer between molecular aggregates through distributed transition dipoles with application to the antenna system in bacterial photosynthesis. *J. Phys. Chem. B*, 103(1): 252–260. https://doi.org/10.1021/jp983477u.

Taniguchi, M. and Lindsey, J. S. (2018). Database of Absorption and Fluorescence Spectra of >300 Common Compounds for use in PhotochemCAD. *Photochem. Photobiol.*, 94(2):290–327. https://doi.org/10.1111/php.12860.

Taniguchi, M., Du, H., and Lindsey, J. S. (2018). PhotochemCAD 3: Diverse Modules for Photophysical Calculations with Multiple Spectral Databases. *Photochem. Photobiol.*, 94(2):277–289. https://doi.org/10.1111/php.12862.

Tanimura, Y. (2006). Stochastic Liouville, Langevin, Fokker–Planck, and Master Equation Approaches to Quantum Dissipative Systems. *J. Phys. Soc. Japan*, 75(8):082001. https://doi.org/10.1143/JPSJ.75.082001.

Tanimura, Y. (2020). Perspective: Numerically "exact" approach to open quantum dynamics: The hierarchical equations of motion (HEOM). *arXiv e-prints*. https://doi.org/10.1063/5.0011599. `arXiv:2006.05501 [physics.chem-ph]`.

Tanimura, Y. and Kubo, R. (1989). Time Evolution of a Quantum System in Contact with a Nearly Gaussian-Markoffian Noise Bath. *J. Phys. Soc. Japan*, 58(1):101–114. https://doi.org/10.1143/JPSJ.58.101.

Thouless, D. (1974). Electrons in disordered systems and the theory of localization. *Phys. Rep.*, 13(3):93–142. https://doi.org/10.1016/0370-1573(74)90029-5.

Trissl, H. W. (1993). Long-wavelength absorbing antenna pigments and heterogeneous absorption bands concentrate excitons and increase absorption cross section. *Photosynth. Res.*, 35(3):247–263. https://doi.org/10.1007/BF00016556.

Trushechkin, A. (2019). Calculation of coherences in Foerster and modified Redfield theories of excitation energy transfer. *J. Chem. Phys.*, 151(7). https://doi.org/10.1063/1.5100967. `arXiv:1902.00554 [physics.chem-ph]`.

Tsukatani, Y., Romberger, S. P., Golbeck, J. H., and Bryant, D. A. (2012). Isolation and Characterization of Homodimeric Type-I Reaction Center Complex from *Candidatus* Chloracidobacterium thermophilum, an Aerobic Chlorophototroph. *J. Biol. Chem.*, 287(8):5720–5732. https://doi.org/10.1074/jbc.M111.323329.

Tsukatani, Y., Yamamoto, H., Harada, J., Yoshitomi, T., Nomata, J., Kasahara, M., Mizoguchi, T., Fujita, Y., and Tamiaki, H. (2013). An unexpectedly branched biosynthetic pathway for bacteriochlorophyll *b* capable of absorbing near-infrared light. *Sci. Rep.*, 3(1):1217. https://doi.org/10.1038/srep01217.

Turner, D. B., Dinshaw, R., Lee, K. K., Belsley, M. S., Wilk, K. E., Curmi, P. M., and Scholes, G. D. (2012). Quantitative investigations of quantum coherence for a light-harvesting protein at conditions simulating photosynthesis. *Phys. Chem. Chem. Phys.*, 14(14):4857–4874. https://doi.org/10.1039/c2cp23670b.

Valkunas, L., van Mourik, F., and van Grondelle, R. (1992). On the role of spectral and spatial antenna inhomogeneity in the process of excitation energy trapping in photosynthesis. *J. Photochem. Photobiol. B Biol.*, 15(1-2):159–170. https://doi.org/10.1016/1011-1344(92)87013-Y.

Valkunas, L., Abramavicius, D., and Mančal, T. (2013). *Molecular Excitation Dynamics and Relaxation*. Wiley-VCH Verlag GmbH & Co. KGaA, Weinheim, Germany. ISBN 9783527653652. https://doi.org/10.1002/9783527653652.

Valkunas, L., Chmeliov, J., and van Amerongen, H. (2018). The exciton concept. In Croce, R., van Grondelle, R., and van Stokkum, I., editors, *Light Harvest. Photosynth.*, chapter 12, pages 249–268. Taylor & Francis/CRC Press, Boca Raton. https://doi.org/10.1201/9781351242899-12.

van Amerongen, H., van Grondelle, R., and Valkunas, L. (2000). *Photosynthetic Excitons*. WORLD SCIENTIFIC, Singapore. ISBN 978-981-02-3280-1. https://doi.org/10.1142/3609.

van der Meer, B. W. (2013). Förster Theory. In *FRET – Förster Reson. Energy Transf.*, chapter 3, pages 23–62. Wiley. ISBN 9783527328161. https://doi.org/10.1002/9783527656028.ch03.

van der Meer, B. W., Coker III, G., and Chen, S.-Y. S. (1994). *Resonance Energy Transfer, Theory and Data*. Wiley-VCH. ISBN 0-471-18589-2.

van der Meer, B. W., van der Meer, D. M., and Vogel, S. S. (2013). Optimizing the Orientation Factor Kappa-Squared for More Accurate FRET Measurements. In *FRET – Förster Reson. Energy Transf.*, chapter 4, pages 63–104. Wiley. ISBN 9783527328161. https://doi.org/10.1002/9783527656028.ch04.

van Grondelle, R. and Novoderezhkin, V. I. (2009). Spectroscopy and Dynamics of Excitation Transfer and Trapping in Purple Bacteria. In Hunter, C. N., Daldal, F., Thurnauer, M. C., and Beatty, J. T., editors, *Purple Phototrophic Bact.*, Advances in Photosynthesis and Respiration, chapter 13, pages 231–252. Springer. https://doi.org/10.1007/978-1-4020-8815-5_13.

Vassiliev, I. R., Antonkine, M. L., and Golbeck, J. H. (2001). Iron-sulfur clusters in type I reaction centers. *Biochim. Biophys. Acta - Bioenerg.*, 1507(1-3):139–160. https://doi.org/10.1016/S0005-2728(01)00197-9.

Vogl, K., Tank, M., Orf, G. S., Blankenship, R. E., and Bryant, D. A. (2012). Bacteriochlorophyll *f*: properties of chlorosomes containing the "forbidden chlorophyll". *Front. Microbiol.*, 3(298):1–12. https://doi.org/10.3389/fmicb.2012.00298.

Vos, M. H. and Martin, J. L. (1999). Femtosecond processes in proteins. *Biochim. Biophys. Acta - Bioenerg.*, 1411(1): 1–20. https://doi.org/10.1016/S0005-2728(99)00035-3.

Vos, M. H., Breton, J., and Martin, J.-L. (1997). Electronic Energy Transfer within the Hexamer Cofactor System of Bacterial Reaction Centers. *J. Phys. Chem. B*, 101(47):9820–9832. https://doi.org/10.1021/jp971486h.

Wakao, N., Yokoi, N., Isoyama, N., Hiraishi, A., Shimada, K., Kobayashi, M., Kise, H., Iwaki, M., Itoh, S., and Takaichi, S. (1996). Discovery of Natural Photosynthesis using Zn-Containing Bacteriochlorophyll in an Aerobic Bacterium *Acidiphilium rubrum*. *Plant Cell Physiol.*, 37(6):889–893. https://doi.org/10.1093/oxfordjournals.pcp.a029029.

Wilkins, D. M. (2015). *A Theoretical Investigation Into Energy Transfer In Photosynthetic Open Quantum Systems*. Master's Thesis, Supervisor: D. E. Manolopoulos, St. Edmund Hall, Oxford University. `arXiv:1503.03277 [physics.chem-ph]`.

Wong, C. Y., Alvey, R. M., Turner, D. B., Wilk, K. E., Bryant, D. A., Curmi, P. M., Silbey, R. J., and Scholes, G. D. (2012). Electronic coherence lineshapes reveal hidden excitonic correlations in photosynthetic light harvesting. *Nat. Chem.*, 4(5):396–404. https://doi.org/10.1038/nchem.1302.

Wraight, C. A. and Clayton, R. K. (1974). The absolute quantum efficiency of bacteriochlorophyll photooxidation in reaction centres of *Rhodopseudomonas spheroides*. *Biochim. Biophys. Acta - Bioenerg.*, 333(2):246–260. https://doi.org/10.1016/0005-2728(74)90009-7.

Wraight, C. A. and Gunner, M. R. (2009). The Acceptor Quinones of Purple Photosynthetic Bacteria — Structure and Spectroscopy. In Hunter, C. N., Daldal, F., Thurnauer, M. C., and Beatty, J. T., editors, *Purple Phototrophic Bact.*, Advances in Photosynthesis and Respiration, chapter 20, pages 379–405. Springer. https://doi.org/10.1007/978-1-4020-8815-5_20.

Yang, M. and Fleming, G. R. (2002). Influence of phonons on exciton transfer dynamics: comparison of the Redfield, Förster, and modified Redfield equations. *Chem. Phys.*, 275(1-3):355–372. https://doi.org/10.1016/S0301-0104(01)00540-7.

Zhang, J. Z. and Reisner, E. (2020). Advancing photosystem II photoelectrochemistry for semi-artificial photosynthesis. *Nat. Rev. Chem.*, 4(1):6–21. https://doi.org/10.1038/s41570-019-0149-4.

Zhang, W. M., Meier, T., Chernyak, V., and Mukamel, S. (1998). Exciton-migration and three-pulse femtosecond optical spectroscopies of photosynthetic antenna complexes. *J. Chem. Phys.*, 108(18):7763–7774. https://doi.org/10.1063/1.476212.

Zwanzig, R. (1960). Ensemble Method in the Theory of Irreversibility. *J. Chem. Phys.*, 33(5):1338–1341. https://doi.org/10.1063/1.1731409.

Zwanzig, R. (1964). On the identity of three generalized master equations. *Physica*, 30(6):1109–1123. https://doi.org/10.1016/0031-8914(64)90102-8.